Studies on Solid Polymer Electrolyte for Direct Electrochemical Reduction of CO_2 to Fuel

Submitted in partial fulfillment of the requirements for the degree of

Doctor of Philosophy

by

LEELA MANOHAR AESHALA

(Roll No. 09610727)

DEPARTMENT OF CHEMICAL ENGINEERING

INDIAN INSTITUTE OF TECHNOLOGY GUWAHATI

Guwahati – 781 039

August, 2014

Dedicated to my beloved,

late mother,

family, and

caring guide

Department of Chemical Engineering
Indian Institute of Technology Guwahati
Guwahati – 781 039
Assam, India

STATEMENT

I do hereby declare that the matter embedded in this thesis is the result of investigations carried out by me in the Department of Chemical Engineering, Indian Institute of Technology Guwahati, Guwahati, Assam, India, under the supervision of Dr. Anil Verma, Associate Professor, Department of Chemical Engineering, Indian Institute of Technology Guwahati, India.

In keeping with the general practice of reporting scientific observations, due acknowledgements has been made wherever the work described is based on the findings of other investigators.

_ _ _ _ _ _ _ _ _ _ _ _ _ _ _ _ _ _ _ _

Dated:
IIT Guwahati

(Leela Manohar Aeshala)
Roll no. 09610727
Sustainable Environergy Electrochemical Research Group (*SEERG*)
Department of Chemical Engineering
Indian Institute of Technology Guwahati
Guwahati – 781 039
Assam, India

Department of Chemical Engineering
Indian Institute of Technology Guwahati
Guwahati – 781 039
Assam, India

CERTIFICATE

It is certified that the work contained in the thesis entitled "Studies on Solid Polymer Electrolyte for Direct Electrochemical Reduction of CO_2 to Fuel", by Mr. Leela Manohar Aeshala, for the award of degree of Doctor of Philosophy, has been carried out under my supervision and that this work has not been submitted elsewhere for a degree.

Dated:
IIT Guwahati

_ _ _ _ _ _ _ _ _ _ _ _ _ _ _ _ _ _ _ _

Dr. Anil Verma
Associate Professor
Department of Chemical Engineering
Indian Institute of Technology Guwahati
Guwahati – 781 039
Assam, India

Preface

The thesis, and the experimental investigations inserted in it, reflect a blend of science and engineering in the study of synthesis and performance evaluation of solid polymer electrolyte in direct electrochemical reduction of CO_2 (dERC). The thesis provides relevant details on the development of solid polymer electrolyte (SPE) for effective reduction of CO_2 to fuels. Moreover, the developed solid polymer electrolyte is tuned as per the selective formation of higher hydrocarbons.

The background and importance of electrochemical reduction of CO_2, and challenges are covered in the 1st chapter. However, the emphasis has been given on finding the solution for the problems associated with the use of electrolyte, especially aqueous and non-aqueous. The importance of SPE in the application of CO_2 electroreduction is discussed at end of the 1st chapter.

A literature review on the solid polymer electrolyte in the application of direct electrochemical reduction of CO_2 (dERC) is covered in the 2nd chapter. The literature review includes a brief discussion on the important scientific findings reported in the recent and past available literatures. The outcomes of the most significant literatures are summarized at the end of the chapter and the objective of the thesis is formulated based on the outcome of the literature review.

The 3rd chapter covers the common experimental procedures for characterizing the solid polymer electrolyte and electrode, development of experimental setup and electrochemical reactor, and evaluation of the reactor using solid polymer electrolyte membrane. Electrochemical techniques used in the experiments, procedure for analysis of products using gas chromatography, and calculation of Faradaic efficiency and selectivity are also discussed in this chapter.

The 4th chapter of the thesis includes the synthesis and characterization of cation and anion exchange membranes. The effect of cation and anion exchange membranes on

the performance of electrochemical reduction of gaseous CO_2 is discussed in this chapter. Moreover, the observations and necessary changes in the system are presented at the end of the chapter to study the role of SPE on the dERC.

The influence of functional groups in the SPEs having same polymer backbone but different functional group (anionic and cationic) is studied and evaluated in dERC. The properties of SPEs, the product distribution, Faradaic efficiency, and selectivity are investigated for ERC and conceptual mechanism is proposed and discussed in the 5th chapter.

The discussions on the tuning of reaction zone by the modification of functional groups in anionic SPE for dERC are covered in the 6th chapter. Materials and methods for the synthesis and evaluation of anionic SPEs with and without hindered bulky quaternary ammonium group for dERC are discussed. Further, the performance of the quaternary SPE is evaluated for dERC and reaction pathway along with conceptual representation of the dERC is discussed at the end of the chapter.

Overall conclusions of the research work are presented in the 7th chapter. Moreover, it also includes the future scope of the research in the dERC. The chapter will help the future researchers in formulating their research objectives to further improve the dERC performance as well as research pertaining to development of solid polymer electrolyte.

In the thesis, I have attempted to cover and cite all the significant literatures relevant to the current research work. However, the off topic scientific reports are avoided carefully throughout the thesis. I have tried to organize thesis in such a manner so that it may depict a clear picture to the reader to the studies on solid polymer electrolyte to evaluate for dERC.

_ _ _ _ _ _ _ _ _ _ _ _ _ _ _ _ _ _ _

(Leela Manohar Aeshala)

Guwahati –781 039

Acknowledgements

It is my pleasure to thank those who made this thesis possible. I recollect numerous occasions and moments, which make me proud to be a part of this world class centre of excellence. It is my privilege to be amidst some intellectual genius, who guided in my pursuit of knowledge. I owe my deepest gratitude to all of them.

First and foremost, with a deepest sense of gratitude, I wish to express my sincere thanks to my supervisor, Dr. Anil Verma whose timely help during the crucial phase of my career has made possible to achieve this target. His valuable guidance, encouragement, inspiration and creative scientific ideas have helped a lot in developing a scientific zeal in me. I am fortunate enough to have his guidance to cultivate scientific thoughts. My everlasting gratitude goes towards him.

I would like to acknowledge my sincere gratitude to all my doctoral committee members Dr. Vaibhav V. Goud, Dr. Tapas K. Mandal, and Dr. Bulu Pradhan for their intuitive review of my work, advices and suggestions. I would like to thank all faculty members of Department of Chemical Engineering of IIT Guwahati for their invaluable suggestions. I would also like to thank Prof. S.V. Naidu, who has motivated me to do the Ph.D. at the time of post-graduation. I might have missed this great opportunity without his kind support.

I express my sincere gratitude and acknowledgements to IIT Guwahati for all the facilities that were made available to me. I am thankful to Mr. Prasun Bhattacharjee of Department of Chemical Engineering, Dr. K.K. Senapati and Mr. M. Borah of Central Instruments Facility and all the non-teaching staff of Department of Chemical Engineering for their help during my Ph.D. tenure.

I extend my sincere thanks to Dr. Biraj, Dr. Lepakshi, and Dr. Avijit, Surya, and Shyam for helping me in different ways. I must acknowledge Ms. Surya Singh for her great help during the thesis writing and putting efforts to finalize the thesis in printable form. I thank my past and present lab mates; Rajmahendar, Hussain, Aanisha, Abhradip, Dhiraj, Raj, Nivedita, Vikas and Shivdeep for their invaluable cooperation, timely help, support and for creating a pleasant atmosphere in our research lab, Sustainable Environergy Electrochemical Research Group (*SEERG*). I also take the opportunity to thank all of my Ph.D. batchmates Ruhit, Giri, Sahu, Prashant, Rajashekar, Chinna,

Murali, Yadav, Satya and the other research scholars at chemical engineering department and all my IITG friends, who have shared their thoughts and views with me.

I extend my sincere thanks to my best friends Anand, Anil, Rajesh, late Sivaiah, Santhosh, Laxman, Kamal, Muni, Ramesh, and Somasekhar for their constant and unfailing support, encouragement and all the help they extended whenever required. I also wish to thank my close friends at IITG: Sushant, Rakesh, Pranjal, Amrita, Deepti for the joyful moments sharing with me at IIT and their support.

I also gratefully acknowledge the financial support of the *Department of Science and Technology* (DST), Government of India, under its *National Programme on Carbon Sequestration Research* (NPCSR), for the project (DST/IS-STAC/CO_2-SR-139/12(G).

Finally, my Ph. D. endeavour would not have been completed without the endless love, unending support, tolerance and blessings from my family. I wish to express my sincere gratitude to my parents (Pandaraiah and Late Rameshwaramma), Mother's younger sister (Balamani), brothers and sister-in-laws (Srinivasulu-Priya, Ramu-Kavitha, Mohan-Saritha), my nieces (Hamsa, Yogasri, Yogitha, Chakrika), nephews (Jhashendra, Dharanidhar), and my grandmother (Anthamma). I am also grateful to my uncles, friends (Veeru, Raj, Sunil, Sridhar, Venkatesh, Amjad) in the village and their family members for their affection and deep concern for career. They are the main soul and inspiration for each and every step that I would achieve in my life. My sincere apology goes to all those to whom I forgot to mention but helped me in any part of the research work.

(Leela Manohar Aeshala)

Abstract

Increasing CO_2 emissions and depletion of fossil fuels are two major concerns in today's society. Renewable energy sources, such as solar, wind etc. can be used as alternatives for the energy production but these are intermittent energy sources. So, the combination of CO_2 reduction with the use of renewable energy sources is an attractive way to solve the problem. The electrochemical reduction of carbon dioxide (ERC) is a technique of particular interest since it may mitigate as well as utilize the CO_2 as a carbon source for the generation of value added products including fuel. Moreover, the synthesis of fuel by the conversion of CO_2 is of special interest for the storage of renewable energy, which may be supplied to the thermodynamically unfavourable CO_2 reduction reaction.

The initial part of the study is focused on the development of electrochemical reactor and analysis of solid polymer electrolyte on direct electrochemical reduction of carbon dioxide. Cast nafion membrane and SPEEK membranes are developed and used as cationic solid polymer electrolyte, whereas alkali doped PVA/GA and Amberlyst/SPEEK composites are developed and used as anionic solid polymer electrolytes. The prepared solid polymer electrolytes are characterized under ex-situ conditions using scanning electron microscopy (SEM), thermogravimetric analysis (TGA), X-ray diffraction (XRD), Fourier transform infrared (FTIR) spectroscopy, water uptake, swelling, ion exchange capacity (IEC), ionic conductivity, and tensile strength. Once the membrane is thoroughly characterized using ex-situ methods, the membrane is used in the electrochemical reactor for the in-situ characterization to evaluate the performance of the SPE using ERC reactor.

The electrodeposited copper on porous carbon paper is used as cathode whereas Pt/C on the carbon paper is used as anode. The products formed after the electrochemical reduction of carbon dioxide is analyzed by gas chromatography. Mainly, formic acid (HCOOH), methanol (CH_3OH), formaldehyde (HCHO), carbon monoxide (CO), and methane (CH_4) are evolved as the products of the ERC apart from the undesired hydrogen gas as a by-product. In case of nafion, the maximum Faradaic efficiency of 4.52% is obtained for CH_4 at a current density of 11.1 $mA.cm^{-2}$, whereas, for SPEEK, Faradaic efficiency of 3.3% is obtained for CH_4 at a current density of 8.9 $mA{\cdot}cm^{-2}$. Primarily, CO is formed along with CH_4 and HCOOH as the minor products using the anionic SPEs (alkali doped PVA/GA and Amberlyst/SPEEK). In case of alkali doped PVA/GA, the maximum Faradaic efficiency of CO is 12% at 2 V with corresponding current density of 5.6 $mA.cm^{-2}$. Moreover, for Amberlyst/SPEEK, Faradaic efficiency of 16% is obtained for CO at 2 V with corresponding current density of 3.3 $mA.cm^{-2}$.

It is observed that anionic SPE has produced good amount of CO as a product and H_2 as by-product. However, the main objective of the study is to evaluate the role of SPE on dERC. Therefore, based on the knowledge gathered, further study is conducted. It may be noted that copper is used as an electrocatalyst and constant potential electrolysis is carried out for the direct electrochemical reduction of CO_2. However, it is observed that copper has some deactivation issues. Therefore, in the remaining part of thesis, cuprous oxide is used as an electrocatalyst along with the pulse potential electrolysis for a shorter time to avoid the effect of any kind of deactivation of electrocatalyst as well as electrolyte on the performance of the ERC system.

Thus, the further study is conducted to evaluate the influence of functional groups in cationic and anionic SPE for dERC. CMI-7000 (proton form) is used as cationic SPE and

AMI-7001 (hydroxyl ion form) is used as anionic SPE. The Cu_2O on porous carbon paper was used as cathode whereas Pt/C on the carbon paper was used as anode. Cationic and anionic SPEs are characterized ex-situ. It is observed that the ionic conductivity of CMI-7000 is twelve times higher than AMI-7001. It is due to the higher ionic size of OH^- ion than H^+ ion. In case of CMI-7000, current density increased from 2 $mA.cm^{-2}$ at 1.8 V to 4.81 $mA.cm^{-2}$ at 3 V in dERC, whereas for AMI-7001 SPE, current density increased from 3 $mA.cm^{-2}$ at 1.8 V to 6.1 $mA.cm^{-2}$ at 3 V. Mainly CH_4, C_2H_4, and CH_3OH are formed as products apart from the undesired H_2 gas as a by-product. It has been found that anionic solid electrolyte is more favorable than cationic solid electrolyte. In case of AMI-7001, Faradaic efficiency for the conversion of CO_2 into the products is more than 45% at 2.5 V and 5.4 $mA.cm^{-2}$, whereas the Faradaic efficiency for any of the products is not more than 6% using CMI-7000.

It may be noted that in earlier section, the anionic and cationic SPEs used were having different functional groups as well as different polymer backbone but the product distribution was not exactly same. However, in this section, the experimental conditions, electrode as well as the backbone of the polymer electrolyte are kept same. Thus it is found that the functional groups are important for the rate of reaction but the polymer backbone, which infact does not take part in the reaction, influences the reaction indirectly. Therefore, with this information, the idea of active reaction zone is conceptualized and thought that it would be possible to change the reaction products by changing the surroundings of the functional group, while keeping all the other parameters fixed. The further study is based on this concept.

Therefore, the electrochemical reduction of gaseous CO_2 is studied for the first time using hindered bulky quaternary ammonium ion in solid polymer matrix at room temperature

and atmospheric pressure in a developed electrochemical reactor. Some new insights are developed for the effective reaction process. It is found that the reaction zone may be tuned in a great extent with the help of fixed functional groups attached in the solid polymer. To illustrate, solid polymer electrolytes with the same backbone and different fixed functional groups are synthesized. Polyethylenimine along with alkali doped PVA/GA (PEI/PVA/KOH) is used as an anionic electrolyte. The other anionic electrolyte is synthesized by quaternizing PEI to fabricate QPEI/PVA/GA membrane. It is found that only the change in functional group of the membrane can dramatically change the efficiency and selectivity of the reaction products. Moreover, the functional group also worked as co-catalyst for the effective electrochemical reduction of gaseous CO_2. In case of PEI/PVA/KOH SPE, the current density increased from 2.42 $mA.cm^{-2}$ at 1.8 V to 5.83 $mA.cm^{-2}$ at 3 V, whereas 1.42 $mA.cm^{-2}$ at 1.8 V to 4.81 $mA.cm^{-2}$ at 3 V is obtained using QPEI/PVA/KOH. C_2H_6 is selectively formed with the QPEI/PVA/KOH apart from the CH_4, CH_3OH and CO. The maximum Faradaic efficiency of C_2H_6 is 17% using QPEI/PVA/KOH SPE at 2.25 V. The concept and the reaction pathway is extended, in which the formation of C-C coupling is proposed to be formed through 2 molecules of $:CH_{3ads}$ to generate C_2H_6. The maximum selectivity of 67.6% is obtained for C_2H_6 using QPEI/PVA/KOH.

Keywords: *Quaternized amine; Electrochemical reduction of CO_2; Functional groups; Solid polymer electrolyte; Ethane; Methane*

Contents

List of Tables

List of Figures

List of Symbols

A	area (cm^2)
E	ion exchange capacity ($meq.g^{-1}$)
F	Faraday constant ($C.mol^{-1}$)
i	current density ($mA.cm^{-2}$)
I	current (A)
l	thickness of the membrane (cm)
L	distance between the electrodes (cm)
n	number of moles of particular product (mol)
P	pressure (MPa)
Q	total charge passed during the experiment (C)
R	resistance (ohm)
V	voltage (V)
z	number of electrons involved for 1 mole of particular reaction product
E^o	equilibrium potential (V)
E_i	initial potential (V)
E_1	potential of interest (V)
V_{NaOH}	volumes of NaOH (mL)
N_{NaOH}	normality of NaOH (N)
V_{HCl}	volumes of HCl (mL)
N_{HCl}	normality of HCl (N)
W_d	weight of dry membrane (g)

W_w	weight of wet membrane (g)
σ	proton conductivity of the membrane ($S.cm^{-1}$)
L_d	length of dry membrane (cm)
L_w	length of wet membrane (cm)
λ	wavelength of the X-ray (cm)
θ	diffraction angle (°)

List of Abbreviations

AEM	anion exchange membrane
CEM	cation exchange membrane
CNT	carbon nanotube
DBE	dibromoethane
DMF	dimethylformamide
DMSO	dimethylsulfoxide
DVB	divinylbenzene
dERC	direct electrochemical reduction of CO_2
EDX	energy-dispersive X-ray spectroscopy
ERC	electrochemical reduction of CO_2
FTIR	Fourier transform infra-red
GDL	gas diffusion layer
GA	glutaraldehyde
IC	ionic conductivity
IEC	ion exchange capacity
IPN	interpenetrating polymer network
ISP	ion-solvating polymer
MEA	membrane electrode assembly
PEI	polyethyleneimine
PEEK	poly(etheretherketone)
PVA	polyvinyl alcohol
PEO	polyethylene oxide
PPy	polypyrrole
PSF	polysulfone

PTFE	poly tetra fluoro ethylene
PDDPCl	poly(1,1-dimethyl-3,5-dimethylene piperidinium chloride)
PAAm	poly(allylamine)
PDDMACl	poly(diallyl dimethyl ammonium chloride)
PDVIBr	poly(1,3-diethyl-1-vinyl imidazolium bromide)
PSEBS	polystyrene ethylenebutylenepolystyrene
PES	polyethersulfone
QPEI	quaternary polyethylenimine
SEM	scanning electron microscopy
SHE	standard hydrogen electrode
SA	silicotungstic acid
SPEEK	sulfonated poly(ether ether ketone)
SPE	solid polymer electrolyte
TEA	triethylamine
TGA	thermogravimetric analysis
TH	thiophene
TMEDA	tetramethyl ethylene diamine
XRD	X-ray diffractometer

Chapter 1

Introduction

Chapter 1

Introduction

1.1 Challenges in energy and climate change

One of the biggest challenges being faced by the scientists and technologists at present is to ensure the energy supply for future generations. The primary energy consumption was increased dramatically and reached 16.3 TW in 2012, representing a growth of around 2% against 2011 data. In 2012, increased energy consumption was the result of increase in energy consumption in emerging economies, mainly in China and India, which accounts for 77.2% and 11.4%, respectively, of the total growth (BP statistical review 2013). The consumption of energy is directly related to the socio-economical growth of the society. However, the use of fossil fuels (primary energy sources) adversely affects our environment. Presently, the dependence on fossil fuels is more than 85% (Rackley, 2009). The combustion of these fossil fuels release large amount of carbon dioxide and other green house gases in the atmosphere and exert a strong influence on the climate change. The current global warming is closely related to the use of increased primary energy consumption. Carbon dioxide is one of the main contributors to the global warming. The large increase in emissions over the past couple of decades has resulted in the substantial accumulation of CO_2 in the atmosphere. The increased amount of CO_2 in the atmosphere causes elevation in global temperature. Concentration of carbon dioxide in the atmosphere is increased by 43.3% from 280 ppm to 401.33 ppm since the industrial revolution. Increase in CO_2 concentration over the past 54 years is shown in fig. 1.1. The data have been recorded at the Mauna Loa Observatory and measurements made by Scripps Institution of Oceanography and the National Oceanic and Atmospheric

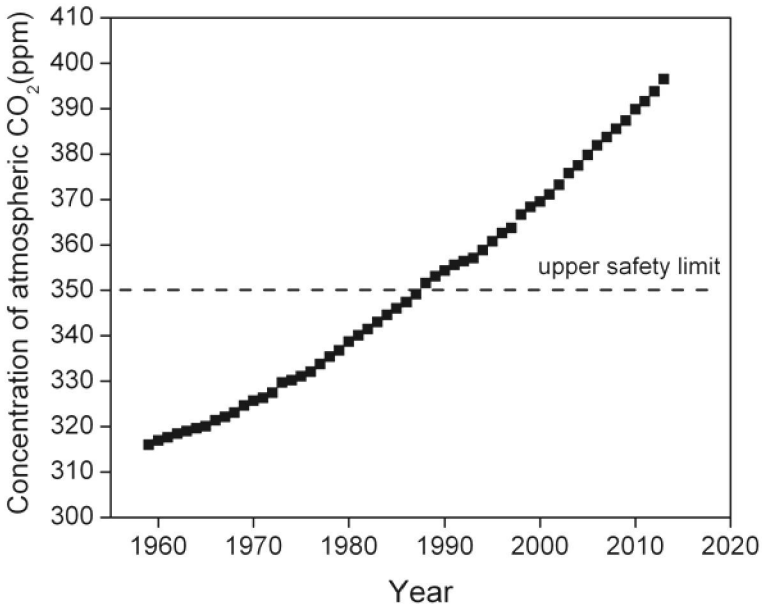

Fig. 1.1 Concentration of CO_2 in the atmosphere during 1959-2013

Administration. A horizontal line in the fig.1.1 indicates the upper safety limit for the atmospheric CO_2, which is equal to 350 ppm. CO_2 concentration has exceeded the safety limit since 1988, while the average annual increase over the 1994−2003 decade was 1.8 ppm per year, whereas the annual increase from 2004-2013 was more severe, reaching 2.09 ppm per year. The aftermath of increased CO_2 concentration poses greenhouse effects, one of the most alarming global environmental problems of today. The change in global atmospheric temperature may cause problems in many areas such as human health, agriculture, natural ecosystems, and coastal areas (Parry, 2007). To avoid severe climate change while relying on fossil fuels, almost all carbon generated from fossil fuels must be captured and sequestered. Climate change may have a significant impact on the future of the human population and the future energy mix. As fossil fuels are being depleted and/or global warming becomes severe, renewable energy (solar photovoltaic, wind, hydroelectric, geothermal, solar thermal, and biomass) and nuclear energy would become the primary energy sources. In future, many energy sources will contribute to meet future

fuel requirements, and it is anticipated that a single source will not be able to meet a large fraction of future fuel requirement. Our present technologies (energy conversion devices) are suitable for the use of hydrocarbon fuel. Therefore, to make the transition energy scheme dependent on fossil fuels to those based on renewable energies is crucial. However, the renewable energies are intermittent in nature and thus the storage of renewable energy is one of the most important steps for the energy supply chain (Armaroli and Balzani, 2011). One of the options for storing renewable energy is use of batteries. However, the energy density of such devices is considerably lower than that of the fossil fuels. Another option is to use the renewable energy to drive chemical reactions and to store the renewable energy in chemicals (reaction products) having high calorific value (Eberle and von Helmolt, 2010). There is abundant CO_2 present in the atmosphere due to various combustion processes of hydrocarbons. Thus it is conceptualized that the CO_2 along with the renewable energy sources may produce useful products (Olah et al., 2009). Therefore, the CO_2 conversion process is particularly attractive, since it can produce compounds with high energy density such as methane and alcohols. These value added products can be used as energy carriers within the existing technology (Gattrell et al., 2007).

1.2 CO_2 utilization and conversion

CO_2 may be used as a feedstock for synthetic fuels, provided that conversion is done by use of renewable energy sources such as nuclear, solar, wind, hydropower etc. Over the past several years, there has been growing interest in the capture of CO_2 emissions, and their subsequent chemical conversion to industrially relevant products.

The Sabatier and the Fischer-Tropsch processes involve the conversion of hydrogen and carbon dioxide into hydrocarbons, which can be used as fuels. Sabatier's reaction scheme

shown in eq. (1.1) involves the conversion of CO_2 and hydrogen gas into methane and water under suitable reaction conditions.

$$\text{Sabatier Reaction:} \quad CO_2 + 4H_2 \xrightarrow[300\text{-}400\ ^oC]{Ni} CH_4 + 2H_2O \tag{1.1}$$

The Fischer-Tropsch process involves two steps and can also be seen as an alternative process for fuel generation. The first step shown in eq.1.2 is the partial oxidation of coal or natural gas into hydrogen gas and carbon monoxide. In the second step shown in eq.1.3 is the conversion of synthesis gas (carbon monoxide and hydrogen) into more useful hydrocarbon fuels.

$$2C + 1/2\,O_2 + 2H_2O \xrightarrow[1073\ ^oC]{Fe} 2CO + 4H_2 \tag{1.2}$$

$$2nH_2 + nCO \xrightarrow[150\text{-}300\ ^oC]{Fe} C_nH_{2n} + nH_2O \tag{1.3}$$

A large number of processes, such as photochemical, biochemical, electrochemical etc., is being studied to generate hydrocarbons by utilizing CO_2. Many of these methods need high temperature and/or high pressure but result in low product yields. Therefore, in recent years, the research on the electrochemical method is taking momentum due to various advantages over other techniques such as the reaction can be performed at atmospheric temperature and pressure. The next section provides the details of the electrochemical reduction of CO_2.

1.3 Electrochemical reduction of CO_2

The electrochemical approach allows mimicking the process occurring in plants in which CO_2 and H_2O are converted into useful products using solar energy. However, in electrochemical process, the energy to reduce CO_2 is derived from renewable energy

conversion device such as photovoltaic panel, to convert CO_2 and H_2O to hydrocarbons and oxygen gas. When the energy used for electroreduction of CO_2 is generated from renewable sources, the process may be referred as artificial photosynthesis (Wilcox, 2012), since it involves the conversion of solar energy to carbon based fuels. Carbon dioxide is a very stable molecule and significant amount of energy is needed to reduce carbon dioxide into useful products. It has been reported that formation of carbon dioxide anion radical ($CO_2^{\bullet-}$) is the rate determining step in the reduction of CO_2. The electrical potential for $CO_2/CO_2^{\bullet-}$ is -1.9V vs. SHE through single electron pathway. However, the requirement of this much high energy may be reduced by proton assisted multi-electron reduction process of CO_2 (Kobayashi and Tanaka, 2014). The energy requirements are critical for the technological development of the process. A brief introduction of the electrochemical principle, for the electrochemical reduction of CO_2 (ERC) is given below.

There are two types of electrochemical cell; one is galvanic cell in which chemical energy of a fuel is directly converted into electrical energy with spontaneous reactions. Second one is electrolytic cell in which electrical energy is required to convert the reactants into products (chemical), that is non-spontaneous reactions take place. The schematic of an electrochemical reactor (electrolytic cell) for conversion of CO_2 into products is shown in fig.1.2. As can be seen in the fig.1.2 that the electrochemical cell consists of two electrodes (anode and cathode), an electrolyte and flow fields for the transport of reactants to the reaction site and removal of the products from the cell. Renewable energy may be used for the reduction of carbon dioxide at cathode along with the oxidation of water at anode. Equation 1.4 shows the electrochemical reaction in which water is oxidized by applying 1.23 V of electrical voltage. Water splits into oxygen, protons and electrons. The anode provides a pathway through which free electrons are conducted via

an external circuit to the cathode. Reduction reaction of CO_2 takes place at the cathode as per eq.1.5. The electrons received by the cathode along with the protons, which are transported to cathode from the anode through electrolyte, react with the CO_2 and form reaction product, e.g. CH_4 as shown in eq. 1.5. The electrolyte acts as the separator between carbon dioxide and water to prevent mixing and completes the electrical circuit by transporting protons from the anode side to the cathode side. The overall reaction in which the carbon dioxide and the water combine to produce products and oxygen is shown in eq.1.6.

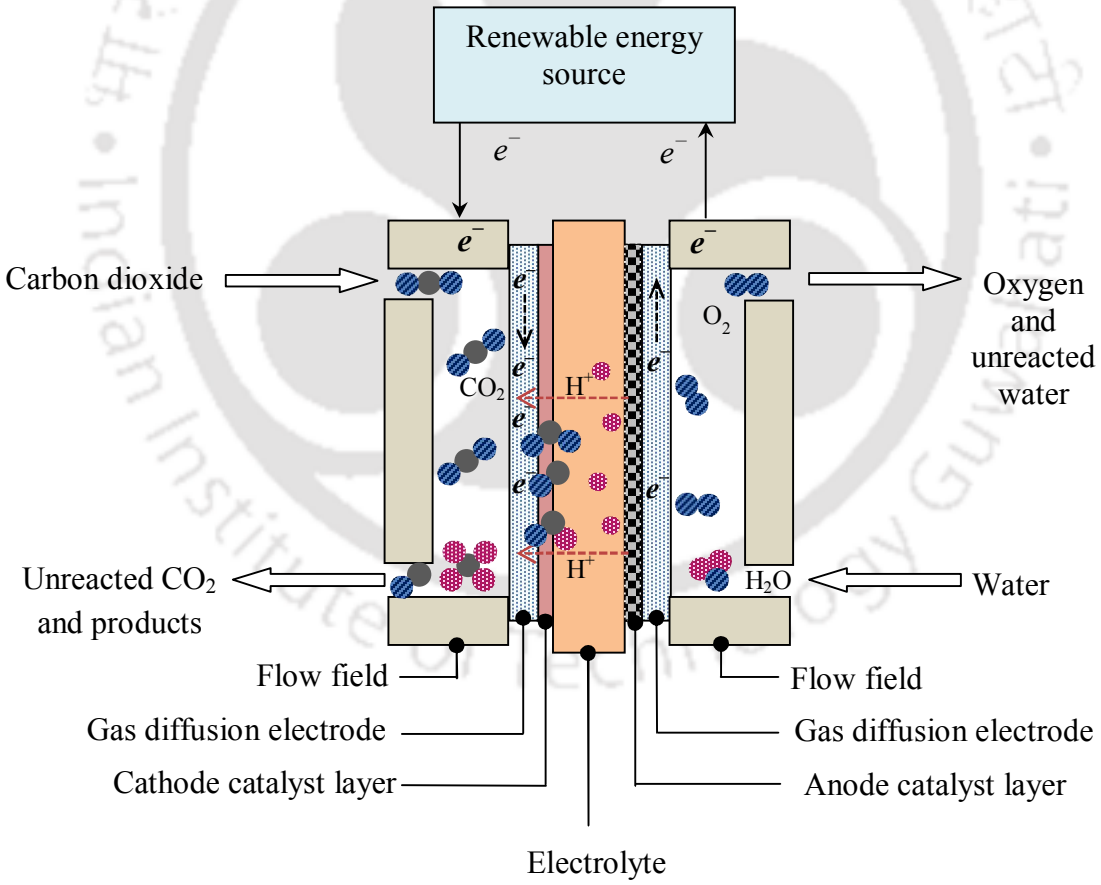

Fig. 1.2 Schematic of an electrochemical reactor for electrochemical reduction of CO_2

Anode reaction : $2H_2O \rightarrow O_2 + 4H^+ + 4e^-$ $E^o = -1.23$ V (1.4)

Cathode reaction : $CO_2 + 8H^+ + 8e^- \rightarrow CH_4 + 2H_2O$ $E^o = +0.17$ V (1.5)

Overall reaction : $CO_2 + 2H_2O \rightarrow CH_4 + 2O_2$ $E^o = -1.06$ V (1.6)

It may be noted that the particular reaction scheme in eq. 1.5 is slightly feasible cathodic reaction, whereas most of the energy is used for the anodic reaction. At a pressure of 1 bar and a temperature of 25°C, the electrical potential required to convert one mole of CO_2 to generate one mole of methane is -1.06 V. The change in Gibbs free energy of the overall reaction, towards the formation of methane from reduction of CO_2 is around 818 $kJ \cdot mol^{-1}$.

In recent years, electrochemical reduction of CO_2 has attracted great attention due to its several advantages. Using ERC process, it is possible to

- reduce the CO_2 concentration from the atmosphere,
- generate fuel/hydrocarbons, in particular CH_4, C_2H_4, C_2H_6, and CH_3OH etc.,
- store renewable energy (e.g., solar energy) in the form of liquid or gaseous reaction product(s), if renewable energy is used as the energy source,
- carry out the reactions at room temperature and pressure,
- minimize the chemical consumption, which may simply be water or wastewater for the proton source along with CO_2, and
- scale-up the electrochemical reactor easily.

However, ERC has several challenges that need attention. Some of the major challenges to overcome the successful technological improvement are to

- reduce hydrogen evolution during the reaction, which takes place while using aqueous electrolyte for the proton availability to perform the reaction,

- reduce the individual half-cell overpotentials of the reactions,
- increase the transport of CO_2 to the reaction site,
- effectively reduce gas phase CO_2,
- reduce catalyst poisoning,
- increase the selectivity of a particular product or increase the current efficiency,
- effectively remove the products from the catalyst layer to avoid the blocking of catalyst active site,
- increase energy efficiency by enhancing the Faradaic efficiency and low overpotential of reactions, and
- analyse and separate the reaction products.

To tackle these problems, it is very important to suppress the hydrogen evolution because the applied energy is used for hydrogen evolution instead of required reduction of CO_2, increase the CO_2 availability at the reaction site and the reduction of CO_2 in the gaseous phase for easy separation of products along with other challenges.

Over the last several decades, the research is being focused especially on electrode materials and it is reported that electrodes play significant role on the electrochemical reduction of CO_2. It is studied and reported that not only the electrode, electrolyte also plays a critical role for effective ERC (Hori et al., 1989; Innocent et al., 2009). There are three different types of electrolytes for ERC viz. aqueous, non-aqueous, and solid electrolyte.

The electrochemical reduction of carbon dioxide in aqueous solutions has been reported by many authors (Alvarez-Guerra et al., 2012; Goncalves et al., 2010; Oloman and Li, 2008; Zhang et al., 2014). The difficulty in ERC appears to be of high overvoltage and low current efficiency. However, the overvoltage and current efficiency depend upon

properties of electrolytic solutions as well as electrodes. Aqueous electrolytic solutions are classified into acidic, neutral, and alkaline depending on the pH value. Acidic solutions have abundant proton availability and may be useful in reduction of CO_2. However, at the same time the protons availability enhances the undesired hydrogen evolution at the cathode. Generation of hydrogen from the reduction of H_2O needs large potential in alkaline solutions.

Therefore, most of the ERC studies are carried out in near neutral aqueous electrolyte solutions, which have the pH range between 7 and 9 (Innocent et al., 2009; Li and Oloman, 2005). Carbon dioxide gets solubilize in the electrolyte solution and exists predominantly in the form of bicarbonate ion. In one hand the poisoning species formation is accelerated at high pH, on the other hand high concentration of CO_2 cannot be maintained in acidic solutions. Due to this reason, neutral and near alkaline solutions may be the best alternatives for reduction of CO_2.

Non-aqueous solvents have been used by many of the workers for the electroreduction of CO_2, because of their ability to solubilize CO_2 to a much greater extent than in aqueous solvents. DMSO can solubilize upto 20 times more CO_2 than corresponding aqueous solutions, such as $KHCO_3$. CO_2 in propylene carbonate is 8 times more soluble and in methanol 5 times more soluble. It has been found that carbon monoxide, oxalic acid, and formic acid were the main products from CO_2 in organic solvents such as propylene carbonate and dimethyl formamide (Ikeda et al., 1987). Faradaic efficiencies of the products from CO_2 in the methanol were better than those obtained in water. Kaneco et al. worked at low temperature (248-290K) because the solubility of CO_2 in methanol strongly depends on temperature and the competitive hydrogen formation diminishes at low temperature (Kaneco et al., 2003; Kaneco et al., 1999).

Moreover, the aqueous and non-aqueous electrolytes have many disadvantages such as high ohmic loss, possibility of leakage from the reactor, increased hydrogen evolution, and mass transfer limitation of the solubilized CO_2 from bulk electrolyte to electrode surface. To overcome the problems associated with the aqueous and non-aqueous electrolyte, solid polymer electrolyte (SPE) may be used.

The next chapter presents the research and development status of the solid polymer electrolyte in the application of electrochemical reduction of CO_2.

Chapter 2

Literature Review

Chapter 2

Literature Review

The issues related to use of liquid electrolyte have been discussed in the previous chapter. The use of solid polymer electrolyte may address the issues. Therefore, extensive research and development efforts are needed to develop the solid polymer electrolytes in order to improve the performance. This chapter provides an extensive literature survey with emphasis on recent advancements in the development of solid polymer electrolytes for electrochemical reduction of CO_2.

Solid polymer electrolyte (SPE) for electrochemical reduction of CO_2 (ERC) is expected to meet the various primary requirements. It should have high ionic conductivity, good thermal stability, and high tensile strength. Additionally, the solid polymer electrolyte is expected to possess,

(i) excellent electrochemical stability,

(ii) substantial morphological and dimensional stability,

(iii) outstanding mechanical properties,

(iv) sufficient water uptake and moderate swelling,

(v) suppressed water transport through diffusion and electro-osmosis,

(vi) easy fabrication to form the membrane electrode assembly, and finally, more important from a practical point of view,

(vii) competitive low-cost and sufficient long-term durability (Zhang et al., 2009).

It would be helpful to discuss the use of electrolyte in ERC before discussing the SPE. Table 2.1 shows the use of various electrolytes along with electrocatalysts, operating

conditions, and the formed products. It can be seen that product distribution varies with the electrode, electrolyte composition, and the operating conditions. Most of the research work was done in aqueous bicarbonate solutions using Pb, Sn, and In electrodes. In many of the situations the pressure in the ERC system was increased to improve the performance. It can be seen that in most of the cases the formate/formic acid was one of the products. Formic acid can be easily formed from CO_2 by the addition of two hydrogen atoms and there is no need to break the bond between C-O in CO_2. However, formation of hydrocarbons from CO_2 is relatively a challenging task. It may also be noted that (table 2.1) copper or its derivative are unique electrocatalysts for the ERC, especially for the formation of hydrocarbons (Goncalves et al., 2010; Yano et al., 2004; Aydin and Koleli, 2004; Lee and Tak, 2001).

Electrochemical reduction of CO_2 on copper electrode was studied in potassium bicarbonate solutions by many groups (Murata and Hori, 1991; Azuma et al., 1990; Kyriacou and Anagnostopoulos, 1993; Hori et al., 1986, 1989; Yano and Yamasaki, 2008; Hara et al., 1985; Kaneco et al., 2003). Murata and Hori, (1991) studied the effect of bicarbonate electrolyte concentration on the reduction of carbon dioxide and showed that ethylene formation became favorable with the decreased HCO_3^- concentration. Methane to ethylene ratio significantly decreased with the decreased HCO_3^- concentration or increased pH at the electrode surface. They observed that methane to ethylene ratio was not varying in a great extent in KCl solutions as compared to bicarbonate solutions. It was reported that methane to ethylene ratios were low since pH values at the electrode were much higher in KCl solutions compared to bicarbonate solutions. Lee et al., (1999) investigated the electrochemical reduction of CO_2 using Cu/PTFE-bonded gas diffusion electrode (GDE) in different $KHCO_3$ electrolyte concentrations.

Table 2.1 Studies on electroreduction of carbon dioxide during 2004-2014

Electrolyte	Electrode	Experimental parameters	Main products (Faradaic efficiency, %)	Reference
$NaHCO_3$	Tin oxide/graphene	10 $mA.cm^{-2}$	Formate (93)	Zhang et al., (2014)
$KHCO_3$	Sn	1 atm, 25°C, pH = 6.98,	Formate (91)	Lv et al., (2014)
$NaHCO_3$	Sn-GDE	27 $mA.cm^{-2}$, pH = 8.3, 25°C	Formate (70)	Prakash et al., (2013)
TBATFB in DMF	Cu based MOF	-2.5V vs Ag/AgCl	Oxalic acid (51)	Senthil et al., (2012)
0.45M $KHCO_3$+KCl	Pb	10.5 $mA.cm^{-2}$, 1 atm, 25°C	Formate (57)	Alvarez-Guerra et al., (2012)
$KHCO_3$	Electrodeposited Cu_2O	25 °C, pH = 7.6	CH_3OH (38)	Le et al., (2011)
$NaHCO_3$	Indium	pH = 8, 40 $mA.cm^{-2}$	Formate (45)	Narayanan et al., (2011)
$KHCO_3$	Copper mesh	1 atm, 25 °C	CH_4 (19.4), C_2H_4 (18.7)	Gonçalves et al., (2010)
KOH/methanol	Cu_2O/Zn disk	243K, pH = 7.5	CH_4 (7.5), C_2H_4 (6.8)	Ohya et al., (2009)
NaOH	Lead	2.5 $mA.cm^{-2}$, 21 °C, pH = 8.5,	Formate (70)	Innocent et al., (2009)
$KHCO_3$	Cu plate/Cu_2O	1 atm, 25 °C,	C_2H_4 (22) / C_2H_4 (28)	Yano and Yamasaki, (2008)
0.5 M $KHCO_3$ + 2 M KCl	Granulated Sn	60 $mA.cm^{-2}$, pH = 7.5, 291 K, 101 kPa	Formate (91)	Li and Oloman, (2007)
0.45 M $KHCO_3$ + 1 M KCl	Tin coated cu mesh	130 $mA.cm^{-2}$, 141 kPa, 299 K	Formate (86)	Li and Oloman, (2006)
0.45M $KHCO_3$	Cu	22 $mA.cm^{-2}$, 298 K	Formate (86)	Hori et al., (2005)
Methanol/$LiClO_4$	Polypyrrole (PPy)	20 bar	HCOOH (40.5) CH_3COOH (62.2)	Aydin and Koleli, (2004)
K_2CO_3	Pb-granules	1.5 $mA.cm^{-2}$, 50 bar, 80°C,	HCOOH (94)	Koleli et al., (2004)
3M KBr	CuBr confined Cu mesh	46.1 $mA.cm^{-2}$, pH = 3,	C_2H_4 (80) ; H_2 (9)	Yano et al., (2004)

It was shown that methane to ethylene ratio tends to have smaller value in a higher concentration of hydrogen carbonate solution when pH becomes higher on the electrode. It was found that methane formation tends to increase in the order of Cs^+, Rb^+, K^+, Na^+, and Li^+, identical to the decreasing order of cationic size. A high Faradaic efficiency of methane was observed in methanol with $LiClO_4$ and $NaClO_4$ supporting salts. Ethylene formation was found to be higher in the methanol with KOH supporting salt. Hydrogen formation decreased with a decreased cationic size in contrast to the aqueous solutions.

Terunuma et al., (1997) studied the relationship between the production of hydrocarbons and characteristics of copper electrode by conducting various pretreatment methods on copper. The copper metal surface was easily contaminated with organic compounds due to its high affinity for adsorbed oxygen. Copper oxide surface has much higher activity for hydrocarbon production along with much higher activity for reduction of protons than the Cu electrocatalyst. It was found that the Cu surface was responsible for the physical adsorption of carbon dioxide and forms carbon monoxide initially. The heat of adsorption of carbon monoxide on Cu_2O was larger than that on metallic copper. So the Cu_2O surface was more favorable for the adsorption of carbon monoxide than on the Cu surface. Recently, experiments on copper (I) halide compounds showed significant improvement in hydrocarbon production (Ogura et al., 2003; Yano et al., 2004). Cu(I) halides not only adsorb the CO stronger than Cu, but also help in the formation of intermediate compound CH_{2ad}, thus enhancing the formation of ethylene. Kim et al., (1988) studied the ERC on Cu foils in 0.5M $KHCO_3$ solution and found methane as a primary product. The highest methane formation rates were observed at 22°C and 0°C. It was reported that polished copper surface results in high methane formation rates.

The electrocatalytic activity of Cu electrode in the electrochemical reduction of carbon dioxide was investigated by Lee and Tak, (2001). They reported that in constant potential mode the degradation of the catalytic activity of Cu was due to the adsorption of amorphous carbon on the Cu substrate and thus the efficiency of hydrocarbons was decreased. They used the potential modulation method and reported the change of the surface structure of copper. This structural change reportedly helped to obtain the constant production rate of methane in long term electrolysis.

Ikeda et al., (1995) employed Cu-loaded gas diffusion electrodes for reduction of CO_2. The products were found to be CH_4, C_2H_4, C_2H_5OH, CO, and $HCOO^-$, but the current efficiencies achieved for gas diffusion electrodes were higher for two orders of magnitude than that for Cu-plate electrodes. Goncalves et al., (2010) reported that presence of Cu electrodeposits on the cathode surface promotes the ethylene formation selectively from reduction of CO_2. Increasing the surface area of Cu electrodeposits, ethylene formation dominates over the methane with an increased Faradaic efficiency from 18.7% to 33%. Hara et al., (1997) studied the reverse arrangement by placing the Pt catalyst layer towards the gas phase CO_2 for getting high Faradaic efficiency of methane (38.8%). They observed that Faradaic efficiency of methane was increased with increase in pressure upto 20 atm and yield was increased by pretreatment of electrode with hydrogen. The investigation on surface oxidized copper electrodes in CO_2 saturated KCl solution was done by Keerthiga et al., (2012). They observed that ethane was formed selectively on surface oxidized copper electrode with low amounts of methane as compared to Cu electrode, where methane formation was prevalent. Christophe et al., (2012) studied the activity of copper single crystal in phosphate buffer solutions in ERC. They reported that methane Faradaic efficiency was increased in the order of Cu (poly) < Cu (100) < Cu (111).

Chang et al., (2009) investigated the ERC by Cu_2O catalyzed carbon clothes and observed methanol as the only major product. It indicates that the Cu(I) species play an important role in the formation of methanol. Le et al., (2011) studied the ERC on three different oxidized copper electrodes viz. air oxidized copper foil, anodized copper foil and electrodeposited Cu_2O thin films. The highest methanol yield was 43 $\mu mol.cm^{-2}.h^{-1}$ and Faradaic efficiency of 38% was obtained at electrodeposited copper oxide thin films rather than anodized or oxidized copper foil. Cu(I) species improved the stability of intermediates and altered the selectivity towards CH_3OH by enabling hydrogenation of oxygen atoms from H_3CO adsorbates.

Most of the notable work has been done on the copper or copper derived electrodes, but significant improvement is still needed in the Faradaic efficiency of hydrocarbons in ERC. Hydrogen evolution was the major problem in the ERC. To overcome these problems, solid polymer electrolyte approach has been introduced in the ERC. However, the success achieved so far is limited and various new electrolytes are being investigated to meet the objectives. We have divided the literature on solid polymer electrolytes into cation exchange membrane (CEM) and anion exchange membrane (AEM). The following sections will address the SPE used in the application of ERC.

2.1 Cation exchange membrane (CEM)

2.1.1 Perfluorinated membrane

The most commonly used perfluorinated polymer is Nafion® produced by DuPont. Similar polymers are Flemion® and Aciplex-S® produced by Asahi Glass and Asahi Chemical, respectively. Among the three major types, the DuPont product is considered to be superior because of its high proton conductivity, good chemical stability and

mechanical strength (Motupally et al., 2000). Two current research areas of interest in nafion are the transport phenomena within the membrane and modifications made to the membrane to increase its performance for any specific application. Several efforts have been made to improve performance of nafion and to ascertain water retention at higher temperatures. The performance of nafion-117 membrane has been improved by equilibrating with phosphoric acid (Wasmus et al., 2000). A significant improvement in the conductivity of nafion, at elevated temperatures, by incorporating perfluorinated ionomers in nafion matrix and by doping it with heteropolyacids such as phosphotungstic acid, phosphomolybdenic acid, phosphoric acid in nafion was targeted and achieved (Bahar et al., 1996). A similar attempt to attain improved ionic conductivity with the incorporation of silicotungstic acid (SA) and thiophene (TH) in nafion-117 membrane was made by Tazi and Savadogo (2001). Water uptake in the nafion incorporated with SA was 60% and with both SA and TH it was 40% compared to the normal value of 27% for nafion-117. It is clear that nafion and related polymers are still being intensely examined in view of the complex electrochemical cell requirements of high proton conductivity and outstanding chemical stability combined with longevity of 60,000 h at 80ºC.

Various studies on the electrochemical reduction of carbon dioxide using solid polymer electrolyte are shown in Table 2.2. Nafion as a cation exchange SPE used in most of the studies (Narayanan et al., 2011; Subramanian et al., 2007). Narayanan et al., (2011) studied the continuous ERC to formate ion in a polymer electrolyte membrane cell. Nafion-115 membrane was treated with NaOH to exchange the protons with sodium ions in the membrane. The Faradaic efficiency of formate ion production was 80% and hydrogen evolution was suppressed with lead and indium as catalysts. It was reported that Faradaic efficiency was strongly dependent on the concentrations of carbon dioxide, bicarbonate, and carbonate at the surface of the electrodes. It was also observed that mass

Table 2.2 Electrochemical reduction of CO_2 having SPE in the electrochemical reactor

SPE	Cathode feed	Electrode	Experimental parameters (conditions)	Main products (Faradaic efficiency, %)	Reference
Nafion-115	$NaHCO_3$ (1M) + CO_2	In	Continuous electrolysis, 1 atm, 25°C	Formate (15-80)	Narayanan et al., (2011)
Nafion-115	$NaHCO_3$ (1M) + CO_2	In	Pulse electrolysis, 1 atm, 25°C	Formate (45-50)	Narayanan et al., (2011)
Nafion-423	NaOH (0.5M) + CO_2	Pb	2.5 $mA.cm^{-2}$, 1 atm, 25°C	Formate (90)	Innocent et al., (2009)
Nafion+buffer layer	Humidified CO_2	Ag	20 $mA.cm^{-2}$, 1 atm, 25°C	CO (82)	Delacourt et al., (2008)
Nafion-430	K_2HPO_4+ H_3PO_4+ CO_2	Pb	298 K, pH = 7, 2 $mA.cm^{-2}$	Formate (93)	Subramanian et al., (2007)
Nafion-117	CO_2 + $KHCO_3$ (0.45M)	Sn-Cu mesh	298 K, 0.2-1.2 bar, pH 7-8	Formate (36-91)	Li and Oloman, (2007)
Nafion-117	K_2HPO_4+ H_3PO_4+ CO_2	In	pH=6, 15°C, 2 $mA.cm^{-2}$	HCOOH (100)	Akahori et al., (2004)
Nafion-117	CO_2	Cu	10-30 $mA.cm^{-2}$	C_2H_4, C_2H_6	Cook et al., (1988)
Nafion-117	CO_2	Cu	1 atm., 25°C	CH_4 (19), C_2H_4 (27)	Komatsu et al., (1995)
Selemion AMV	CO_2	Cu	1 atm., 25°C	HCOOH (15), CO (10)	Komatsu et al., (1995)
SF-17	CO_2	Au	10 $mA.cm^{-2}$, 5 atm	CO (90)	Nishimura et al., (1995)

transport limitations can be mitigated and high efficiencies can be realized by conducting the electrolysis in pulse mode. Subramanian et al., (2007) developed an electrochemical reactor using a perfluoro polymer CEM (nafion-961 and nafion-430) as a separator between anode and cathode chambers for the electroreduction of dissolved carbon dioxide under ambient conditions to formate ion. The flow reactor enhanced the mass transfer of carbon dioxide compared to the batch reactor and maximum current efficiency of 93% for formate ion formation was obtained. Akahori et al., (2004) reported a cell using a nafion membrane to separate a lead cathode and carbon fiber anode. In this design, CO_2 saturated buffer solution (0.2M K_2HPO_4 + H_3PO_4; pH 6) flowed over the cathode and a solution with sulfite ions was used on the anode. The oxidation of sulfite ions instead of producing oxygen lowered the total cell potential. They also described process by which both the CO_2 and sulfite could be absorbed from flue gases. The main products were formate ion and small amounts of CO, but exact amounts were not reported. Current densities of 3 $mA.cm^{-2}$ were hardly obtained.

Some of the most notable work on the reactors for CO_2 reduction has been done by Li and Oloman who have published several papers on their design of a continuous reactor for the production of formate ion (Li and Oloman, 2005, 2006, 2007). Their design uses 2-phase (gas and liquid) flow through a 3-D cathode of tinned copper mesh or tin granuels, with a nafion-117 membrane as separator. In the work limited study over several parameters such as temperature, catholyte species, CO_2 pressure, and other reactor parameters was also made. They also achieved high efficiencies (63-91%) and high current densities (60-310 $mA.cm^{-2}$).

Gas phase electrochemical reduction of CO_2 was investigated using metal deposited SPE (Dewulf and Bard, 1988; Komatsu et al., 1995; MacHunda et al., 2010). Dewulf et al.,

(1988), and Cook et al., (1988) investigated the nafion as a cation exchange SPE coated with Cu using electroless plating. C_2H_4 was obtained during the ERC as the major product. Komatsu et al., (1995) fabricated Cu-nafion electrode by an electroless plating method by combination of Cu-Rochelle salt as the plating agent and 10% $NaBH_4$ as the reducing agent. With the electrodes made of cation exchange membrane (nafion) as SPE materials, the total current efficiencies for reduction product of CO_2 had maximum values of 19% for CH_4 and 27% for C_2H_4. Mainly hydrocarbons were observed as CO_2 reduction products but at lower yields. Formate ions were produced with good Faradaic efficiency and current density by the use of alkali metal hydroxides at anolyte side than water in the electrochemical reactor. Machunda et al., (2010) carried out electrochemical reduction of gas phase CO_2 using SPE membrane on electrodeposited Pb on GDE. The maximum Faradaic efficiency reached was 65% for formic acid and structural change provided high surface area and increased current density during the initial stage of reduction. Delacourt et al., (2008) developed an electrolysis-cell design for the electrochemical reduction of CO_2 and H_2O to make syngas ($CO+H_2$) at room temperature. They represented several cell designs based on polymer exchange membranes. The most effective design had a modified configuration with a buffer layer of $KHCO_3$ between the cathode and the nafion membrane. This allowed much greater efficiency for reduction of CO_2 to CO. With this design they achieved a CO/H_2 ratio of 1/2 (for methanol synthesis) at -1.8 V NHE with a current density of 80 $mA.cm^{-2}$ (Delacourt et al., 2008). Recently, breakthrough research has done by converting gas phase conversion of carbon dioxide to liquid carbon chain hydrocarbons ($>C_5$) at room temperature and ambient pressure using Pt nanoparticles on carbon based electrode used as catalyst and nafion membrane as an electrolyte (Centi et al., 2007).

Gangeri et al., (2009) reported the conversion of CO_2 to 18 electron reduction product, isopropanol, using Fe/CNT and Pt/CNT electrocatalysts. It is noticeable that reactions were carried out at 60^oC, which was contrary to the usual belief that CO_2 reduction performs well at low temperature conditions. However, there is difference in the activity of the two electrocatalyst used. Fe/CNT is able to give good productivity, mainly isopropanol, plus minor amounts of other lighter alcohols or acetone. However, it deactivates faster, due to the crossover of the electrolyte, particularly of K^+ ions, as confirmed by SEM-EDX study. On the other hand, Pt/CNT retained its electrocatalytic activity in a better way but it showed lesser productivity as compared to Fe/CNT. Over all, the research lightens up the path of CO_2 reduction by enabling its reduction to higher alcohols.

Kuhl et al., (2012) reported the new insights into the electrochemical reduction of CO_2 on a metallic copper surface. They studied reduction of CO_2 on copper in $KHCO_3$ electrolyte across a range of potentials and observed a total of 16 different CO_2 reduction products. The products with the larger current efficiencies were the hydrocarbons such as methane, ethylene, while the remaining 14 products were oxygenates, 11 of which were C_2 and C_3 products. They suggested that intermediate species formed on the electrode surface through a series of dehydroxylation steps, influenced the reaction rate and selectivity for products (ethane and other higher hydrocarbons).

Till date, perfluoro membranes (eg. nafion) are the only SPEs used by the most of the researchers in the application of ERC. A few authors studied the electrochemical cell configuration based on the solid polymer electrolytes in the application of ERC. Even then perfluoro membranes were used for the ERC, hydrogen evolution reaction was significantly higher as compared to the hydrocarbon products of ERC. To reduce the

hydrogen evolution, researchers treated the nafion membrane with sodium/potassium based aqueous electrolytes to exchange the protons with sodium/potassium ions respectively (Li and Oloman, 2005; Narayanan et al., 2011). However, the performance could not be improved significantly.

A few of the researchers studied the ERC using anion exchange membranes. Narayanan et al., (2011) reported that both cationic and anionic exchange SPEs performed equally in the ERC. They have used the aqueous electrolytes at the cathode in the electrochemical cell configurations. The following section shows the relevant literature survey on anion exchange membrane especially membrane preparation. It may be noted that hardly any literature discuss about the role of anion exchange membrane in electrochemical reduction of carbon dioxide.

2.2 Anion exchange membranes (AEM)

AEMs can be divided according to their structure and preparation procedure, which can be classified into three categories: heterogeneous membranes, interpenetrating polymer networks, and homogeneous membranes (Agel et al., 2001). Table 2.3 gives an overview of AEMs and some of the important properties.

2.2.1 Heterogeneous membranes

A heterogeneous membrane is an anion exchange material embedded in an inert compound. In turn, this category of membrane is divided according to the nature of the inert compound. If the compound is a salt, the membrane is an ion solvating polymer; if it is an inorganic segment, the membrane is called hybrid membrane. Ion-solvating polymer (ISP) complexes are based on polyethylene oxide (PEO) polymers, discovered forty years ago by Armand et al., (1979) and Fenton et al., (1973).

Table 2.3 Properties of a few important anion exchange membranes

	Anion exchange membranes	IEC ($meq.g^{-1}$)	Temperature (^oC)	IC ($mS.cm^{-1}$)	References
1A:	**Heterogeneous Membranes (Ion-solvating polymers)**				
	PVA/KOH	0.95	20-25	47	Yang et al., (2002)
	PVA/PEch/KOH	0.86	20-25	20	Yang et al., (2003)
	PVA/TEAC/KOH	0.82-0.99	25	23.1	Yang et al., (2005)
	PVA/KOH	-na-	20-25	1	Lewandowski et al., (2000)
1B:	**Interpenetrating polymer networks**				
	PVA/PEI cross-linked DBE	0.6-0.7	-na-	-na-	Lebrun et al., (2002)
	PVA/poly(1,3-diethyl-1-vinylimidazolium bromide)	1.1	-na-	-na-	Lebrun et al., (2004)
	PVA/PAAm cross-linked	4.9	-na-	-na-	Nishimura et al., (2008)
	PVA-poly(acrylonitrile-co-2-dimethylaminoethyl methacrylate)	1	20-25	3.45	Kumar et al., (2010)
1C:	**Homogeneous membranes**				
	PCMS/DVB/benzyltrialkylammonium	0.83-2.38	-na-	-na-	Huda et al., (1998)
	PSEBS/TEA	-na-	20-25	0.69-1	Vinodh et al., (2010)
	Tetramethylethylenediammonium PSU	-na-	95	73	Wang et al., (2009a)

Note: "-na" - Not Available

Ion-solvating polymers consist of a matrix, which is a water soluble polymer, a hydroxide salt and sometimes one or more plasticizers. These combinations have the mechanical properties of the polymer and the electrochemical and conductive properties of the alkaline salt. The polymer contains electronegative heteroatoms such as oxygen, nitrogen, or sulfur, which interact with the cations of the salt by a donor–acceptor link. Ionic conduction within the structure is based on these heteroatom-cation interactions, and on the mobility of amorphous polymer chains (Armand et al., 1979). Mechanical studies of ion transport in polymer electrolytes have demonstrated that the ionic conductivity is enabled by segmental motion of the polymer hosts and the binding energy between cations and anions (Druger et al., 1985; Minier et al., 1984).

Other work on ion-solvating polymers focused on polyvinyl alcohol (PVA) which shows good properties such as chemical stability and hydrophilicity (Mohamad et al., 2002; Mohamad et al., 2003; Palacios et al., 2003; Sang et al., 2008; Vargas et al., 2004; Yang et al., 2005). PVA has high hydrophilicity due to the presence of hydroxyl group pendant on the backbone, which can interact very strongly with water. Lewandowski et al., (2000) studied this system and found that the ionic conductivity of the PVA/KOH polymer electrolyte was around 1 $mS.cm^{-1}$ at room temperature, as the ionic conductivity is highly dependent of the proportions of KOH and water in the membrane (Lewandowski et al., 2000). Yang and Lin, (2002) developed this alkaline polymer electrolyte by increasing the quantities of KOH and water in the PVA matrix. They measured ionic conductivity of their ion-solvating polymer and found it to be in the order of 47 $mS.cm^{-1}$ at room temperature (Yang and Lin, 2002).

The disadvantage of PVA is that the polymer electrolyte is damaged when higher amounts of KOH (up to 4M) are introduced. In order to obtain membranes that exhibit a much higher conductivity, some research is focused on PVA blends to decrease the crystalline phase to the benefit of the amorphous region (Yang et al., 2003). Since the initial discovery of Armand et al., (1979) there has been a growing interest in ion-solvating polymers and considerable effort has been made to develop new types of polymer electrolytes (Table 2.3). Most of the investigations have enhanced the ionic conductivity to about 10 $mS.cm^{-1}$. Further improvements can be made, such as decreasing the thickness of the membrane without decreasing its physical strength. However, the stability of this material is very low due to the presence of KOH within the matrix. Moreover, the ionic conductivity decreases continuously due to the leaking out of KOH. In reality, this leads to the same problems as found with liquid electrolyte such as blocking of the gas diffusion electrodes. It is clear that dramatically new approaches are required to hold the KOH inside the matrix.

2.2.2 Interpenetrating polymer

An interpenetrating polymer network (IPN) is a combination of two polymers in network form of which at least one is synthesized and/or cross-linked in the presence of the other without any covalent bonds between them. These polymers are closely related to other multi-component materials containing completely entangled chains, such as polymer blends, grafts and blocks. However, the IPN can swell in solvents, without being dissolved, and creep and flow are suppressed. Most IPNs are heterogeneous systems. They possess an excellent combination of electrochemical and mechanical properties. They are composed of a hydrophobic polymer that has good thermal, chemical and mechanical properties, and a conductive polymer to transport anions. IPN materials have

drawn great interest because of the special properties brought about by the interlocking of polymer chains (Sperling, 1981). Recently, research on IPN materials made from PVA yielded interesting results. A series of anion exchange membranes based on PVA was prepared. The film-forming polymer is constituted by PVA as the cross-linked matrix and a polyelectrolyte for the specific ion-exchange properties. Polyethyleneimine (PEI), poly(1,1-dimethyl-3,5-dimethylene piperidinium chloride) (PDDPCl), and poly(diallyl dimethyl ammonium chloride) (PDDMACl) were used as cationic polyelectrolytes (Lebrun et al., 2002), and the gaseous cross-linking was done by dibromoethane. The best anion exchange capacity was obtained for PVA/PEI as 0.6–0.7 meq.g^{-1}. On the basis of the same polymer matrix (PVA), poly(1,3-diethyl-1-vinyl imidazolium bromide) (PDVIBr) was used as polyelectrolyte and gaseous DBE as cross-linking agent for the preparation of an IPN. The ion exchange capacity obtained was 1.1 meq.g^{-1} (Lebrun et al., 2004). Moreover, PVA was blended with poly(allylamine) and cross-linked with glutaraldehyde (Nishimura et al., 2008). Recently, AEMs based on cross-linked PVA-poly(acrylonitrile-co-2-dimethylaminoethyl methacrylate) were developed (Kumar et al., 2010). PVA was used because of its high chemically reactive hydroxyl groups favorable for chemical cross-linking. The copolymer poly(acrylonitrile-co-2-dimethylaminoethyl methacrylate) was used for the mechanical, chemical and thermal properties of the poly(acrylonitrile) and the poly(dimethylaminoethyl methacrylate) for its tertiary amine favorable for quaternization. These membranes showed good ion exchange capacities of 1 meq.g^{-1}, and reasonable ionic conductivities in the range of 3.45 mS.cm^{-1}.

Work on interpenetrating polymer network has produced interesting results. IPNs exhibit a low electrical resistance due to the presence of the polyelectrolyte, good mechanical strength, chemical stability and durability (due to the stable polymer matrix) at reasonable cost. Nevertheless, because the polyelectrolyte is not bound to the other polymer, a slow

extraction was observed over time, leading to loss of conductivity as well as ion exchange capacity.

2.2.3 Homogeneous membranes

In homogeneous membranes, the cationic charges are covalently bound to the polymer backbone. These polymers present ionic sites such as quaternary ammoniums grafted on the skeleton of the polymer chain. A mobile counter ion is associated with each ionic function in order to preserve the electro-neutrality of the polymer. The stability of the polymer electrolyte is dependent on the alkaline media, but temperature also plays a role. The development of a resistant anion exchange membrane requires a good stability of the polymer backbone along with fixed charges.

Sata and colleagues prepared highly cross-linked anion exchange membranes (Huda et al., 1998; Sata et al., 1998). Two series of poly(styrene)-based copolymer membranes with low and high contents of divinyl benzene as cross-linking agent were used. Different tertiary amines were reacted into the base membranes as anion-exchange groups. Although a good ion exchange capacity (IEC) was obtained (0.83–2.38 meq.g^{-1}), the electrical resistance was high and the water content was very low. Another method was developed which consisted of preparing a membrane based on chloromethylated polysulfone, a copolymer of chloromethyl styrene cross-linked with divinylbenzene and a series of diamines (by varying the length of the alkyl chain). These highly cross-linked AEMs exhibited a high electrical resistance because of the high cross-linking rate and anion exchange capacity in the order of 1.8 meq.g^{-1} (Sata et al., 1996). No other data such as ionic conductivity or thermal and chemical stability were presented.

Introduction of cationic moieties by chemical modification into a polymer is great deal to prepare ion exchange membranes from polymer films. Most commonly, styrene and divinyl benzene used as starting material to prepare quaternary AEM membranes. The membrane is obtained in two steps: copolymerization and chloromethylation followed by quaternary amination (Galeazzi, 1976; Sata, 1978; Strathmann, 1995). The preparation procedure for a membrane based on styrene is complicated. The styrene-based membranes exhibited low electrical resistance and good mechanical strength. In order to avoid the use of chloromethylmethyl ether, AEM was prepared via chloromethylation and quaternization by the triethylamine of a tri-block co-polymer matrix called polystyrene ethylenebutylenepolystyrene (PSEBS) (Vinodh et al., 2010). These membranes exhibited ionic conductivities in the order of 1 $mS.cm^{-1}$ at room temperature and it was found that the modification provided a flexible, chemically and mechanically stable membrane. The same synthetic route was used in order to obtain a chloromethylated polystyrene block-poly(ethylene-ran-butylene)-block-polystyrene (Zeng et al., 2010). After introduction of chloromethyl groups, these were converted into ammonium groups in the presence of trimethylamine. The membranes showed ion conductivity of 9.37 $mS.cm^{-1}$ at 80ºC.

Zschocke and Quellmalz demonstrated the excellent chemical properties of polyethersulfone (PES), by soaking the membrane in NaOH (40 wt.%) at 70–80ºC for 300 h (Zschocke and Quellmalz, 1985). Because of the extremely high chemical (and physical) stability of PES, the researchers modified the PES by introducing an anion exchange group in two steps: chloromethylation, followed by quaternization. The membranes exhibited an IEC between 0.5 and 1.8 $meq.g^{-1}$ having electrical resistances between 0.5 and 5 $\Omega.cm^{-2}$. One approach to promote the hydroxyl conductivity of quaternized polymers is to increase the basicity of the functional groups. Synthesis of a functionalized polysulfone was demonstrated and investigated the effects of reaction

temperature and time on chloromethylation, and studied several quaternization approaches for enhanced ionic conductivity in water (Wang et al., 2009b). The preparation of this alkaline AEM was conducted in three steps: (1) chloromethylation, (2) quaternization and (3) alkalization. Quaternization was carried out via three approaches: Quaternization of a pre-formed membrane via a tertiary amine; quaternization of the chloromethylated polymer via tetramethyl ethylene diamine (TMEDA), followed by treatment with a tertiary amine; quaternization of the chloromethylated polymer via TMEDA, followed by treatment with bromoethane. The results showed that both temperature and time exhibited significant impacts on chloromethylation and gelation. It was also found that using an appropriate quaternization approach could significantly improve the ionic conductivity. The developed AEM showed ionic conductivity of up to 31 $mS.cm^{-1}$ at room temperature (Wang et al., 2009b). Increasing the temperature to 95ºC the ionic conductivity was increased up to 73 $mS.cm^{-1}$. These membranes offered better homogeneous fixed ionic charge distribution over the entire polymer matrix.

The most successful AEMs were prepared by copolymerization of chloromethylstyrene and divinyl benzene or butadiene. Radiation-induced grafting is a method widely investigated for the preparation of AEMs. Nevertheless, the success of these membranes is limited. Concerning polysulfone, even if the membranes showed high mechanical strength, they exhibited a low IEC. Moreover, defects and flocculation of the polymer during AEM synthesis and the introduction of the ionic group can occur in polysulfone membranes. A way to avoid this is to synthesize blocks of PES, which can be functionalized afterwards. This provides a better dimensional stability but unfortunately also a decrease in ionic conductivity. Membranes based on PVA showed good ionic conductivities, and water content but lack of mechanical stability.

2.3 Summary of literature review

Solid polymer electrolyte membranes (SPEs) with the suitable characteristics have great potential in achieving an effective reduction of CO_2. SPEs are attractive because it may be tuned as per the requirement. SPE contains polymer backbone and functional groups. They allow blending or modification of the different properties of component in the membrane to improve overall ERC performance. Basically, the solid polymer membranes evaluated for ERC usually possess a few of the important properties, namely hygroscopic property, ion (proton/hydroxyl) conducting property, and reactant/product (eg. methanol) impermeability. The two desirable primary parameters required during evaluation of SPEs for ERC are reduction of CO_2 due to modification of functional groups while maintaining the proton or hydroxyl conductivity of membrane. The modification of functional groups resulted in a change in properties of the membranes such as ionic conductivity, ion exchange capacity and water uptake. The water uptake by the heterogeneous membrane containing ion solvating polymers is generally higher than that of the pure nafion. They also exhibited improved thermal and mechanical stability than the parent polymer, and in most cases exhibited reduced proton conductivity compared to pure nafion membrane. However, other problems such as reduction in mechanical stability when the chemical modification of polymer backbone reached a critical level, and decreased electrochemical cell performances were encountered. However, increasing crosslinking usually resulted in a simultaneous reduction in proton conductivity and mechanical failure. The acid-base blend membranes were found to have low ionic properties of membrane, attributed to lack of interactions between the polymers creating a crude dispersion impairing the transport trend. Chemical modification into a polymer can lower the water uptake while increasing the anionic conductivity along with maintaining the good mechanical stability without reducing the electrochemical performance.

However, it has been indicated that membrane which is highly acidic in nature results in more hydrogen evolution. Neutral or less basic nature of anion exchange SPEs could alleviate the problem of hydrogen evolution. Modification of polymer with functional groups which have good affinity for CO_2 may be a good strategy. Therefore, the search for a modified membrane possessing the good affinity toward CO_2 is required. For a proper assessment of the SPEs, a detailed characterization of the modified membranes both under ex-situ environment and electrochemical cell conditions is necessary. Another significant point to be noted is that ERC has advantages such as (i) the process can be carried out at room temperature and pressure; (ii) overall chemical consumption can be minimized to simply water or wastewater for the proton source; (iii) renewable energy may be used to drive the process, which can ultimately be stored as the reaction products; (iv) the compact electrochemical system can easily be scaled-up; and (v) the by-product (H_2) of ERC may be minimized. The mechanical properties of the modified membranes namely, tensile strength has not been taken into consideration while studies have shown that the ionic properties of the membranes are extremely important for the performance and longevity of the electrochemical cell. Even though, the membrane of an electrochemical cell is subjected to various stresses, including those due to solvent mass uptake and clamping between flow plates. Hence, an accurate knowledge of the physico-chemical properties of the developed membrane under a range of environmental conditions is crucial to identify the suitability of membranes for ERC. However, there are barely any reports especially focused on the evaluation of solid polymer electrolytes for ERC.

It is seen that the solid polymer electrolyte have some influential role on the electrochemical reduction of carbon dioxide. From the literature, it is understood that primarily cation exchange membrane is used in the ERC. Various authors have used

various cation exchange membranes but the study was limited to the electrocatalyst only. Though some of the researchers emphasized about the role of various cations or anions but it was limited to the aqueous or non-aqueous electrolyte. As far as anion exchange membranes are concerned, only a few of the researchers have employed these membranes in ERC but again the aim was on electrocatalyst or reactor design and not on the study of anion exchange membrane. Thus it is very important to study the role of solid polymer electrolyte on the electrochemical reduction of carbon dioxide. Therefore, the objective of the current research is set as per the above literature survey and discussed in the next section.

2.4 Aim and objectives

It is evident from the literature review that the solid polymer electrolyte has great role in the ERC applications. However, it is not explored in great extent. Hence, **the main objective of this thesis is to understand the significance of solid polymer electrolyte and suitably develop it for direct electrochemical reduction of gaseous CO_2 (dERC) into fuel.** In order to achieve the main objective, first, an electrochemical reactor was designed and developed to perform the electrochemical reduction of gaseous CO_2. Second, various solid polymer electrolyte membranes were synthesized and evaluated in the reactor. The knowledge gained by the results was used to further explore the SPE in greater depth. Thus, thirdly, the research work was done using two similar SPEs having same polymer backbone but anionic and cationic functional groups. Finally, the insight gained was used to further enhance the understanding and subsequently two new SPEs were synthesized and evaluated. The new mechanisms, insights as well as quite a good knowledge base were established for the SPE. The next section shows the research and development work, which was conducted to achieve the objective of the thesis.

Development of an electrochemical reactor for dERC

- An electrochemical reactor was developed for the direct electrochemical reduction of gaseous CO_2 to fuel in continuous mode. The work was published in *ASME Proceedings and in International Journal of Innovative Research and Development*.

Performance evaluation of dERC using developed SPEs

- Synthesis of cation and anion exchange membrane using casting technique. Ex-situ characterization of the developed cation and anion exchange membrane by Scanning electron microscopy (SEM), X-ray diffraction (XRD), Thermogravimetric analysis (TGA), Fourier transform infrared (FTIR) spectrometer analysis, water uptake, swelling behavior, ion exchange capacity, ionic conductivity, and tensile strength. Finally, in-situ charactetrization was conducted using the membranes in the reactor to evaluate the performance towards ERC.

The following cation exchange membranes were synthesized:

- Nafion
- SPEEK (Sulfonated polyether ether ketone)

The following anion exchange membranes were synthesized:

- Alkali doped polyvinyl alcohol (PVA/GA/KOH)
- Amberlyst/SPEEK

The research work was published in *Separation and Purification Technology, an Elsevier journal*.

Influence of functional groups in cationic and anionic SPE on dERC

- Two SPEs having similar polymer backbone but with different functional group were used. The ex-situ as well as in-situ characterization was performed to know the efficacy and understand the influence of the functional groups.
  - CMI-7000 (Polystyrene crosslinked with divinyl benzene in protonic form) chosen as cationic SPE, and
  - AMI-7001 (Polystyrene crosslinked with divinyl benzene in hydroxyl form) chosen as anionic SPE.

This research work was published in *Journal of CO_2 Utilization, an Elsevier journal*.

Tuning of reaction zone by modifying functional group in anionic SPE

- The quaternary SPEs (anionic) were synthesized and characterized using ex-situ techniques and ERC performance was evaluated using developed anionic SPEs.

The following anion exchange membranes were synthesized:

- PEI/PVA/KOH (Polyethylenimine/Polyvinyl alcohol in hydroxyl form),
- QPEI/PVA/KOH (Quaternary Polyethylenimine/Polyvinyl alcohol in hydroxyl form).

This research work was published in *Physical Chemistry Chemical Physics, a journal of Royal Society of Chemistry*.

Next chapter provides the details of various materials and methods used in the study along with the details of the developed electrochemical reactor. The common materials and methods used in the thesis are provided in the chapter 3; however, other necessary details are given in the relevant chapters.

Chapter 3

Experimental

Chapter 3

Experimental

The experimental methodologies for characterization of the solid polymer electrolytes are discussed in the first part of the chapter. In the subsequent sections, the design and development of the electrochemical reactor, product analysis technique, along with analysis procedures of electrochemical system are discussed in detail. It may be noted that only common experimental techniques are discussed in this chapter, however, the synthesis of SPE along with materials will be discussed in the relevant chapters.

3.1 Membrane characterization techniques

The developed solid polymer electrolyte membranes were characterized under ex-situ conditions by, scanning electron microscopy (SEM), thermogravimetric analysis (TGA), X-ray diffraction (XRD), Fourier transform infrared (FTIR) spectroscopy analysis, water uptake, swelling, ion exchange capacity (IEC), ionic conductivity, and tensile strength. Once the membrane was thoroughly characterized using ex-situ methods, it was used in the electrochemical reactor for the in-situ characterization to evaluate the performance for the ERC. Moreover, the detailed procedure for the fabrication of the membrane electrode assembly (MEA) and characterization of the ERC is provided in the relevant sections as stated above.

3.1.1 Scanning electron microscopy (SEM)

Scanning electron microscopy is a technique that takes advantage of the shorter wavelength of the electrons in comparison to the visible light, used in optical microscopy,

to get images with higher resolution. It directs a beam of high energy electrons, also known as primary electrons, towards a sample in an ordered pattern. When the primary electrons interact with the sample, secondary electrons are emitted together with back scattered electrons and X-rays. The secondary electrons come from the region near the surface and contain topographic information, so these electrons are detected to generate an image of the sample.

Surface morphologies of the membranes and electrodes used in the study were evaluated using scanning electron microscope (make: LEO; model: 1430vp). The membrane samples were mounted on a stub and subjected to gold coating to make them conductive for SEM analysis (Aeshala et al., 2013).

3.1.2 Thermogravimetric analysis (TGA)

SPE used in the electrochemical reactor was operated at atmospheric temperature and pressure. However, while fabricating the membrane electrode assembly, the membrane experiences a temperature of 110^{o}C. Therefore, the thermal stability of the SPE was evaluated using thermogravimetric analyzer (make: Mettler Toledo; model: SDTA 851e). Approximately 5 mg of the membrane was cut into very small pieces and taken in the alumina crucible of the analyzer. A heating rate of 10°C.min^{-1} was used in the range of 25-600°C under nitrogen atmosphere to study the thermal behavior of the membrane (Aeshala et al., 2012).

3.1.3 X-ray diffraction (XRD)

X-Ray diffraction is a powerful non-destructive method for determining a range of physical and chemical characteristics of materials. The applications include the type and quantities of phases present in the sample (phase analysis), the crystallographic unit cell

and crystal structure, crystallographic texture, crystallite size, macro-stress and micro-strain, and electron radial distribution functions. X-ray diffraction results from the interaction between X-rays and electrons of the material. Depending on the atomic arrangement, interfaces between the scattered rays are constructive, when the path difference between two diffracted rays differs by an integral number of wavelengths, which is described by the Bragg equation shown in eq. 3.1,

$$2d \sin\theta = n\lambda \tag{3.1}$$

where, λ is the wavelength, d is the spacing between the crystal planes and θ is the Bragg angle, which is the angle between incident and reflected beam.

X-ray diffraction (XRD) analyses of the membranes and electrodes were carried out in an advanced diffractometer (make: Brucker; model: D8 Advanced X-ray diffractometer). The sample was kept over a slide, which was later fixed in the XRD analyzer. The X-ray guns in the XRD analyzer used a monochromatized Cu-Kα radiation. The wavelength of the Cu-Kα X-ray was approximately 1.54 Å at 40 kV and 40 mA. The XRD gun was swept from 5–80° with a step size of 0.05° and scan rate of 0.5 s^{-1}.

3.1.4 Fourier transform infrared (FTIR) spectroscopy

The membranes were analyzed in a Fourier transform infrared (FTIR) spectrometer (make: Perkin–Elmer; model: Spectrum One Spectrometer) to identify the presence of functional groups. The transmission spectra of the membrane was recorded in a spectral range of 450-4000 cm^{-1} at a resolution of 4 cm^{-1} (Barbora et al., 2009a).

3.1.5 Water uptake

Water uptake of the membrane was evaluated by suspending the dry membrane sample of known weight in de-ionized water for 24 hours. Thereafter, the membrane was removed from the water and the excess surface water was quickly wiped off from both the surfaces. The weight of the wet membrane sample was measured and the water uptake of the membrane was calculated using eq. (3.2),

$$\text{Water uptake} = \frac{(W_w - W_d) \times 100}{W_d} \tag{3.2}$$

where, W_w and W_d are the weights of wet and dry membranes, respectively (Aeshala et al., 2012).

3.1.6 Swelling

The swelling of the membrane was determined by measuring changes in the membrane length upon equilibrating the membrane in water solution at room temperature (Ahmad et al., 2006). Determination of linear expansion is an effective method to interpret the swelling. Therefore, the linear expansion factor (L%) was calculated using eq. (3.3),

$$\text{Swelling (L\%)} = \frac{(L_w - L_d) \times 100}{L_d} \tag{3.3}$$

where, L_w and L_d are the lengths of wet and dry membranes, respectively.

The measurements were repeated at least five times for each sample and the arithmetic mean is reported. The variations in the experimental values were in the range of ±5% (Aeshala et al., 2013).

3.1.7 Ion exchange capacity

The ion exchange capacity (IEC) of the anion exchange membrane was determined by volumetric titration method. The membrane was immersed in 0.1N HCl solution for 24 hours. To assure complete ion exchange, the membrane was immersed again in another 0.1N HCl solution for an additional 24 hour. In the process, hydroxyl ions from the anion exchange membrane were replaced by Cl^- using HCl solution. The two solutions were then mixed and a sample was taken from the solution mixture. The sample was then titrated against 0.1N NaOH solution using phenolphthalein as an indicator to determine the displaced OH^- ions present in the sample. The ion exchange capacity of the membrane, E ($meq.g^{-1}$), was calculated using eq. 3.4 (Aeshala et al., 2013; Zeng et al., 2010).

$$E\left(meq.g^{-1}\right)=\frac{(V_{HCl}\times N_{HCl}-V_{NaOH}\times N_{NaOH})}{W_d} \qquad (3.4)$$

where, V_{HCl} and V_{NaOH} are the volumes (in ml) of HCl and NaOH solutions, respectively, used in the titration. N_{HCl} and N_{NaOH} are the normalities of HCl and NaOH solutions, respectively. W_d is the weight of the dry membrane in gm.

Similarly, the IEC of the cation exchange membranes was evaluated by immersing the membrane in NaOH and titrated with HCl to determine the displaced H^+ ions present in the sample. The calculation procedure was same as in the case of anion exchange membrane.

3.1.8 Ionic conductivity

Solid polymer electrolyte membranes must have good ionic conductivity for ERC applications. It should have fixed charged sites surrounded by water molecules, which

facilitate the transport of ions. Through-plane ionic conductivity of the membrane was determined by an ion conductivity cell as shown in fig. 3.1 (Barbora et al., 2009b). The conductivity cell was fabricated using perspex. Two cylinders having internal diameter of 3.2 cm and length of 30 cm were taken. A perspex flange was attached to one end of each of the cylinders. The other ends were sealed by the teflon blocks. Silicon gasket was used in between the flanges. Both the cylindrical compartments have the arrangements to fix three electrodes (working, counter, and reference) as shown in fig. 3.1. These arrangements were also used to pour/drain the solutions into/from the cell compartments.

The ionic conductivity was measured at 30°C by AC impedance technique over a frequency range of 10 kHz to100 mHz using a potentiostat (CH instruments Inc., USA, model no. CHI6002B).

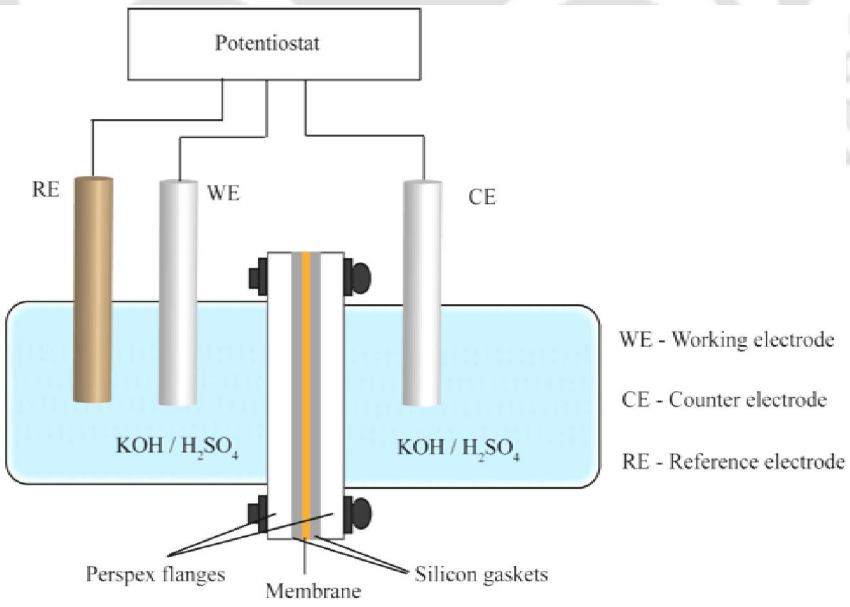

Fig. 3.1 Schematic of the ionic (hydroxyl/proton) conductivity experimental setup

The hydroxyl conductivity measurements were performed after hydrating the membrane in de-ionized water for 24 hours. The membrane was fixed between the flanges as shown in fig 3.1. A platinum sheet electrode (0.25 cm^2), working electrode, was placed in one of the chambers, facing the membrane. Another platinum sheet electrode (0.25 cm^2), counter electrode, was placed in the other chamber facing the membrane. Both of these two electrodes were kept near to the membrane. A third electrode (reference electrode) was placed in the chamber, where the working electrode was kept as shown in fig 3.1.

To measure the hydroxyl conductivity of anion exchange membranes, both chambers were filled with KOH solution. Thereafter, resistance was measured with and without the membrane in the conductivity cell. Resistance of the membrane was obtained by subtracting the resistance due to the electrolyte solution from the combined resistance, due to the membrane and electrolyte solution. The ionic conductivity of the anion exchange membrane, σ ($S.cm^{-1}$), was calculated using eq. 3.5 (Aeshala et al., 2012),

$$\sigma = \frac{L}{RA} \tag{3.5}$$

where *L*, *R*, and *A* denote the distance between the electrodes (cm), the measured resistance (ohm), and the area of the membrane (cm^2) exposed to the solution, respectively.

Similarly, proton conductivity was measured for cation exchange membrane using H_2SO_4 solution instead of KOH solution. The calculation procedure was same as in the case of anion exchange membrane (Aeshala et al., 2012).

3.1.9 Tensile strength

The membrane was cut into dog-bone shaped samples as per ASTM (D-638) standard with a gauge length of 2.2 cm and a width of 0.5 cm (Aeshala et al., 2012). The tensile strength of the dry membrane was examined under ambient conditions using a universal tensile tester.

3.2 Evaluation of membrane in ERC Reactor

3.2.1 Fabrication of electrochemical setup

ERC reactor hardware was developed and fabricated to study the performance of the synthesized membrane in real environment of the ERC reactor. Two graphite plates with proper flow channels and ribs were used as monopolar plates or end plates and machined to deliver the reactants at anode and cathode. Figure 3.2 shows the picture of a machined graphite plate along with parallel channels and ribs and an assembly of electrochemical reactor. The channels are connected to a supply-head at one end and outlet at other end so as the reactant can be fed in, as well as the product and unreacted reactant can be taken out from the ERC cell. The gold terminals of the cathode and anode were used to supply suitable electrical potential to the ERC reactor. The electrons generated at the reaction sites are collected by the ribs at anode, which migrate to the gold plated terminal attached at the anode monopolar plate. Similarly, the electrons that are transported to the cathode via the external circuit and reaching to the cathode are first received by the gold plated terminal attached at the cathode monopolar plate then transported to the ribs to the cathode reaction sites. One of such graphite plates with flow arrangement along with the gold plated terminals can be seen in the fig. 3.2a. The developed membrane electrode assembly (MEA), as described in section 3.2.2, was sandwiched between these two

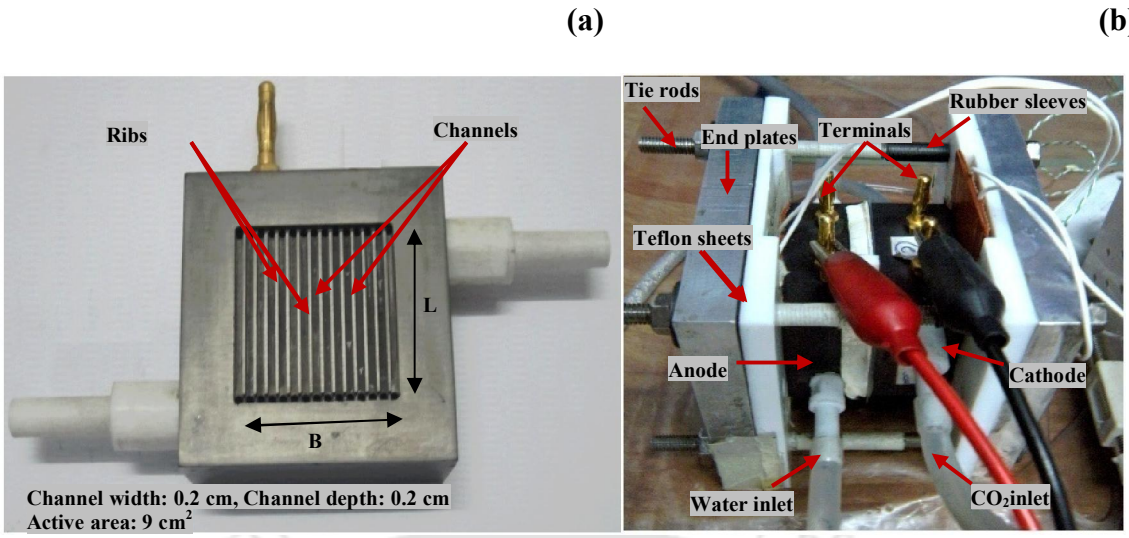

Fig. 3.2 Snapshot of (a) a machined graphite plate along with parallel flow channels and ribs, and (b) ERC reactor

aligned graphite monopolar plates. Two stainless steel plates were used to integrate the full assembly using tie rods. It can also be seen in the fig. 3.2b that teflon sheets and teflon/rubber sleeves were used to make the ERC reactor isolated from any short-circuiting. The ERC reactor (or ERC cell) was checked for any short-circuiting as well as leakage of any of the reactants (Aeshala et al., 2011; Singh et al., 2012).

3.2.2 Fabrication of membrane electrode assembly (MEA)

Porous carbon paper or gas diffusion layer (GDL) (TGP-H-120) from Toray, USA, was used as support for anode and cathode catalysts in the ERC reactor. Anode catalyst layer was developed on the carbon paper by depositing a thin catalyst layer with the help of a spray gun. The catalyst layer was prepared by making catalyst slurry, by mixing isopropyl alcohol and the nafion dispersion with 40 wt.% Pt/C for the anode ink followed by sonication for 20 min. The metal catalyst loading was maintained at 0.5 mg.cm^{-2} for the anode. Nitrogen gas was used as carrier for spraying the catalyst dispersion onto the electrode. The electrodes with the catalyst layer were heat treated in an air oven for about

12 h at 100°C to obtain the anode. The cathode was developed by electroplating copper onto the carbon paper. The electroplating was done by dipping a copper rod and the carbon paper into a solution of copper sulphate. The copper rod and carbon paper were used as the anode and cathode respectively and 1 V potential was applied between them. The electrodeposition of copper on the carbon paper was carried out for different time intervals (Aeshala et al., 2011). The carbon paper electrodeposited by Cu was dried to obtain the cathode. The treated membrane (SPE) was placed in between anode and cathode and the assembly was then hot pressed at 100°C for 3 min under 54 $kg.cm^{-2}$ pressure to obtain membrane electrode assembly. Thereafter, the MEA was cooled to room temperature by setting a cooling time of 30 min in the hot press machine. Figure 3.3 shows the sequence of the different layers of MEA and a snapshot of a MEA. The final MEA was then ready to be tested in the ERC. The details of the experimental setup of ERC are given in the next section (Aeshala et al., 2011).

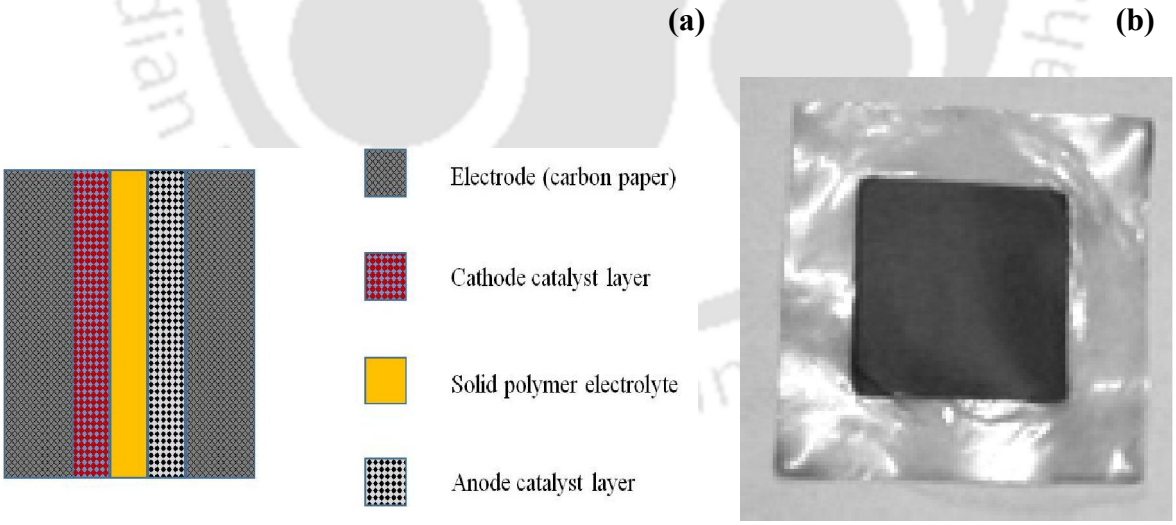

Fig. 3.3 Representation of (a) the developed MEA, and (b) its snapshot

3.2.3 Performance evaluation of ERC

The developed MEA was sandwiched between two similar monopolar plates and tested for evaluating the performance in the ERC reactor. Schematic of the experimental setup for ERC is shown in fig. 3.4. It can be seen in the fig. 3.4 that CO_2 gas (99.995%) was taken from a cylinder (1) through regulator (2) and fed at the cathode side of the electrochemical reactor (7) through a humidifier (4) with a flow rate of 20 $ml.min^{-1}$ set by the rotameter (3). Deionized water source (5) was used to flow the water at the anode of the electrochemical reactor using peristaltic pump (6) with a flow rate of 1.5 $ml{\cdot}min^{-1}$. Membrane electrode assembly (8-12), which is a combination of anode gas diffusion layer, anode catalyst layer, solid polymer electrolyte (SPE), cathode catalyst layer, and cathode gas diffusion layer is fabricated and detailed in section 3.2.2. Required energy for the reduction of carbon dioxide was supplied by the potentiostat (CH instruments Inc., USA, model no. CHI6002B). Different potential values ranging from 1.8 V to 3 V were applied to the electrochemical reactor through the potentiostat. The anode outlet is connected to vent (13) and the cathode outlet is connected to a gas/liquid separator (14) to separate the gaseous and liquid reaction products.

The ERC was conducted at different electrical potentials for 60 minutes and the collected reaction products were analyzed by gas chromatograph (GC) (15). Each experiment was conducted for a short time (25 min.) with a new membrane electrode assembly so that the effect of degradation of membrane and/or electrocatalyst, if any, would not influence the study. The same was assured by studying the current behavior of the system before finalizing the experiment time. All the experiments were performed at room temperature ($25^{o}C$) and atmospheric pressure (Aeshala et al., 2013).

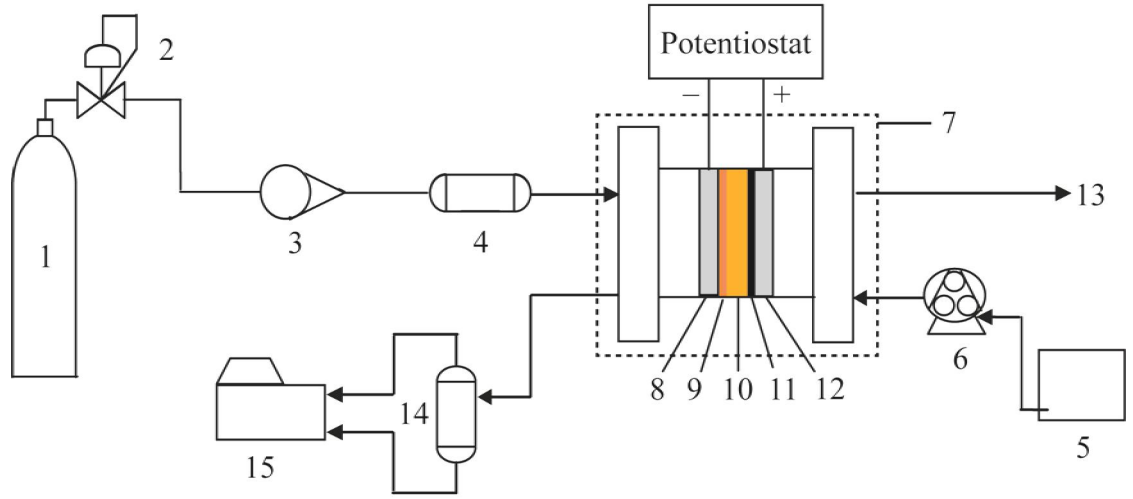

Fig. 3.4 Schematic of the experimental setup for ERC; (1) CO_2 source, (2) pressure regulator, (3) rotameter, (4) humidifier, (5) water source, (6) peristaltic pump, (7) electrochemical reactor, (8) cathode gas diffusion layer, (9) cathode catalyst layer, (10) SPE, (11) anode catalyst layer, (12) anode gas diffusion layer, (13) anode vent (O_2 and unreacted H_2O), (14) gas/liquid separator, (15) gas chromatography

3.3 Electrochemical technique for the dERC analysis

The electrochemical measurement performed in the developed electrochemical reactor were controlled by potentiostat (CH instruments Inc., USA, model no. CHI6002B). As discussed earlier, the details of the common electrochemical technique to analyze the reactor performance is given in this section.

3.3.1 Chronoamperometry

Chronoamperometry is a technique that consists of keeping the potential fixed and measuring the current as a function of time.

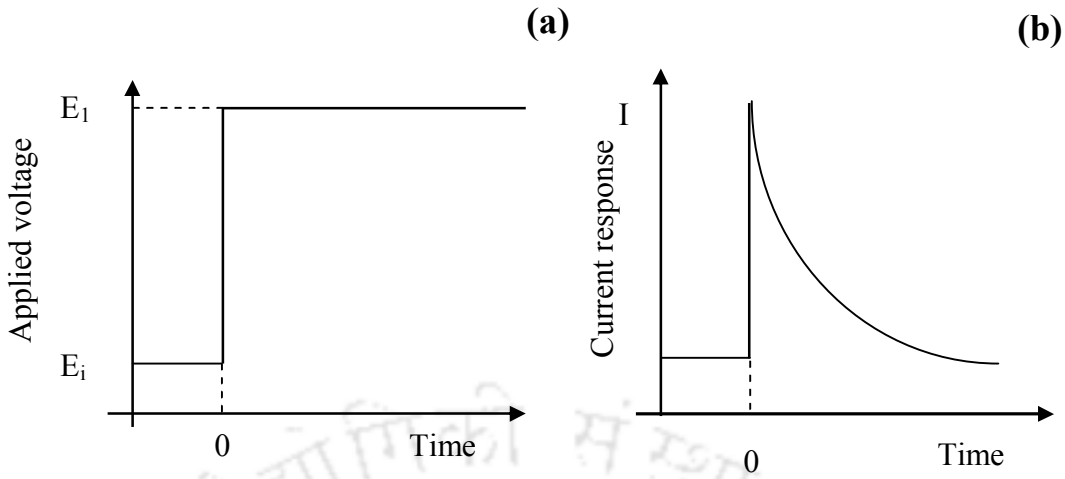

Fig. 3.5 The chronoamperometric measurement: a) The potential-time profile applied during experiment, E_i is initial value and $E_1$is the potential of interest, and b) The corresponding response of the current due to changes of the potential

In this work, the electroreduction of CO_2 is studied by chronoamperometry for constant mode electrolysis. The total charge measured during the reaction corresponds to the electrons used in the reduction reactions and thus it is proportional to the amount of products formed. The difference between the applied potential and the reaction equilibrium potential is known as overpotential and it is a measure of how much extra energy one needs to supply to drive the reaction.

The chronoamperometric experiment was conducted in which the potential of the working electrode is held at E_i as shown in fig. 3.5a. At t=0, the potential instantaneously change to a new value E_1, and corresponding current time response is recorded as shown in fig. 3.5b. The charge was calculated (eq. 3.6) by integrating the current response (fig. 3.6) which will be useful to calculate the Faradaic efficiency. The Faradaic efficiency is discussed in section 3.4.2.

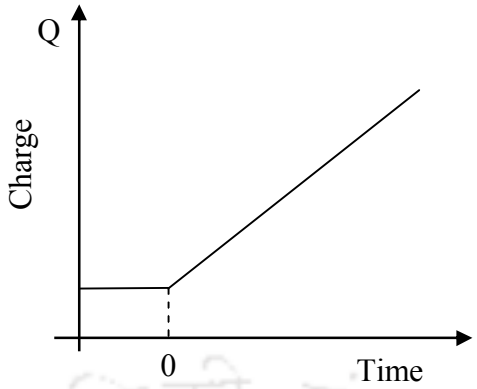

Fig. 3.6 A representative charge-time profile measured by integration of current response in the chronoamperometric experiment

$$Q = \int_{t_1}^{t_n} i\, dt \approx \sum_{j=1}^{n-1} (t_{j+1} - t_j) \frac{1}{2} [i_{j+1} + i_j] \quad (3.6)$$

where, n = duration of the experiment

3.4 Product analysis

3.4.1 Gas chromatography

The reaction products of the ERC process, as shown in the fig. 3.4, need to be analyzed for the evaluation of the ERC performance. Therefore, the reaction products from the ERC reactor were sent to a gas-liquid separator to separate the gas and liquid streams, which were analyzed by gas chromatography. This analytical technique allows to separate and to identify the different components of the product mixture. For the analysis, a small volume of the sample was mixed with a carrier gas, usually an inert gas such as argon, known as mobile phase. This mobile phase passes through a column, which has the stationary phase. The components of the sample interact with the stationary phase in the column and depending on strength; it may take longer or shorter time to elute through the column. A strong interaction between the column and a given product results in long

retention time, whereas a weak interaction implies a short retention time. The retention time can be modified by changing the column temperature or the flux of the carrier gas. When the optimal conditions are used, the different compounds will have different retention times as well as sufficient time gap in the elution of the species, such that allowing its adequate separation. It can easily be measured and analyzed. At the end of the column, the products were analyzed with the help of appropriate detector, giving a signal when one of the components of the sample leaves the column (fig. 3.7). It may be noted that evaluation of the reaction products of ERC is one of the major challenges in the ERC research (Kuhl et al., 2012). Therefore, after struggling for more than one year to identify the reaction products, reliability could be developed, and the further ERC work proceeded.

The gas chromatographs comprised thermal conductivity detector (TCD). The detection in TCD was generally used to detect both organic and inorganic compounds. It is based on the change of thermal conductivity of the carrier gas when another compound is present. For this work this detector type was primarily used for the quantification of H_2, and CO. Other detector of the GC was flame ionization detector (FID). The detection in FID was generally used to detect organic compounds, since it works by passing the sample through a hydrogen flame and measuring the ions produced while burning the compounds of the sample. FID detector was used for the quantification of CH_4, C_2H_4, and C_2H_6 etc.

The gaseous products were analyzed by GC with packed column (Carbosieve S-II, 3.05 m, 1/8 in., 2.1 mm) using thermal conductivity detector (TCD), and flame ionization detector (FID). Argon was used as carrier gas to carry the sample into the column, where separation of H_2, CH_4, CO, CO_2, and C_2H_6 etc. was achieved.

(Scheme - 1)

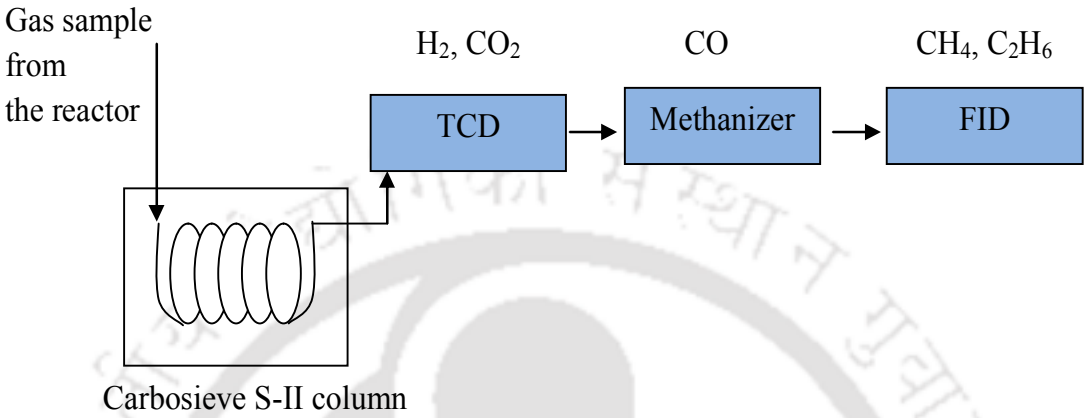

(Scheme - 2)

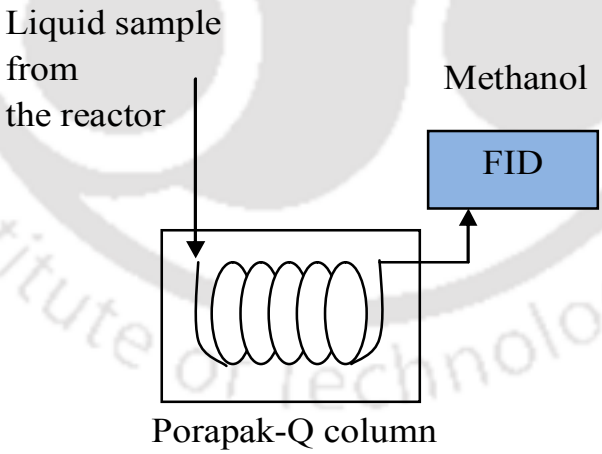

Fig. 3.7 A representative flowchart of gas chromatography for gas phase product analysis (scheme-1) and liquid phase product analysis (scheme-2).

After leaving the columns, the gas sample was first analyzed by TCD detector where H_2 and CO_2 gases were detected. Then, gas sample passed through methanizer where CO and CO_2 were converted to methane and analyzed by FID detector where the remaining hydrocarbons (CH_4, C_2H_4, C_2H_6) were also detected as shown in scheme-1 of fig. 3.7. It may be noted that there was no interference of the CH_4 from the reactor and methane from methanzier (which was obtained from CO and CO_2 conversion), because the later reached FID at different time. The liquid products like CH_3OH and higher alcohols were analyzed by GC using packed column (Porapak-Q) using FID (scheme-2 of fig. 3.7). The products were quantified by using calibration curves of known concentration of the standard samples.

3.4.2 Faradaic efficiency

Gas chromatography provides information about the concentration of different compounds, which is used to calculate the amount of different products formed during the reaction. However, Faradaic efficiency is a measure of how selective an electrolyte is towards a particular product. The Faradaic efficiency was calculated by determining the charge passed to produce a particular product with respect to the total charge passed during the experiment (sampling time) (Kuhl et al., 2012) and shown in eq. 3.7.

$$\text{Faradaic efficiency} = \frac{n \times F \times z}{Q} \tag{3.7}$$

where, n = number of moles of particular product (mol)

F = Faraday constant ($C.mol^{-1}$)

z = number of electrons involved for 1 mole of particular reaction product

Q = total charge passed during the experiment (C)

It is important to mention that the Faradaic efficiency depends not only on the amount of product formed, but also on the amount of electrons needed to reduce CO_2 into that particular product. Therefore, if the same amount of CO and methane is formed the Faradaic efficiency towards methane would be 4 times higher, since there are 8 electrons involved in the formation of one mole of methane while only 2 in the formation of one mole of CO.

3.4.3 Selectivity

Selectivity is defined as the amount of desired product to amount of total CO_2 reduction products obtained (based on the carbon content) during reaction (Ogura et al., 2004). As an example, if the CH_4, CO, C_2H_6 products were formed in the reaction, then selectivity of methane and ethane would be calculated by eq. 3.8 and eq. 3.9, respectively.

$$\text{Selectivity of } CH_4 = \frac{(\text{number of moles of } CH_4)}{\left((\text{number of moles of } CH_4) + (\text{number of moles of CO}) + (2 \times \text{number of moles of } C_2H_6)\right)} \quad (3.8)$$

$$\text{Selectivity of } C_2H_6 = \frac{2 \times (\text{number of moles of } C_2H_6)}{\left((\text{number of moles of } CH_4) + (\text{number of moles of CO}) + (2 \times \text{number of moles of } C_2H_6)\right)} \quad (3.9)$$

It needs one mole of CO_2 to form one mole of methane, whereas two moles of CO_2 are required to form one mole of ethane.

Chapter 4

Analysis of Solid Polymer Electrolytes for dERC

Chapter 4

Analysis of Solid Polymer Electrolytes for dERC

This chapter covers experimental procedures for synthesis and characterization of cationic and anionic solid polymer electrolytes. The casting technique is used to synthesize the solid polymer electrolytes. The formation of solid polymer electrolytes and their properties are evaluated by various characterization techniques and described in details. The cationic and anionic solid polymer electrolytes are evaluated in an electrochemical reactor to study the role of solid polymer electrolyte membranes on electrochemical reduction of CO_2. The chapter will provide the insight for the further research and development work and lay down the basic understanding for the next chapters.

4.1 Overview

This chapter shows the investigation on the effect of different SPE in the gas phase CO_2 electroreduction process. A compact electrochemical reactor was developed for the gas phase ERC, which could employ the SPE for continuous electrochemical reduction of CO_2. Copper and Pt/C were used on carbon paper to develop the cathode and anode, respectively. Four different SPEs (nafion, alkali doped PVA, SPEEK, and Amberlyst/SPEEK) were developed. The solid electrolytes were characterized for thermal gravimetric analysis (TGA), X-ray diffraction (XRD), Fourier transform infrared spectroscopy (FTIR), water uptake, swelling, ion exchange capacity, ionic conductivity, and tensile strength. The reactants were supplied to the electrochemical reactor and the

products of the ERC were identified qualitatively and quantitatively to evaluate the effects of the SPEs on ERC. This chapter presents the cationic and anionic SPE membranes. Cationic membranes were nafion, and SPEEK, whereas anionic membranes were alkali doped PVA, and Amberlyst/SPEEK. It may be noted that the Amberlyst/SPEEK is kept in anionic membrane category, which is confirmed and described in the later section of the chapter.

4.2 Experimental

4.2.1 Materials

Amberlyst A26 is a strong base, anionic, macroreticular polymeric resin based on crosslinked styrene divinylbenzene copolymer containing quaternary ammonium groups. The amberlyst A26 is a product of Dow Chemical Company and procured from Sigma Aldrich. The properties of amberlyst are shown in table 4.1.

Nafion dispersion (SE-5112), 5 wt.% solid, was procured from DuPont, USA. Pt/C (40 wt.%) was purchased from Electro-Chem., USA. Polyether ether ketone (PEEK) was procured from Gharda Chemicals Ltd., Mumbai. Polyvinyl alcohol (PVA) was purchased from Sigma Aldrich. Porous carbon paper (TGP-H-120) from Torayca was used as backing layer for electrode preparation. Other chemicals like DMF, HCl, H_2O_2, H_2SO_4, and KOH were procured from Merck, India. All the chemicals were used without further purification unless specified and de-ionized water was used in all the experiments.

Table 4.1 General properties of amberlyst A26 resin

Properties	**Values**
Appearance	White powder
Ionic form	Hydroxide (OH^-)
Surface area	30 $m^2.g^{-1}$
Bulk density	16.01 $kg.m^{-3}$
Matrix	Styrene-divinylbenzene (macroreticular)
Functional group	Quaternary ammonium

4.2.2 Method

4.2.2.1 Development of nafion and SPEEK electrolytes

The nafion membrane was fabricated using nafion dispersion (5 wt.%). In order to synthesize the nafion membrane, a measured amount of the dispersion was first dried in a petridish at 30°C. The obtained dried nafion residue was then solubilized in dimethyl formamide to obtain nafion solution. The nafion solution was used to cast the nafion membrane in a petridish using a well aligned oven to get a uniform film of definite thickness. The temperature of the oven was kept at 165°C (Silva et al., 2005). The membrane thus prepared will now be referred as pure cast nafion membrane. A representative structure of nafion polymer is shown in fig. 4.1a.

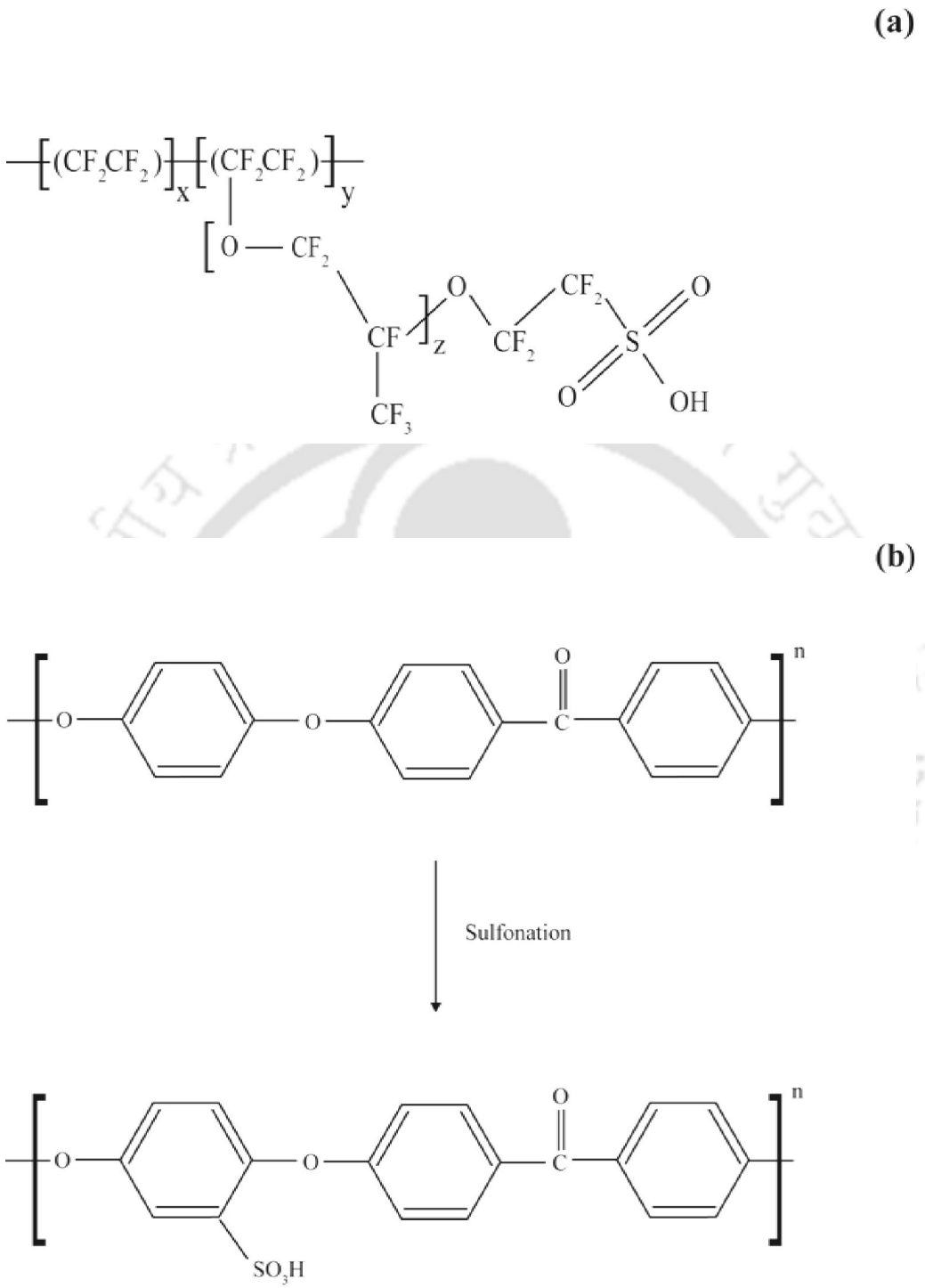

Fig. 4.1 Representative structure of (a) nafion, and (b) SPEEK

SPEEK was synthesized using PEEK polymer (27000 $g.mol^{-1}$). The PEEK polymer was dissolved in concentrated (95–98%) sulfuric acid and vigorously stirred at room temperature for a long time until a homogeneous solution was formed. The sulfonated PEEK (SPEEK) was precipitated by cooling the solution at subzero temperature. The polymer precipitate was filtered and washed several times with the water until neutral pH was obtained. The SPEEK polymer was dried at 100°C in which the degree of sulfonation was kept at 50%. The dried SPEEK polymer was dissolved in dimethyl sulfoxide (DMSO) and membrane was fabricated using solution casting method. Representative structure of SPEEK is shown in fig. 4.1(b).

4.2.2.2 Development of alkali doped PVA and Amberlyst/SPEEK electrolytes

PVA (99% hydrolyzed, average mol. wt. = 1,10,000 –1,25,000) was fully dissolved in water at 90°C to make 10 wt.% solution. The PVA membrane was developed using solution casting method. The developed membrane was soaked in a solution containing 10 wt.% glutaraldehyde (GA) in acetone at 30°C. The chemical cross-linking takes place between the -OH of PVA and the –CHO of GA in HCl catalyzed reaction. Further, to obtain the PVA anionic membrane, the cross-linked membrane obtained was equilibrated in a 2M KOH by immersing for at-least 24 hours. Thereafter, the membrane was taken out and the excess KOH on the surface of the membrane was removed by rinsing the membrane many times using de-ionized water. The structure of crosslinked PVA is shown in fig. 4.2a.

In order to prepare the Amberlyst/SPEEK polymer membrane, 1 wt.% of amberlyst A-26 anion exchange resin was added into the SPEEK solution. Thereafter, the dispersion was used to prepare the composite membrane using solution casting method. The representative structure of Amberlyst/SPEEK is shown in fig. 4.2b.

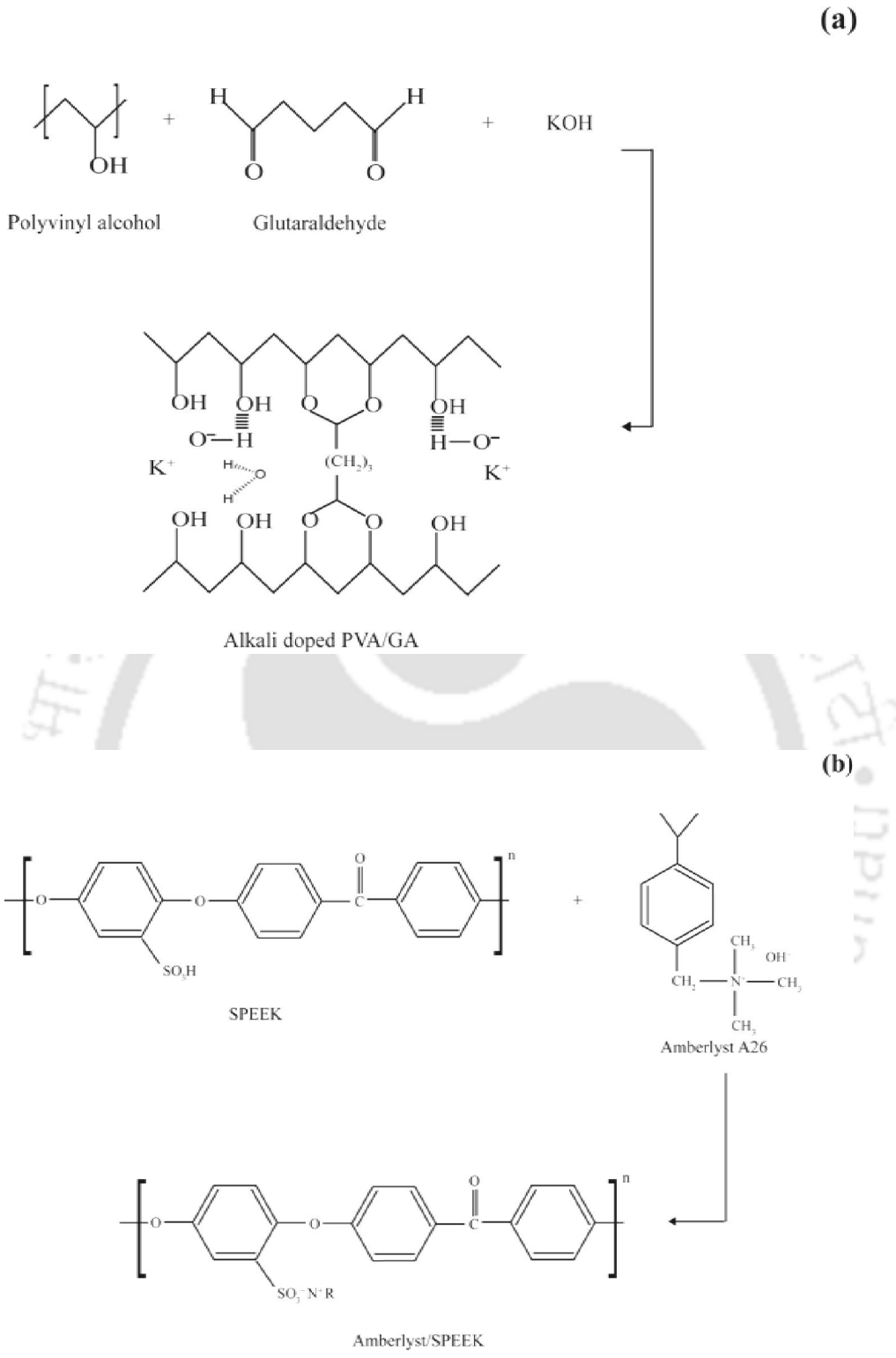

Fig. 4.2 Representative structure of (a) alkali doped PVA/GA, and (b) Amberlyst/SPEEK

4.3 Results and discussion

4.3.1 Membrane characterization

The prepared membranes were characterized using SEM, TGA, XRD, FTIR, water uptake, swelling, ion exchange capacity, ionic conductivity, and tensile strength before testing into the electrochemical reactor for the ERC.

4.3.1.1 SEM images

Figure 4.3 shows the SEM images of the membranes for studying the surface morphology, and for ascertaining the physical compatibility between polymers and the resin additive in case of the composite membrane (Amberlyst/SPEEK). The thickness of the SPEs were evaluated by the SEM images (not shown) and confirmed by measuring with screw guage at various locations. The thickness of all the membranes was around 80±10 μm.

Figure 4.3a shows the SEM image of the pure cast nafion membrane. The surface morphology of the nafion membrane appears uniform without formation of pores or cracks. Figure 4.3b shows the SEM image of SPEEK. It can be seen that membrane morphology shows a dense structure and there is no evidence of pores or cracks. Figure 4.3c shows the SEM image of cross-linked polyvinyl alcohol/glutaraldehyde (PVA/GA) membrane. It appears from the membrane morphology that the glutaraldehyde was well cross-linked with the polyvinyl alcohol in the membrane. Similarly, the fig. 4.3d shows the SEM image of Amberlyst/SPEEK composite membrane. It can be seen that amberlyst resin was uniformly distributed in the SPEEK matrix and no crack or pore formation was observed. Thus by the help of SEM analysis it can be concluded that all the SPEs were dense solid membranes without any pore or cracks on the surface of the membrane.

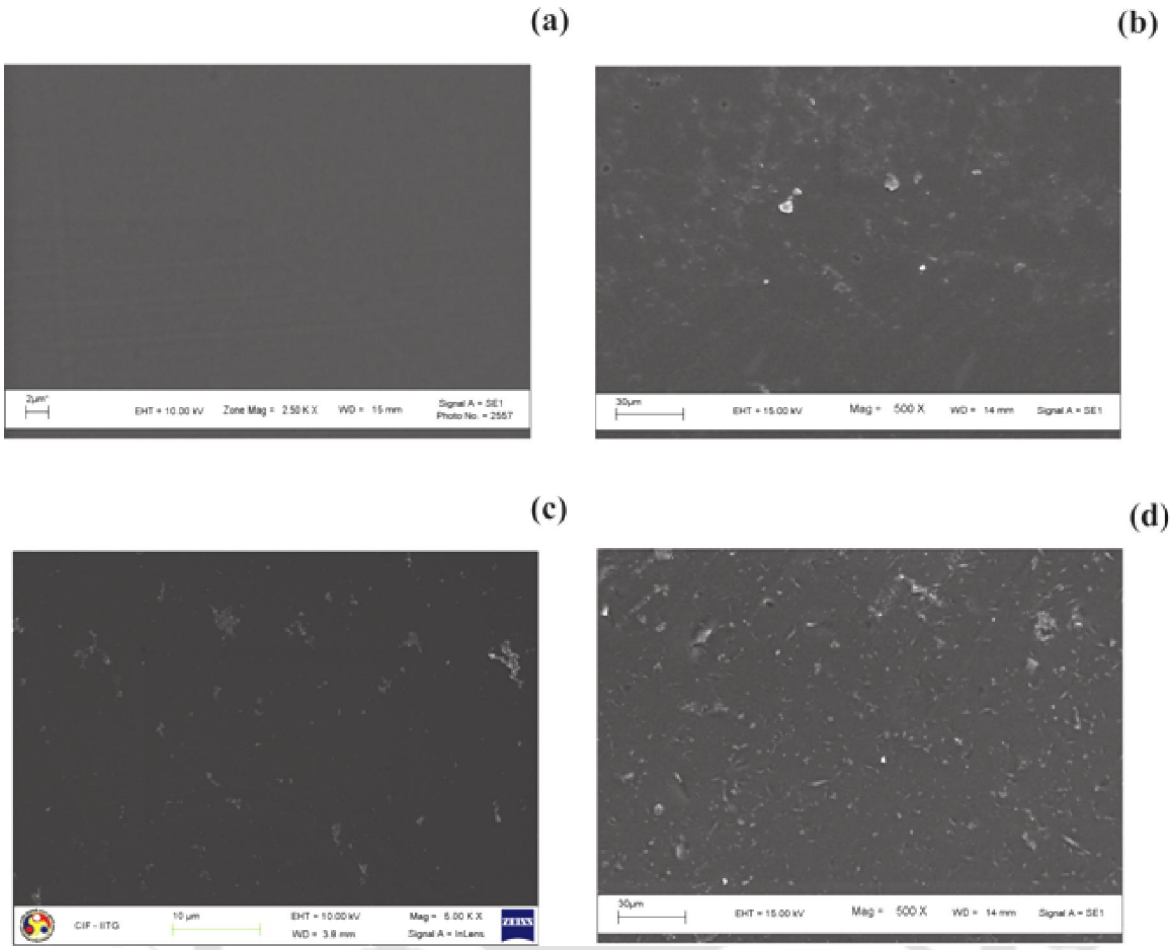

Fig. 4.3 SEM images of (a) pure cast nafion, (b) SPEEK, (c) crosslinked PVA/GA, and (d) Amberlyst/SPEEK

4.3.1.2 TGA

Thermal stability of the membranes was evaluated as the membranes experience temperature of 110°C during the fabrication of membrane electrode assembly fabrication process. TGA curves in fig. 4.4 shows the thermal degradation of nafion, SPEEK, cross-linked (PVA/GA), and Amberlyst/SPEEK membranes. The TGA of SPEEK was also compared with the PEEK powder and shown in the fig. 4.4a. Figure 4.4 shows the initial weight loss from the membrane samples, which is primarily because of the water loss

from the samples. The water loss from the SPEEK is higher as compared to nafion membrane. It is because of the sulfonation of PEEK, which provide more hydrophilic nature and accommodates higher amount of water as compared to the pure cast nafion membrane. Further increase in the temperature degrades the polymer sample and a continuous weight loss is observed. The nafion is stable up to 300°C and above this temperature the solid polymer electrolytes (membrane) are not thermally stable. PEEK is a temperature resistant polymer; weight loss for this polymer is mainly due to the chain decomposition after 520°C. The pyrolytic degradation of PEEK starts at about 520°C and results in the formation of phenols and benzene (Zaidi et al., 2000). Two weight loss steps are observed for SPEEK. The first weight loss step in SPEEK is due to the splitting-off of sulfonic acid groups at around 290°C. The second major weight loss starts at about 480°C against 520°C corresponding to the main chain degradation of PEEK. It indicates that SPEEK membranes are thermally stable up to approximately 290°C as shown in fig. 4.4a.

Figure 4.4b shows the TGA profile for anionic membranes (PVA/GA and Amberlyst/SPEEK). The increase in temperature degrades the polymer sample and continuous weight loss is observed. The PVA/GA is stable up to 350^{o}C, and further increase in temperature results in thermal degradation of membranes (solid electrolytes). In case of Amberlyst/SPEEK membrane (fig. 4.4b), the initial weight loss was quick due to water loss-upto 80^{o}C and thereafter slow weight loss was observed and profile followed the same trend as of PEEK membrane (Aeshala et al., 2012). The results show that all the cationic and anionic membranes used in the study was thermally stable not only upto the desired temperature (110^{o}C) but upto significantly higher temperature.

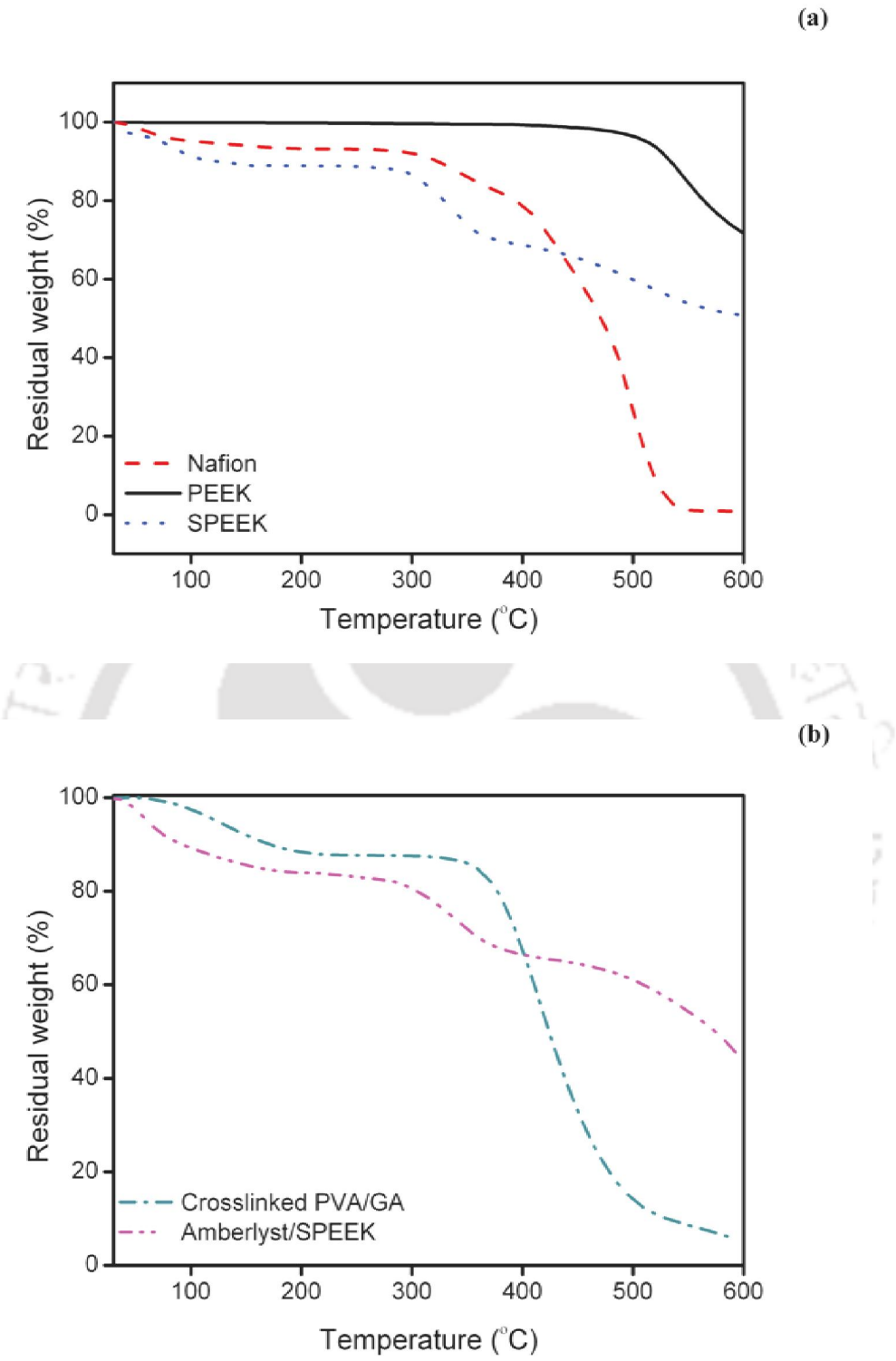

Fig. 4.4 TGA profiles for (a) nafion, PEEK, SPEEK, and (b) crosslinked PVA/GA, Amberlyst/SPEEK

4.3.1.3. XRD

Figure 4.5 shows the representative XRD patterns of the cationic and anionic membranes under study. The pure cast nafion membrane shows a broad peak at 14°–18° (2θ) (fig. 4.5a). According to the literature (Dimitrova et al., 2002), this broad peak can be deconvoluted into two peaks, assigned to amorphous (2θ =16°) and crystalline (2θ = 17.5°) scattering from the polycarbon chains of nafion (Barbora et al., 2012).

XRD pattern for SPEEK membrane can also be seen in fig. 4.5a. It may be noted that the base material for SPEEK (i.e. PEEK), is a semicrystalline polymer, thus showing a slight semi-crystalline peak in the range of 20°–30° (Zaidi et al., 2000). After sulfonation the crystallinity was further decreased and made the SPEEK amorphous.

Figure 4.5b shows that PVA/GA membrane exhibits semi-crystalline structure with a broad peak at 2θ angle of 18°–22° and a small peak at 39°–40°. XRD pattern of Amberlyst/SPEEK composite was shown in fig. 4.5b. It exhibits a broad peak in the 2θ range of 10°–30° with the maxima at around 20° due to the adjacent chains of polymer.

4.3.1.4 FTIR

FTIR spectra were obtained to find out the structural information of the cationic and anionic membranes. The FTIR spectra of pure cast nafion, SPEEK, PVA/GA, and amberlyst/SPEEK are shown in fig. 4.6.

Figure 4.6a shows FTIR spectra of pure cast nafion membrane, and SPEEK membrane. The FTIR spectra of pure cast nafion shows five major bands, namely, SO_3^- and $-SO_3H$ band, C=O and C-O-C band, C-F band, band for H_2O bending, and a band for stretching

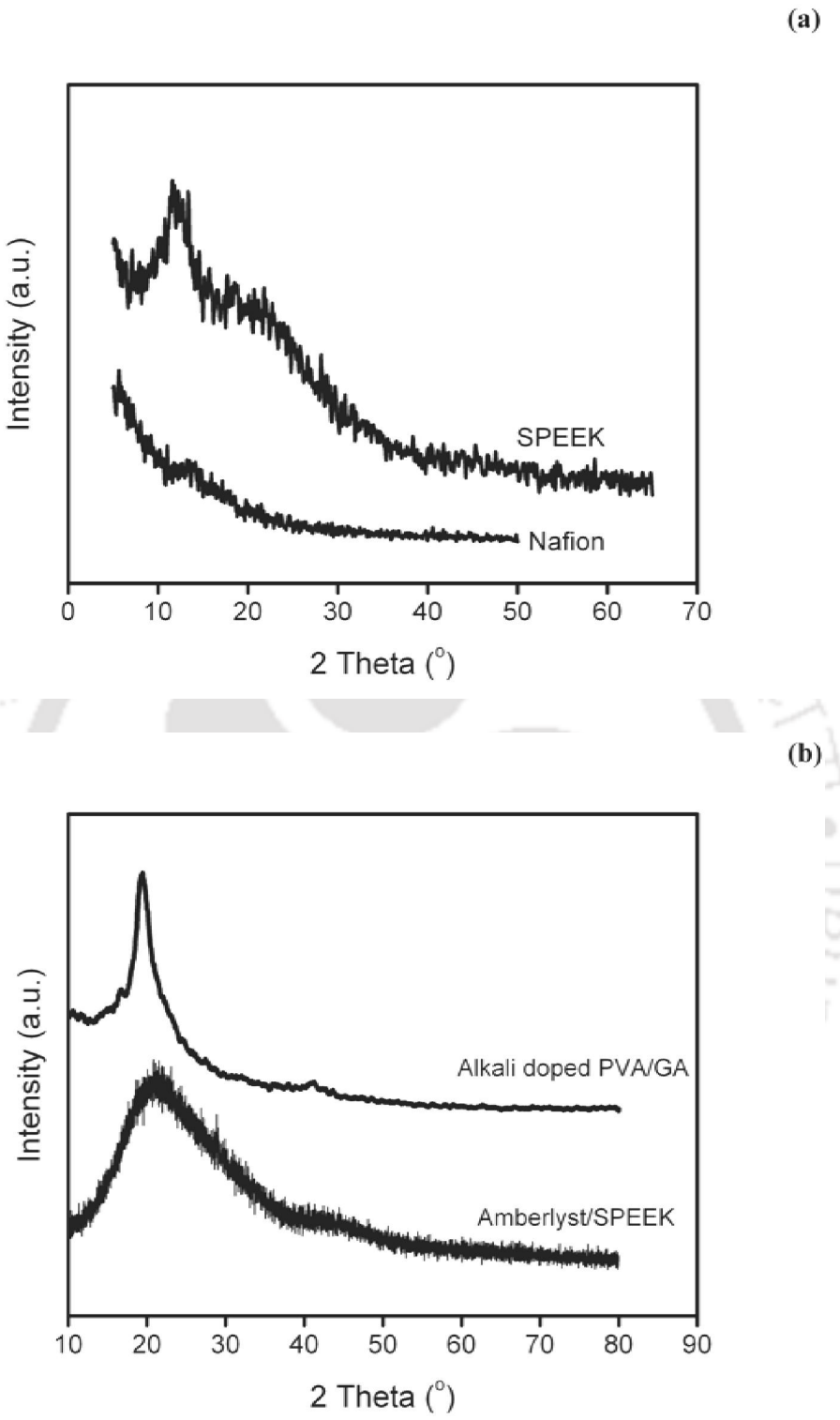

Fig. 4.5 XRD patterns of (a) nafion, SPEEK, and (b) alkali doped PVA/GA, Amberlyst/SPEEK

vibration of water. The observations made for pure cast nafion are discussed. The peaks at 518 and 633 cm^{-1} for the pure cast nafion membrane (fig. 4.6a) may be assigned to SO_3^-, and at 718 cm^{-1} to C=O bending (Kumutha and Alias, 2006). A peak is observed at 982 cm^{-1} for the vibration of C-O-C bonding in pure cast nafion membrane (Mahreni et al., 2009). Similarly, the peak for the stretching vibration of SO_3^- is observed at 1055 cm^{-1} (Ramani et al., 2005). A band for water bending occurs in the region 1400-2000 cm^{-1} (Park and yamzaki, 2005) and the peak for stretching vibration of water molecules is obtained within 3200 and 3700 cm^{-1} (Ludvigsson et al., 2000).

The FTIR spectrum for SPEEK is shown in fig. 4.6a along with PEEK for the comparison. The aromatic C–C bond is observed for PEEK at 1488 cm^{-1}, whereas the peak at 1648 cm^{-1} corresponds to the carbonyl group of the PEEK. Significant differences in the spectrum of SPEEK are observed as compared to pure PEEK. The broadband at 3440 cm^{-1} in fig. 4.6a corresponds to O–H vibration from sulfonic acid groups interacting with water molecules. The bands at 1252, 1024, and 709 cm^{-1} show the presence of sulfonic acid groups (Intaraprasit et al., 2011). It shows that the SPEEK was successfully prepared by the sulfonation of the PEEK.

Figure 4.6b shows the FTIR spectra of PVA/GA membrane. It reveals two important bands at 2869 and 2750 cm^{-1} which corresponds to C-H stretching related to aldehydes, duplet absorption with peaks attributed to alkyl chain (Mansur et al., 2008). Another strong band of carbonyl group (C=O) was observed at 1716 cm^{-1}. Moreover, the large bands between 3550 and 3200 cm^{-1} are linked to the O-H stretching in the PVA/GA. The reaction of PVA with GA results in a considerable reduction of the O-H peaks from pure PVA (shown in the figure), indicating possible formation of acetal bridges. The spectrum

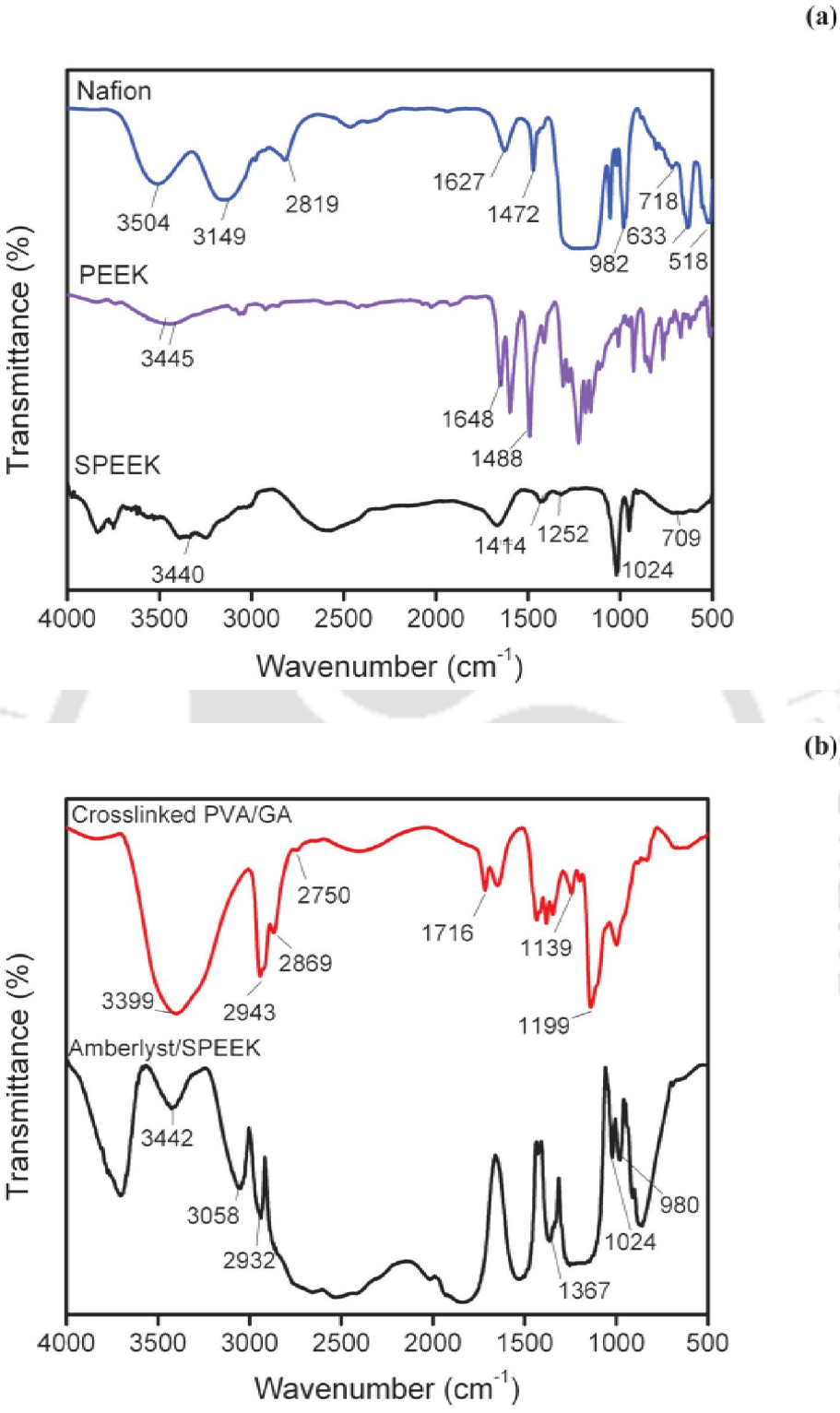

Fig. 4.6 FTIR spectra of (a) nafion, PEEK, SPEEK, (b) crosslinked PVA/GA, Amberlyst/SPEEK

for Amberlyst/SPEEK membrane is also shown in fig. 4.6b, where strong bands of the -OH stretching vibrations are observed at 3442 cm^{-1}. Stretching vibrations of the ring C-H bonds and CH_2 groups of the matrix (cross-linked polystyrene) are observed at 3058 cm^{-1}, 2932 cm^{-1}. The scissoring vibrations of the methylene groups appeared at 1367 cm^{-1}. The deformation vibrations of 1,4-disubstituted benzene ring were also noticed at 980 cm^{-1}. Thus it can be seen that incorporation of amberlyst in the SPEEK formed a significantly different SPE as compared to pure SPEEK (fig. 4.6a).

4.3.1.5 Water uptake

Water uptake is one of the important properties for the solid polymer electrolytes. The water uptake is closely related to other important properties of SPE such as, swelling behavior, ion exchange capacity, and ionic conductivity. The presence of water in the SPE greatly influences the ionomer microstructure, cluster, channel size, as well as plasticizes, and modifies the mechanical strength (Baglio et al., 2005). However, the extremes of water uptake may not be a beneficial property for a suitable SPE for the purpose and may adversely affect the SPE performance. Thus, this section discusses the water uptake by the various SPEs, and the other properties are correlated with the water uptake of the SPEs in the further sections.

Figure 4.7 shows the water uptake of developed SPEs. Water uptake of nafion and SPEEK is shown in fig. 4.7a. It is observed that the water uptake of nafion is less than SPEEK. It is known that 50% sulfonation of PEEK enhances hydrophilicity by introducing the sulfonic acid groups. It depicts that SPEEK is having more sulfonation sites as compared to the nafion membrane thus attracting more water as compared to the nafion membrane due to increased intermolecular association through the polar ionic

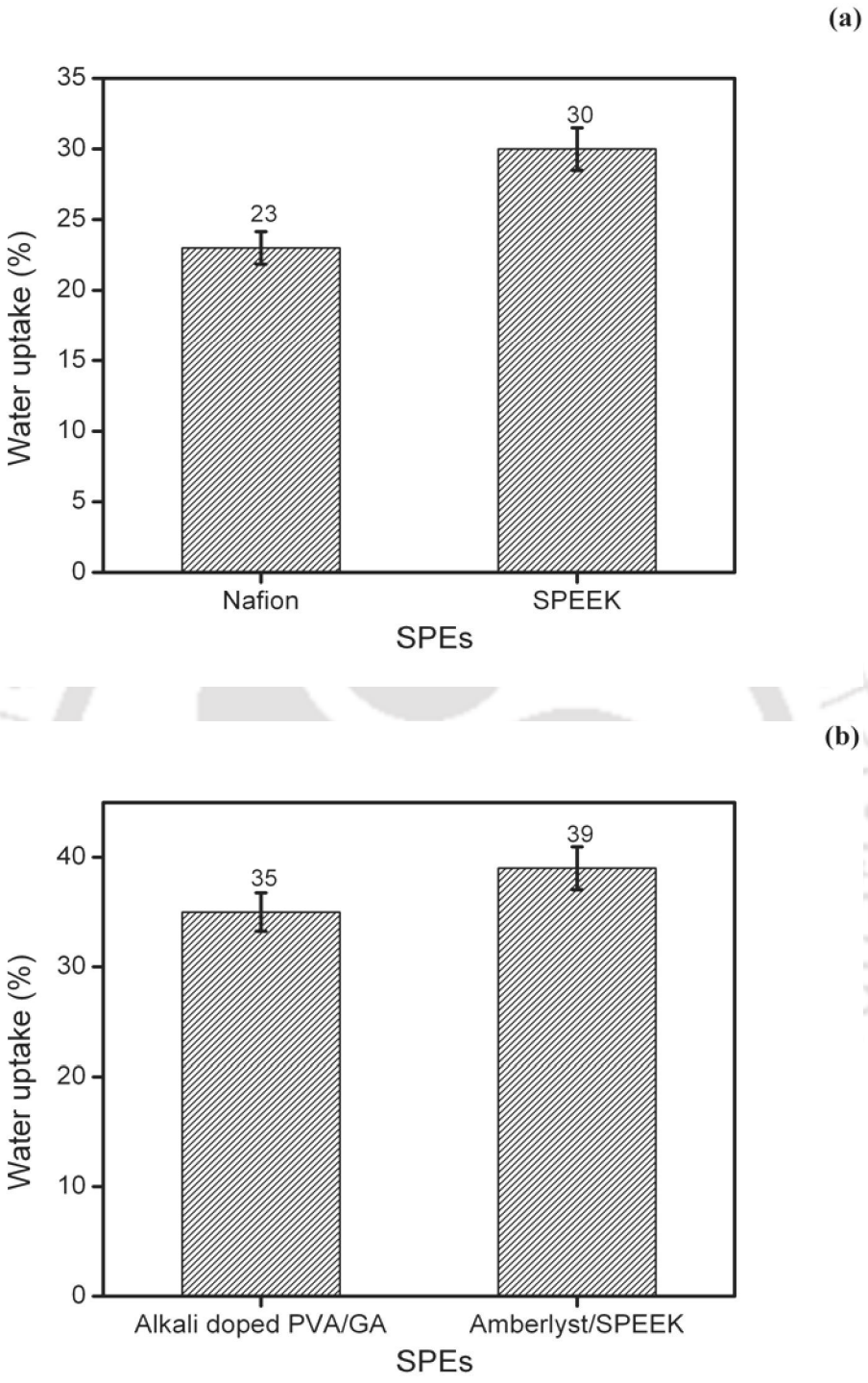

Fig. 4.7 Water uptake of (a) nafion, SPEEK, and (b) alkali doped PVA/GA, Amberlyst/SPEEK

sites. The equivalent weight of SPEEK (degree of sulfonation, 50%) and nafion was 657 $g.eq^{-1}$ and 1100 $g.eq^{-1}$ respectively. Thus lower equivalent weight of SPEEK as compared to the nafion resulted in more water uptake. Figure 4.7b shows the water uptake of alkali doped PVA/GA and Amberlyst/SPEEK anion exchange SPEs. In case of anion exchange SPEs, water molecules get attached to hydroxyl sites. The water enters and exists within the polymer structure as free water, which is presumably located in free volume within the polymer. The action of water molecules to attach the hydroxyl groups on the macromolecules destroys crystallinity by forcing the chains to change configuration from the crystalline planar zig-zag to an amorphous configuration in order to accommodate the effective increase in size of the hydroxyl groups. Amberlyst/SPEEK composite SPE has higher water uptake due to the hydrophilicity of the main structure. The quaternary ammonium groups enable the membrane to accommodate high water content (fig. 4.7b) as compared to the alkali doped PVA/GA. It is supposed that the abundant water may form continuous transfer channel to make the movement of ion easy through the SPEs.

4.3.1.6 Swelling

Swelling is a key factor for mechanical integrity of membranes in the electrochemical cell. During ERC operation, the H^+ ions along with water molecules (hydrated protons) are transported from anode to cathode in case of cation exchange membranes whereas, OH^- ions are transported from cathode to anode along with water molecule for anion exchange membranes. The membrane hydration is very important for the transport of protons through the cation (proton) exchange membranes (nafion, and SPEEK). However, the nafion membrane swells because of water uptake (section 4.3.1.5) by the membrane. The hydration level in the membrane does not decrease due to the plenty of water present at the anode side of the electrochemical reactor. However, there should be a balance

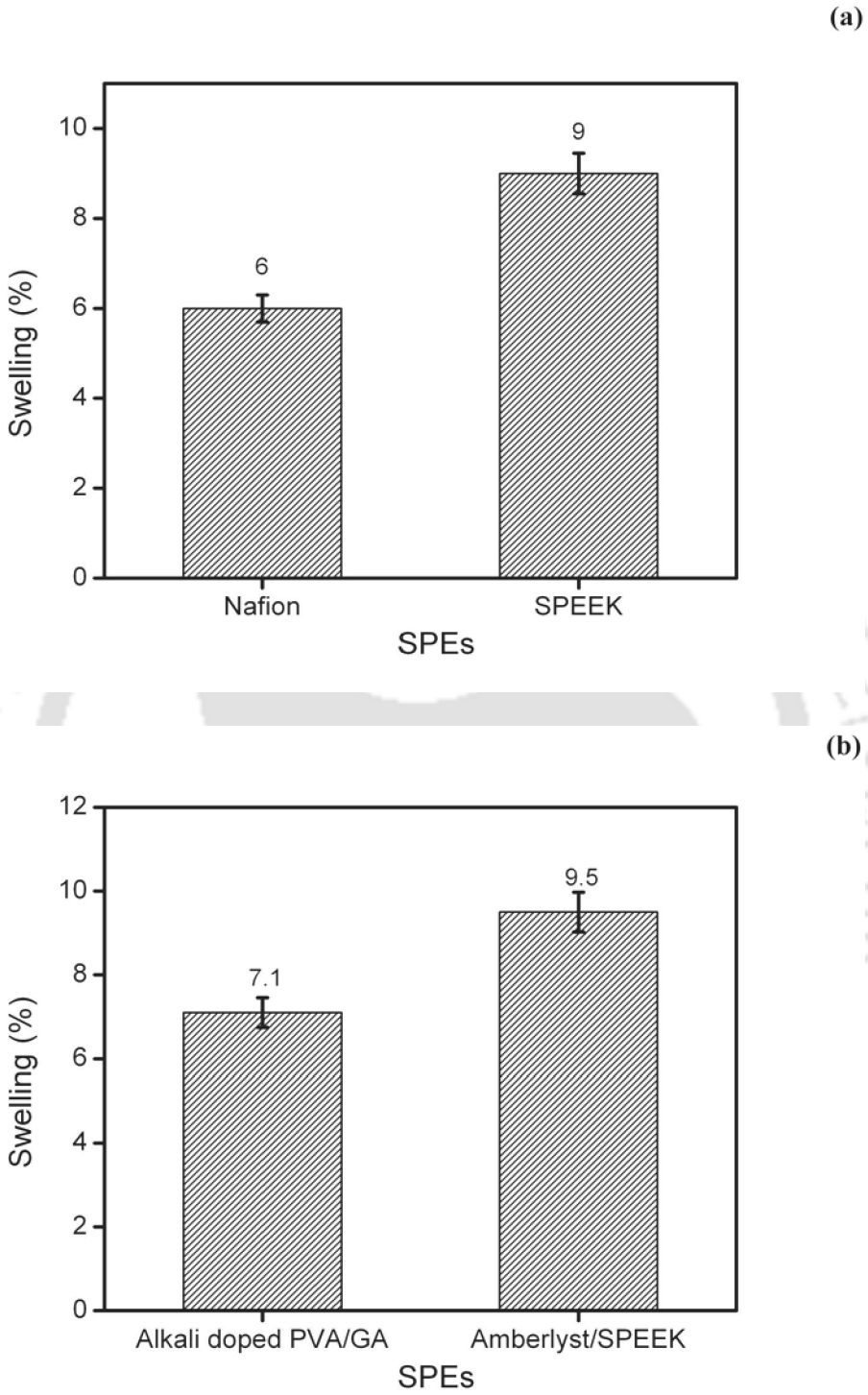

Fig. 4.8 Swelling of (a) nafion, SPEEK, and (b) alkali doped PVA/GA, Amberlyst/SPEEK

between the water uptake (a desired property, upto certain extent, to have proton conductivity) and the swelling (an undesired property). The higher swelling of the membrane during the operation and idle situations may lead to the membrane delamination from the membrane electrode assembly and/or may crack the electrode. Therefore, swelling is one of the most important properties, which is to be evaluated for SPEs. Figure 4.8 shows the swelling of the developed SPEs. SPEEK swells by 9%, which is higher than the nafion (6%) due to the high water uptake of the SPEEK (fig. 4.7a). The alkali doped PVA/GA has around 25% less swelling than the Amberlyst/SPEEK composite membrane. It may be due to the high water uptake of the Amberlyst/SPEEK as shown in fig. 4.7b.

4.3.1.7 Ion exchange capacity

Ion exchange capacity (IEC) is defined as the number of replaceable ions per unit mass of the dry membrane. It is one of the very important characteristics of the polymer electrolyte membrane as it provides an estimate of the acid groups having replaceable H^+ ions in case of cationic SPE and alkali group having replaceable OH^- in case of anionic SPE. The H^+ ions are relatively loosely attached to SO_3^- groups. Therefore, H+ ions are able to move from anode to cathode (as shown in eq. 3.4) via the Grotthuss mechanism, which involves rapid 'hopping' of protons amongst neighboring sites involving solvated H^+ ions (Sandhu et al., 2005; Barbora et al., 2009a) or through vehicular mechanism using hydronium, Zundel, and/or Eigen ions (Kreuer, 2001; Barbora et al., 2010). Similarly, the quaternary ammonium ion having replaceable OH^- are able to move from cathode to anode for the further reaction as shown in eq. 3.4.

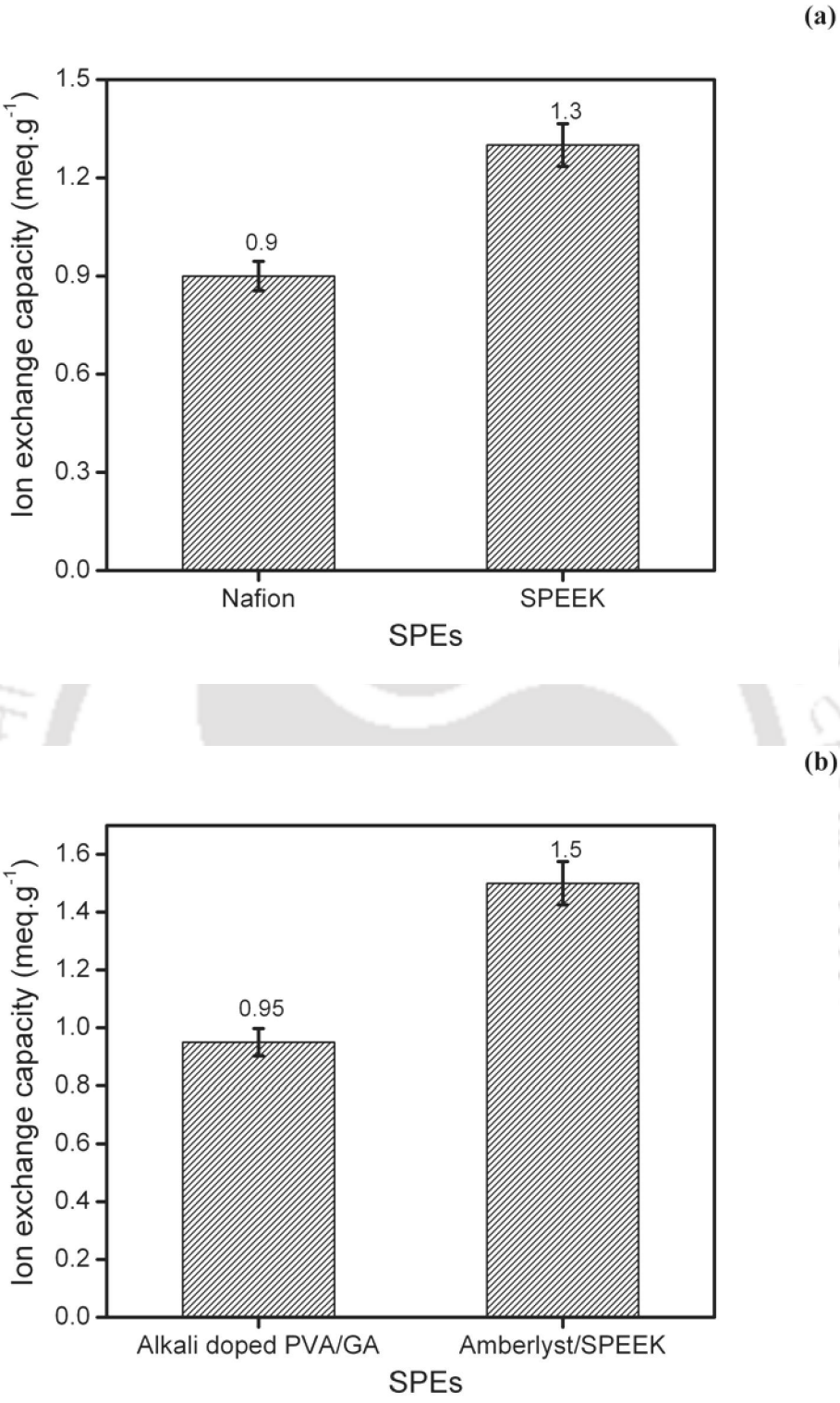

Fig. 4.9 Ion exchange capacity of (a) nafion, SPEEK, and (b) alkali doped PVA/GA, Amberlyst/SPEEK

Figure 4.9a shows the ion exchange capacity of cation exchange SPEs (nafion and SPEEK). It can be seen in the figure that IEC is more for SPEEK than nafion (Li et al., 2003). Usually Perfluorosulfonic polymers combine with the extremely hydrophobic perfluorinated backbone with the highly hydrophilic sulfonic acid functional group in a macromolecule. This gives rise to some hydrophobic/hydrophilic nano-separation especially in the presence of water (Kreuer, 2001). The sulfonic acid functional groups aggregate to form a hydrophilic domain. When the membrane is sufficiently hydrated, protonic charge carriers are formed within the inner space charged layers by the dissociation of the acidic functional groups, and proton conduction occurs with the help of water molecules. The well connected hydrophilic domains are responsible for the transport of protons and water, whereas hydrophobic domains provide the morphological stability and strength to the polymer and prevent the polymer from getting dissolved in the water. Moreover, the hydrophilic zone also assists the proton/water transport in the channels formed within the polymer which is detailed in the next section (Kreuer, 2001). IEC is associated with the mean separation distance between the sulfonic acid groups. The mean separation distance of sulfonic groups in SPEEK is less than the nafion due to low equivalent weight of the former (Mendil-Jakani et al., 2014).

Figure 4.9b shows the ion exchange capacity of alkali doped PVA/GA and Amberlyst/SPEEK. It can be seen that the ion exchange capacity of the alkali doped PVA/GA is lower than the Amberlyst/SPEEK. It can directly be related with the water uptake of the SPEs. The OH^- are easily released by the Amberlyst/SPEEK membrane due to the increased water content of the membrane.

4.3.1.8 Ionic conductivity

Ionic conductivity of the solid polymer electrolyte is another important property. In ERC, the reaction performs efficiently at the interface of the electrolyte and the electrocatalyst. The CO_2 gets adsorbed at the electrocatalyst site and receives the electrons from the outer circuit. The H^+, which was produced at the anode, reach to the site via the electrolyte, and reacts with the adsorbed CO_2 at the interface of the electrolyte/electrocatalyst. Whereas, in case of alkaline electrolyte, the OH^- is produced at electrocatalyst/electrolyte interface of cathode and gets transported to the anode. The OH^- forms O_2 and produce electrons to complete the reaction. It can be seen from the fig. 4.10a that the ionic conductivity of the cationic SPEs is significantly more as compared to the ionic conductivity of the anionic SPEs (fig. 4.10b). It is well known that the conductivity of the solid polymer electrolyte should be as high as possible for the smooth ionic transport in order to complete the reactions for efficient ERC.

Nafion membrane is a good proton conductor due to the presence of loosely held hydrogen ions (protons), which are attached to the fixed sulphonic acid sites in the polymer chain. The protons along with the surrounded water molecules available in the membrane form hydronium ions and diffuse through the flooded pore channels of the membrane to contribute for the proton conductivity (Choi et al., 2005a). Moreover, the protons are also transported through hopping mechanism via hydronium, Zundel and/or Eigen ions (Kreuer, 2001, Barbora et al., 2009b). Thus water is important for the transport of protons in both the mechanisms (vehicular or hopping). Moreover, as the protons should be loosely held with the sulphonic acid groups, the IEC also plays an important role as discussed earlier. The replaceable character of the hydrogen ion from the sulphonic site has been discussed in terms of the IEC (section 4.3.1.7). The fixed charged (SO_3^-) sites within the main polymer chain provide the centers where the moving ions (protons) can be accepted or released.

The ionic (H^+) conductivity of the nafion was found to be around 80 $mS.cm^{-1}$. However, the H^+ conductivity of the SPEEK was only about 19 $mS.cm^{-1}$. It is quite interesting to observe that, though the water uptake as well as the ion exchange capacity of SPEEK was more than the nafion but the ionic conductivity was found less. Usually the trend followed by ionic conductivity is similar to IEC and water uptake. Nevertheless, this may not necessarily be the rule of thumb as increase in water uptake or ion exchange capacity may not necessarily increase the proton conductivity of the membranes. The IEC and water uptake contribute to proton conductivity by facilitating the transfer of protons while at the same time the connectivity of the ion exchange channels within the membrane are also crucial for effective proton conductivity (Kreuer, 2001). Immersion of SPEEK membrane in water allows the molecular rearrangements of nanostructure in the membrane and provides a well-defined interface between hydrophilic and hydrophobic phases whereas nafion has intrinsically nano-phase separated channels (Mendil-Jakani et al., 2014). This nano-phase separation observed in case of nafion and provides the explanation for its higher conductivity than SPEEK. Therefore, in spite of having higher IEC and water uptake than nafion in Amberlyst/SPEEK membrane, it does not possess high ionic conductivity. The channels size and geometry present in the membrane also influences the ionic conductivity by a large extent. It is discussed earlier that the equivalent weight of the SPEEK is quite low as compared to the nafion and thus the water filled channels of SPEEK may be narrower as compared to those in nafion, which is conceptualized in the fig 4.11. It can be seen that the channels in the SPEEK are having less separation and more branched with more dead-end "pockets". These features correspond to the larger hydrophilic/hydrophobic interface and, therefore, a larger average separation of neighboring sulfonic acid functional groups. The strong

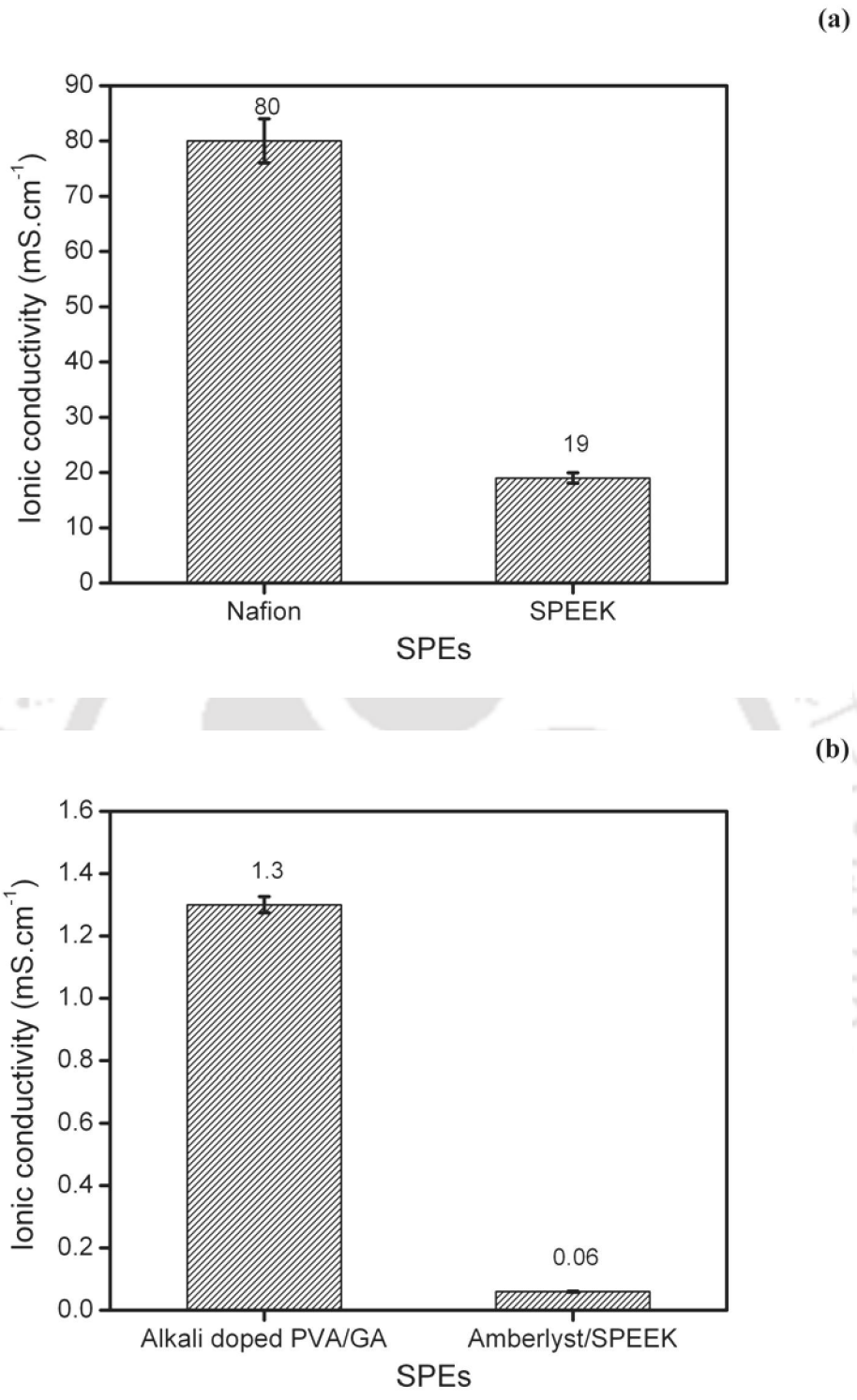

Fig. 4.10 Ionic conductivity of (a) nafion, SPEEK, and (b) alkali doped PVA/GA, Amberlyst/SPEEK

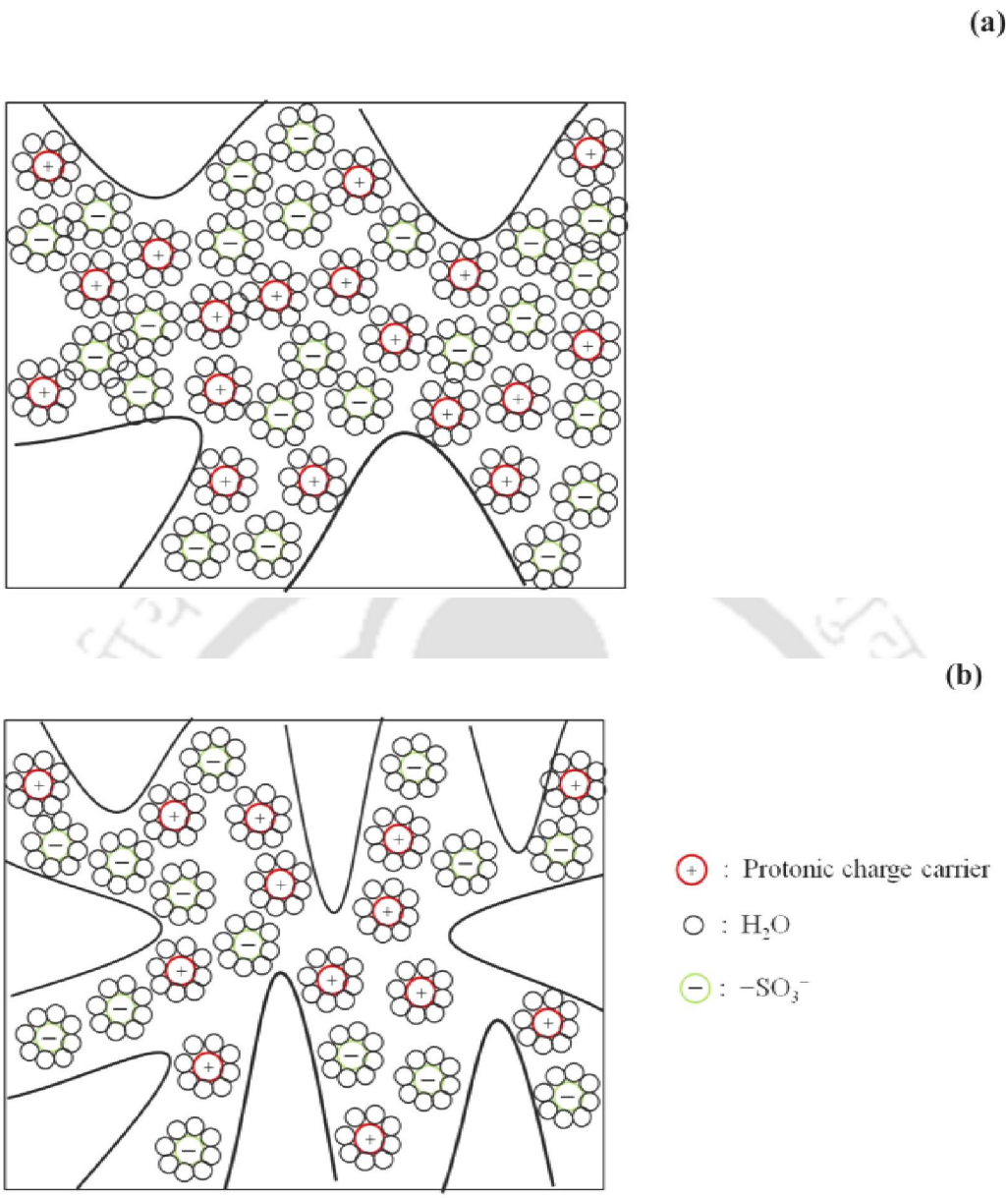

Fig. 4.11 Comparsion of structures: (a) nafion, (b) SPEEK

confinement of the water in the narrow channels of the aromatic polymers leads to significant resistance to the transport of hydrated ion. The absorbed KOH in the PVA/GA matrix was the primary source of the hydroxyl ion conductivity, whereas in case of Amberlyst/SPEEK the hydroxyl ions were the functional sites in the amberlyst. Therefore, the ionic conductivity of alkali doped PVA/GA was 1.3 $mS.cm^{-1}$ as compared to 0.06 $mS.cm^{-1}$ for Amberlyst/SPEEK as shown in fig. 4.10b. The OH^- ion conductivity

obtained by the doping of 2 M KOH solution was used and reported for the alkali doped PVA/GA as it was the maximum ionic conductivity found for this case. However, it was observed that the ionic conductivity was decreased with the increased concentration of KOH. The doping by higher KOH concentration (above 2M) in solution does not simply make additional contribution to the conductivity. The membrane samples were found to be supernatant with KOH at high doping concentration. It seems that more OH^- can not be taken into the polymer due to the weak ionic mobility (such as formed ion-pairs or increased viscosity), thus resulting in decreased ionic conductivity. The ionic conductivity of Amberlyst/SPEEK was significantly low as compared to alkali doped PVA. It may be due to the incorporation of quaternary ammonium based resin in the SPEEK, which might cause some disruption in the continuum of hydrophilic channels or the sulfonic group clusters. Thus, either the ion movement is taking a longer path or the hindrance in the ion movement is resulting in the drop of hydroxyl ion conductivity. Infact, on comparing the ion exchange capacity, water uptake, and hydroxyl ion conductivity of the Amberlyst/SPEEK composite membrane, it was found that higher water uptake did not inevitably result into the higher hydroxyl ion conductivity (Choi et al., 2005b). Inclusion of additives in SPEEK changes the morphology of the membrane by changing the shape of the ionic cluster and water content, which subsequently results in variation of the ionic conductivity of the composite membranes.

4.3.1.9 Tensile strength

It has been already discussed that the membrane is sandwiched between the electrodes and placed into the ERC cell casing under a particular pressure. The cation exchange SPEs and anion exchange SPEs have different compressive strength.

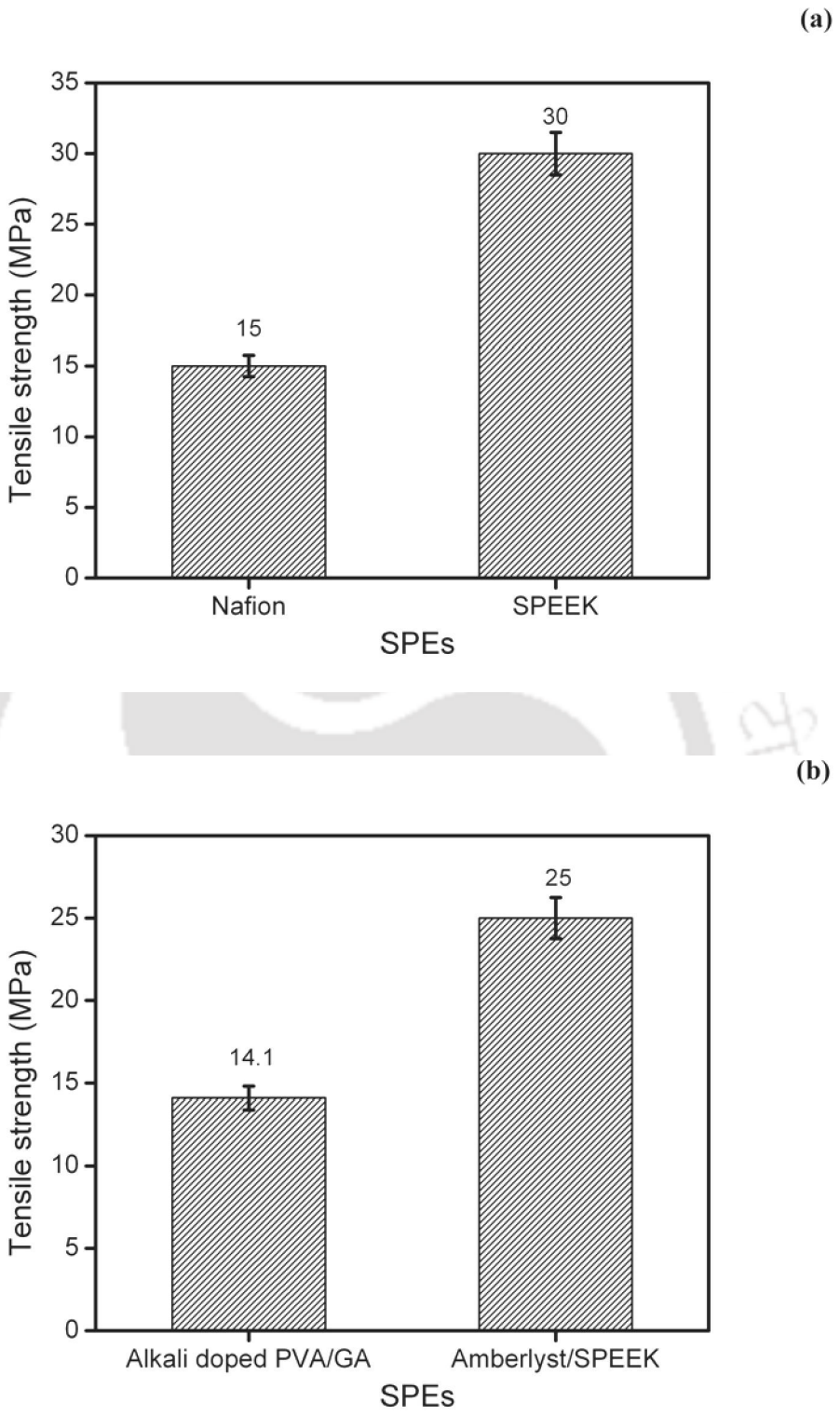

Fig. 4.12 Tensile strength of (a) nafion, SPEEK, and (b) alkali doped PVA/GA, Amberlyst/SPEEK

However, membrane swelling occurs during the ERC cell operation, which may produce linear variation in the longitudinal direction. Thus, the membrane is generally tested for its mechanical strength using tensile strength (Liu et al., 2003; Park et al., 2012). Therefore, tensile strength is an important property, which needs to be evaluated. A membrane with good tensile strength is expected to be used for longer duration in the reactor and can cope up with various mechanical conditions. The tensile strength for the nafion and SPEEK was found to be 15 MPa and 30 MPa, respectively as shown in fig. 4.12 a. The tensile strength of the alkali doped PVA/GA and Amberlyst/SPEEK membrane is found to be 14.11 MPa and 25.7 MPa, respectively as shown in fig. 4.12 b.

4.3.2 Electrode characterization

Electrode plays a vital role in the performance of any electrochemical system. In electrochemical conversion of CO_2, the gas phase CO_2 has to reach upto the electrocatalyst layer at the electrode, which is made up of carbon paper. The morphological structure of carbon paper is shown in the SEM image in the fig. 4.13a. The carbon paper (gas diffusion layer) was used to support the Pt/C catalyst to fabricate the anode for the ERC system. The morphology of the anode shows the porous structure for the transport of water from one face (which was not coated by the catalyst) to the other face of the carbon paper having Pt/C catalyst layer. It can be seen that the carbon paper is made up of compressed carbon fibers (fig. 4.13a) and it has significant porosity. However, after the deposition of catalyst layer the porosity of the electrode is comparatively reduced but still enough porosity is present (fig. 4.13b) to transport water through it.

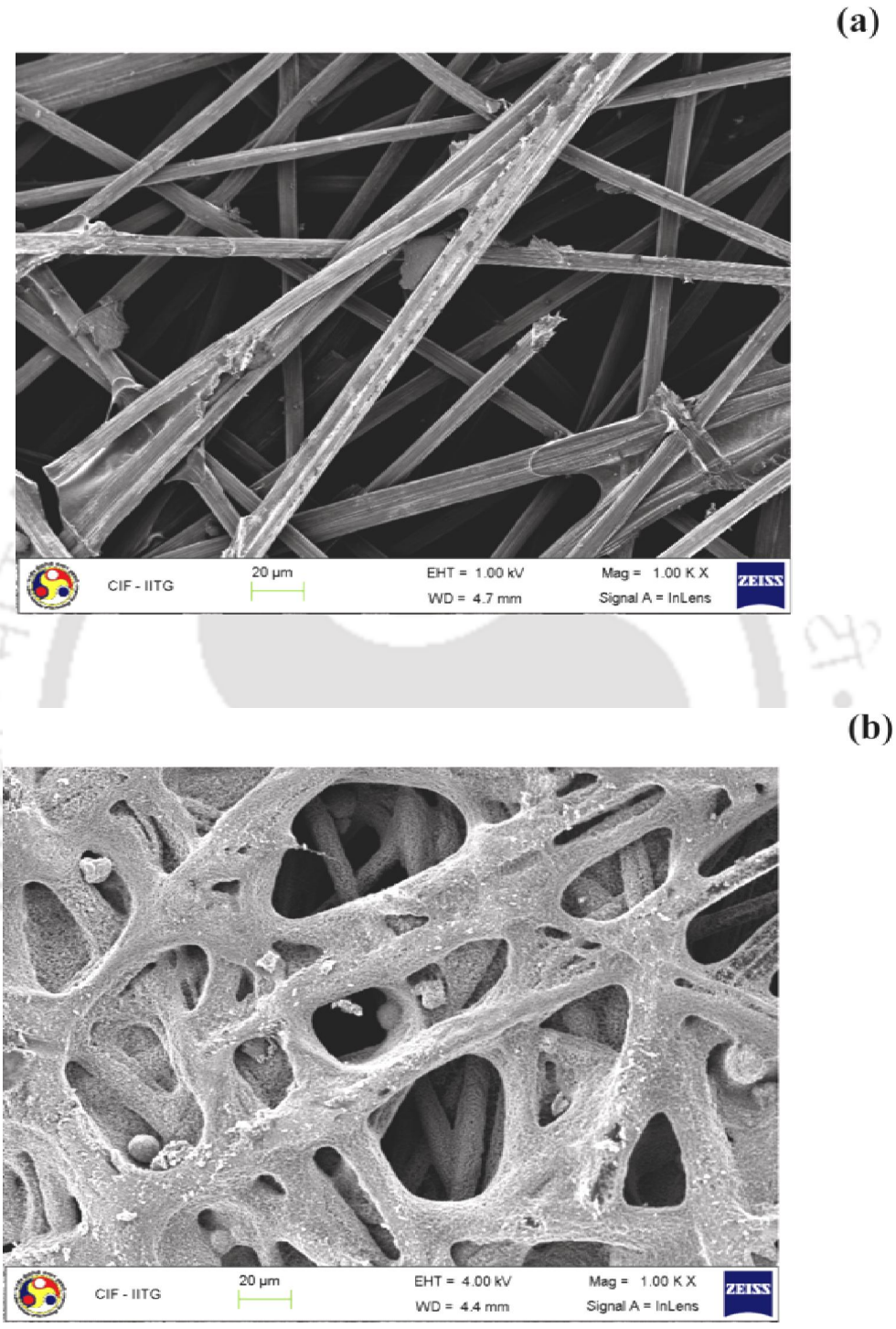

Fig. 4.13 SEM image of (a) pure carbon paper and (b) Pt/C on carbon paper.

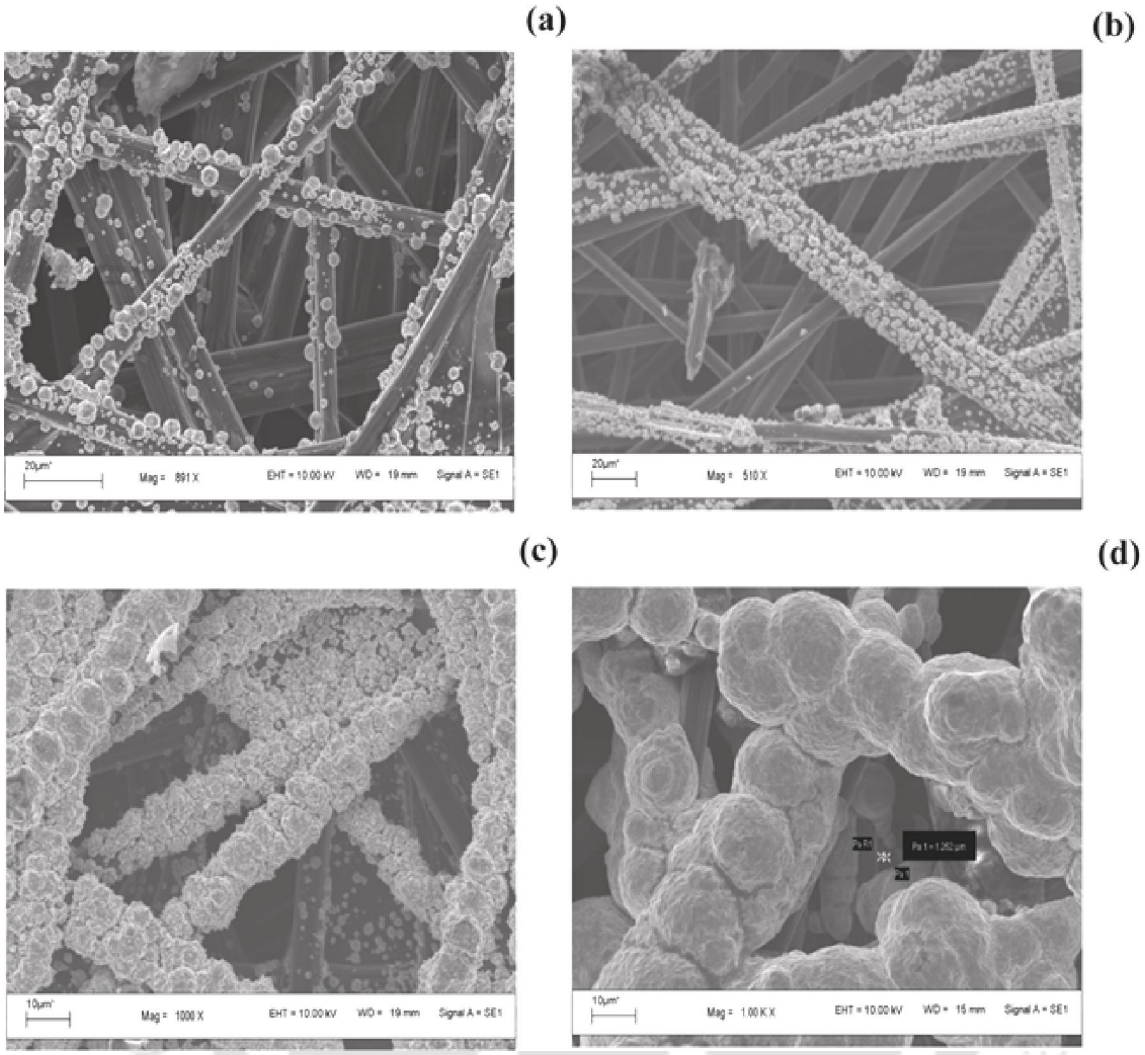

Fig. 4.14 SEM images of electrodeposited copper on carbon paper for different time of electroplating: (a) 1 min, (b) 2 min, (c) 5 min, and (d) 15 min

The cathode was also prepared using carbon paper as a support. The cathode electrocatalyst (Cu) was electroplated on one face of the carbon paper as discussed in section 3.2.2. The SEM images of the electrodeposited Cu on the carbon paper for different electroplating time are shown in the fig. 4.14. The aim to perform the electroplating for different time is to know (qualitatively) the porous structure of the cathode so as to facilitate gaseous CO_2 transport through the electrode. Therefore, the

electrodeposition was conducted for different time intervals to find out the optimum Cu loading on the carbon paper.

Figure 4.14 shows the deposition of copper on to the carbon fibers for different time intervals. In fig. 4.14a and 4.14b, it can be observed that the porosity of the carbon paper was hardly reduced but at the same time the copper deposition was not done thoroughly on to the carbon fiber strands. When the copper deposition was conducted for 5 min (fig. 4.14c) almost all the carbon fibers were coated by the copper. Moreover the porosity was not reduced significantly. The electrodeposition was conducted for different time intervals but it was observed that the agglomerates of the copper significantly increased and the porosity of carbon paper reduced quickly. A representative SEM image for the Cu electrodeposited on carbon paper for 15 min is showed in fig. 4.14d. The catalyst loading of copper on the carbon paper was calculated with the help of Faraday's laws of electrolysis. In order to have the catalyst loading of 2 $mg.cm^{-2}$, theoretically 4.56 min are required. However, practically 5 min are required (confirmed by weighing method) to prepare the cathode with 2 $mg.cm^{-2}$ catalyst loading (Aeshala et al., 2012).

4.3.3 Performance evaluation of dERC using developed SPEs

The following section provides the results and discussion on the evaluation of dERC using cationic and anionic SPEs.

4.3.3.1 Cationic SPE

4.3.3.1.1 Nafion SPE

The gaseous CO_2 was fed into the electrochemical reactor and various products were obtained at different applied voltages in the range of 1.8 V to 3 V. Figure 4.15 shows the current density as a function of applied voltage in the direct electrochemical reduction of CO_2 (dERC). The current density increases with the increase in the applied voltage for nafion SPE, which indicate that the rate of the reactions increases with the increase in the applied voltage. The increased reaction rate corresponds to the increased rate of electrical charge consumed by the various electrochemical reactions at the electrodes. Current density increases from 8.8 $mA.cm^{-2}$ at 1.8 V to 14.8 $mA.cm^{-2}$ at 3 V. This current density corresponds to formation of products such as CH_4, CH_3OH, CO, and HCHO during the reaction in ERC along with H_2 as by-product. It can be seen in the fig. 4.16 that amount of methane increases sharply up to 2 V, thereafter decreases gradually along with the formation of comparatively minor quantities of CH_3OH, CO, and HCHO. Hydrogen is generated due to water electrolysis (competitive reaction at the cathode) as a by-product in ERC. The H_2 generation increases with increase in current density at all applied voltages. It is interesting to note (fig. 4.16) that increasing the applied voltage up to a certain extent, results in increased product formation. However, on further increase in the applied voltage, the H_2 evolution follows the pattern of current density, whereas products except H_2 formation reactions reduces as reaction kinetics increases significantly at higher

applied voltages. It can be seen that most of the energy was utilized for H_2 generation as compared to the ERC products. It can be seen that 8.8 µmol of methane was formed during ERC (25 min) at 2 V. Thereafter, methane formation decreases but hydrogen evolution increases up to 952 µmol.

The applied voltage was primarily utilized for hydrogen evolution, which was in competition with CO_2 reduction reaction. The possible reason may be that proton and electron transfer were heavily favoured at high potential values and as a result, either the coverage of adsorbed H was increased or the Heyrovsky mechanism for H−H bond formation becomes more dominant pathway for hydrogen evolution (Kuhl et al., 2012).

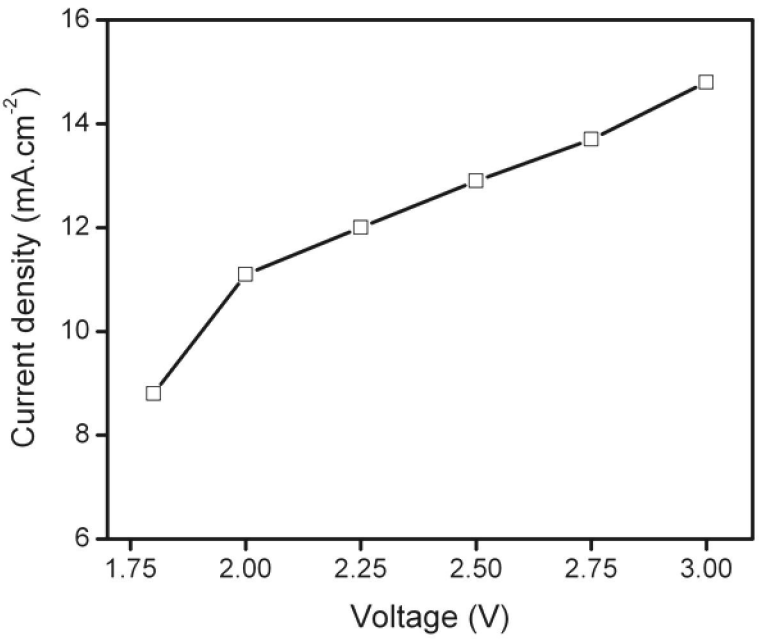

Fig. 4.15 Current density obtained as a function of applied voltage using nafion

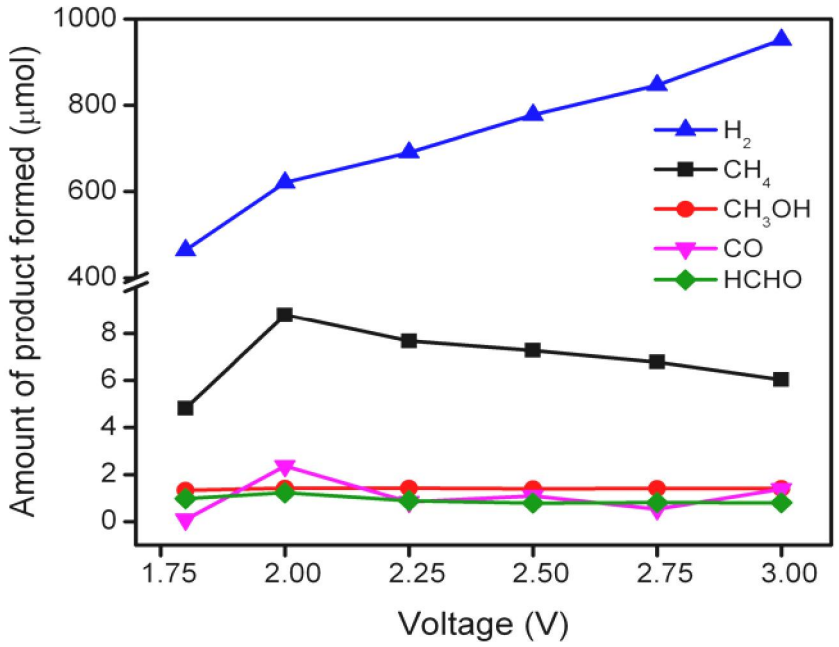

Fig. 4.16 Amount of products formed as a function of applied voltage using nafion

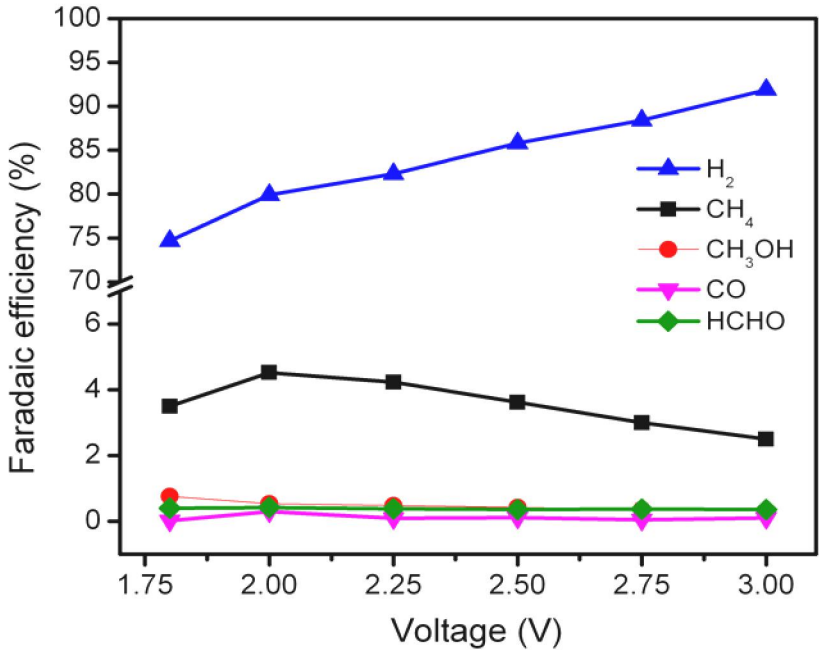

Fig. 4.17 Faradaic efficiency as a function of applied voltage using nafion

Figure 4.17 shows the Faradaic efficiency of the products obtained in ERC using the nafion membrane. Calculation of Faradaic efficiency was discussed in section 3.4.2. Faradaic efficiency is an important parameter to understand the CO_2 reduction selectivity (Jhong et al., 2013).

The products obtained were CH_4, CH_3OH, CO, and HCHO with maximum Faradaic efficiencies of 4.52%, 0.54%, 0.3, and 0.42%, respectively, at 2 V with a corresponding current density of 11.1 $mA{\cdot}cm^{-2}$. Faradaic efficiency follows the same trend as product distribution for dERC using nafion membrane as SPE. Higher Faradaic efficiency of methane at 2 V may be due to the increase in mass transfer of CO_2 to the electrode surface, leading to an increase in the concentration of CO_2 available for the reaction. Thereafter, Faradaic efficiency decreases continuously. It may be noted that at higher voltages the current density increases (fig. 4.15) resulting in more hydrogen generation, which is evident in fig. 4.16, results due to consumption of H^+ reaching at the cathode from the anode. Hence, reduced H^+ concentration at the cathode affects the further ERC.

4.3.3.1.2 SPEEK SPE

Figure 4.18 shows the current density as a function of applied voltage in the direct electrochemical reduction of CO_2 using SPEEK as a SPE. The current density increases with the increase in the applied voltage for SPEEK SPE. Current density increases from 7.7 $mA.cm^{-2}$ at 1.8 V to 11.8 $mA.cm^{-2}$ at 3 V. This current density corresponds to formation of products such as CH_4, CH_3OH, CO, and HCHO during the reaction in ERC along with H_2 as by-product. The current densities are slightly less using SPEEK SPE in ERC compared to current densities obtained using nafion SPE. It is mainly due to the higher resistance posed by SPEEK due to its low ionic conductivity as compared to nafion.

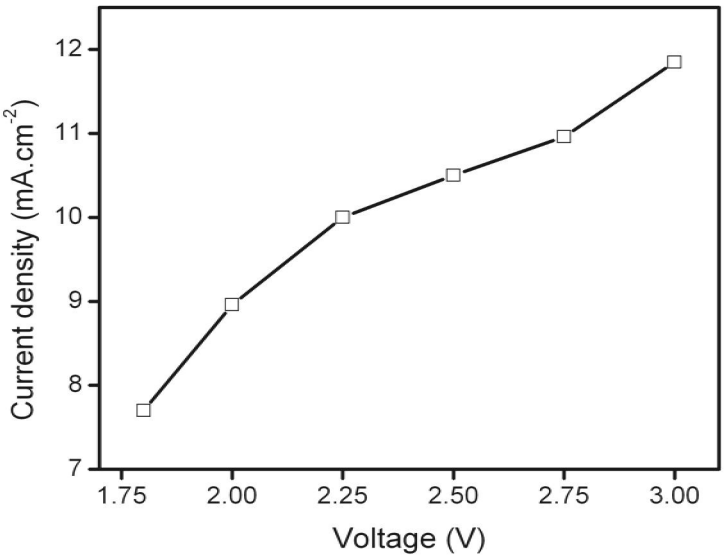

Fig. 4.18 Current density obtained as a function of applied voltage using SPEEK

Figure 4.19 shows that product distribution as a function of applied voltage in dERC using SPEEK. It was found that the proton conducting membranes (nafion and SPEEK) resulted in the formation of same kind of products. Maximum amount of methane was formed at 2 V similar to the nafion SPE and corresponds to total current density of 8.96 $mA.cm^{-2}$ (fig. 4.18). As the potential increases, the amount of methane formation decreases and hydrogen evolution increases. It follows the same trend as the nafion. It happens because both the nafion and SPEEK are acidic membranes having similar functional groups. Even though ionic conductivity is less as compared to the nafion but water uptake is more in SPEEK, therefore hydrogen generation was quite comparable with the nafion. The amount of hydrogen generated is 753 µmol at potential of 3 V, which is 26% less than the nafion SPE (fig. 4.19). Minor amounts of product such as CH_3OH, CO, and HCHO were formed, which were not varied significantly with increased voltage.

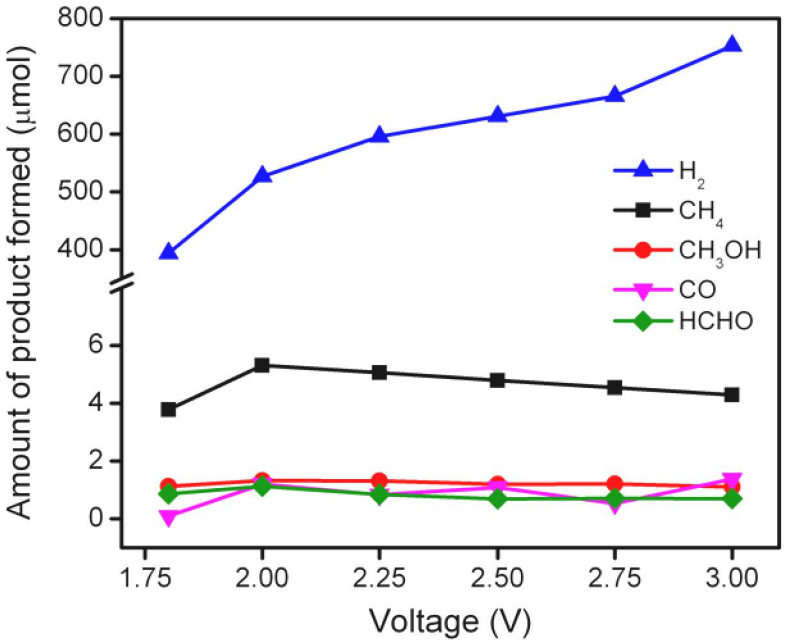

Fig. 4.19 Products obtained as a function of applied voltage using SPEEK

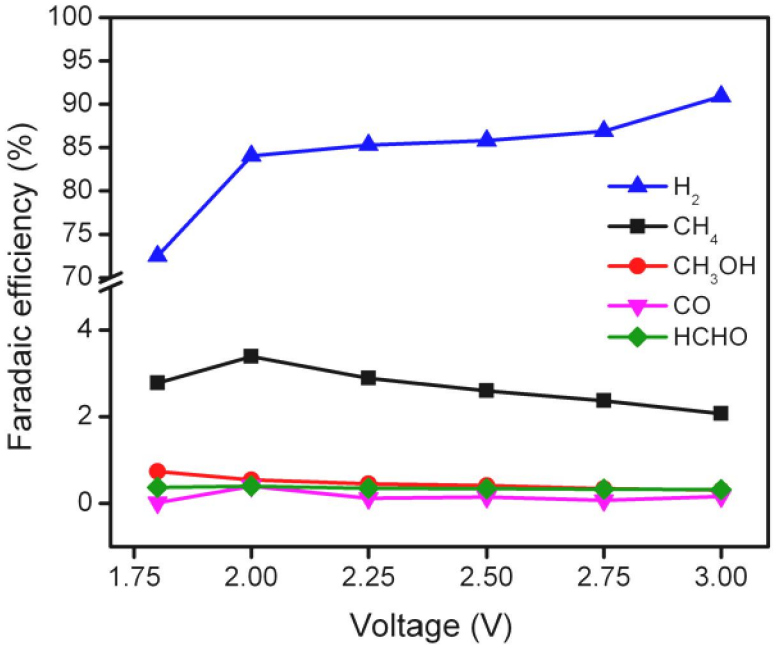

Fig. 4.20 Faradaic efficiency as a function of applied voltage using SPEEK

The Faradaic efficiency of H_2 reaches 90% in ERC using SPEEK as shown in fig. 4.20. The maximum Faradaic efficiency of 3.3% was obtained for CH_4 at a voltage of 2 V and current density of 8.9 $mA \cdot cm^{-2}$. The Faradaic efficiencies of the products using SPEEK membrane were less as compared to the nafion. It is because of the low proton conductivity of the SPEEK as compared to nafion. The Faradaic efficiency of methane increases upto 2 V, and decreases gradually afterwards due to the same reasons as in case of nafion.

4.3.3.2 Anionic SPE

4.3.3.2.1. Alkali doped PVA/GA SPE

Figure 4.21 shows the current density as a function of applied voltage in the direct electrochemical reduction of CO_2 using alkali doped PVA/GA. It is observed that the current density or rate of the reaction increases with increase in the applied voltage for alkali doped PVA/GA SPE. The increased reaction rate due to increase in current density corresponds to the increased rate of electrical charge being used in the process. The current density increases from 5.18 $mA.cm^{-2}$ at 1.8 V to 8 $mA.cm^{-2}$ at 3 V. It may be noted that the current densities corresponding to various voltages are lower in the case of alkali doped PVA compared to cation exchange membranes (nafion and SPEEK). It may be due to the lower ionic conductivity of the alkali doped PVA SPE than nafion and SPEEK SPEs.

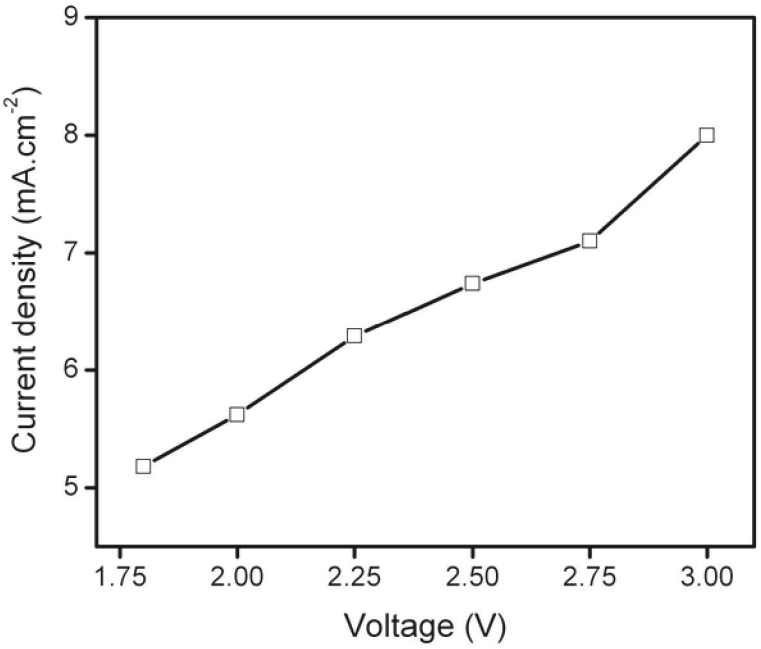

Fig. 4.21 Current density obtained as a function of applied voltage using alkali doped PVA/GA

Figure 4.22 shows the product distribution as a function of applied voltage in the direct electrochemical reduction of CO_2 using alkali doped PVA/GA. The CO was formed as a major product along with CH_4 and HCOOH as minor products during dERC. Amount of CO increases sharply up to 2 V, and decreases gradually thereafter along with the formation of comparatively minor quantities of CH_4 and HCOOH. Amount of hydrogen formed was less compared to cation exchange SPEs. The hydrogen evolution increases with voltage and reaches 459 µmol at 3 V. It may be interesting to note that in case of alkali doped PVA/GA membrane, the major product obtained was CO. It shows that reaction mechanism is entirely different and probably the reaction zone has selectivity for hydrogen. However, the generation of CO was significantly higher than any of the products formed in case of cationic membranes as discussed in the previous sections.

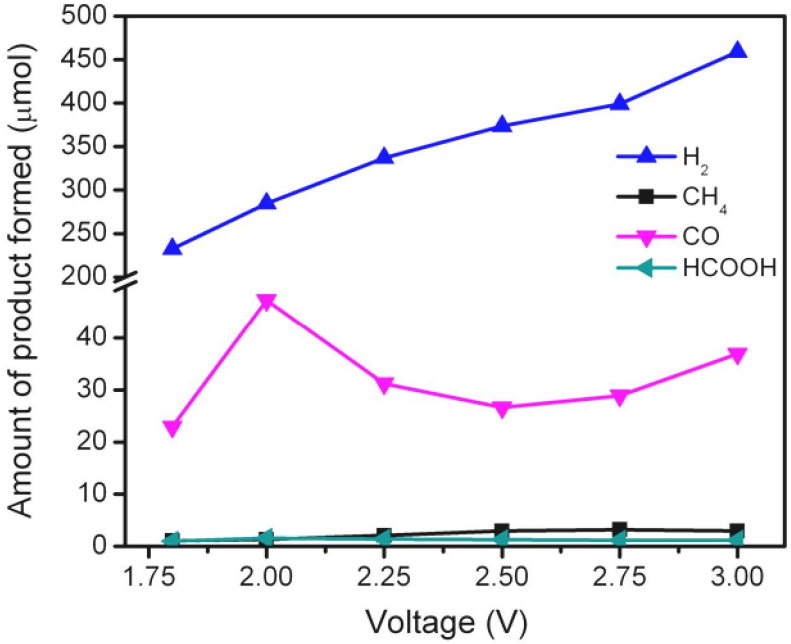

Fig. 4.22 Product obtained as a function of applied voltage using alkali doped PVA/GA

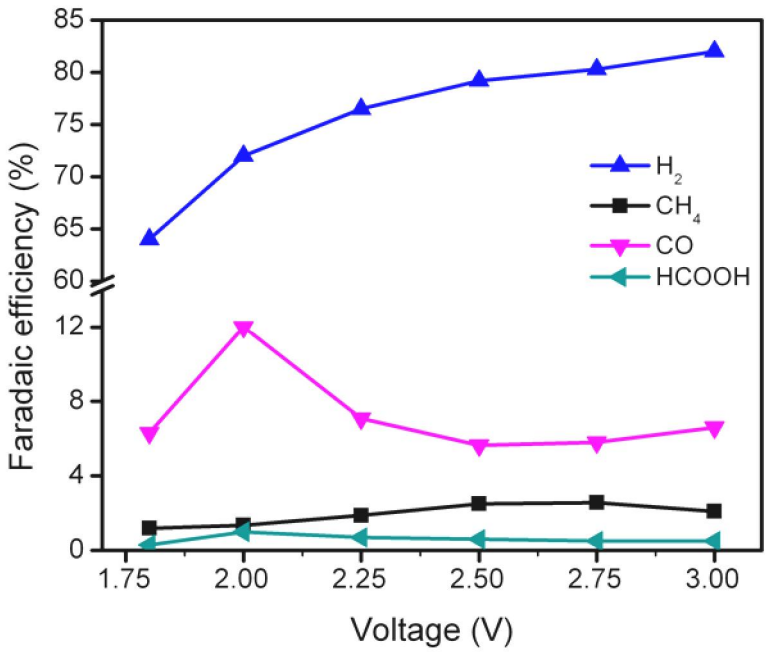

Fig. 4.23 Faradaic efficiency as a function of applied voltage using alkali doped PVA/GA

Although the generation of CH_4 and HCOOH was in minor quantities but it was higher than any other minor product formed in case of cationic membranes.

Figure 4.23 shows Faradaic efficiency of the products obtained in ERC using the alkali doped PVA/GA. Primarily, CO was formed and thus shows the maximum Faradaic efficiency of 12% at a voltage of 2 V and corresponding current density of 5.6 $mA{\cdot}cm^{-2}$ apart from the undesired hydrogen gas as a by-product. The Faradaic efficiencies of CH_4 and HCOOH were low but in case of CH_4 the Faradaic efficiency was around 2.5 %, which was almost double of the minor products reported for cationic membranes (nafion and SPEEK). The Faradaic efficiency of hydrogen evolution was found as high as 82% at 3 V (Aeshala et al., 2012).

4.3.3.2.2. Amberlyst/SPEEK SPE

Figure 4.24 shows the current density as a function of applied voltage in the direct electrochemical reduction of CO_2 using Amberlyst/SPEEK membrane. Similar to other cases, the current density increases with the increase in applied voltage for Amberlyst/SPEEK SPE too. Moreover, the current density increases almost linearly with the voltage. The overall current density increases from 3.11 $mA.cm^{-2}$ at 1.8 V to 4.66 $mA.cm^{-2}$ at 3 V showing the increased rate of the reaction with applied voltage.

Figure 4.25 shows the product distribution obtained as a function of applied voltage in the ERC using Amberlyst/SPEEK. It is quite interesting to see that though the Amberlyst/SPEEK was a composite made up of 1% anion exchange resin (amberlyst) and cationic polymer (SPEEK) but the reaction products were same as in the anionic SPE (alkali doped PVA/GA). Moreover, it has significant ionic conductivity for hydroxyl ion as shown in fig. 4.10b. Therefore, it can be concluded that the Amberlyst/SPEEK

composite membrane worked as an anionic SPE. The product distribution follows the same trend as for alkali doped PVA/GA. It can be seen that the CO was formed primarily as the product with the maximum amount of 37.4 µmol at 2 V. The formation of other products (CH_4 and HCOOH) is quite low and the quantity formed is less than 2 µmol at any of the applied voltage as shown in fig. 4.25.

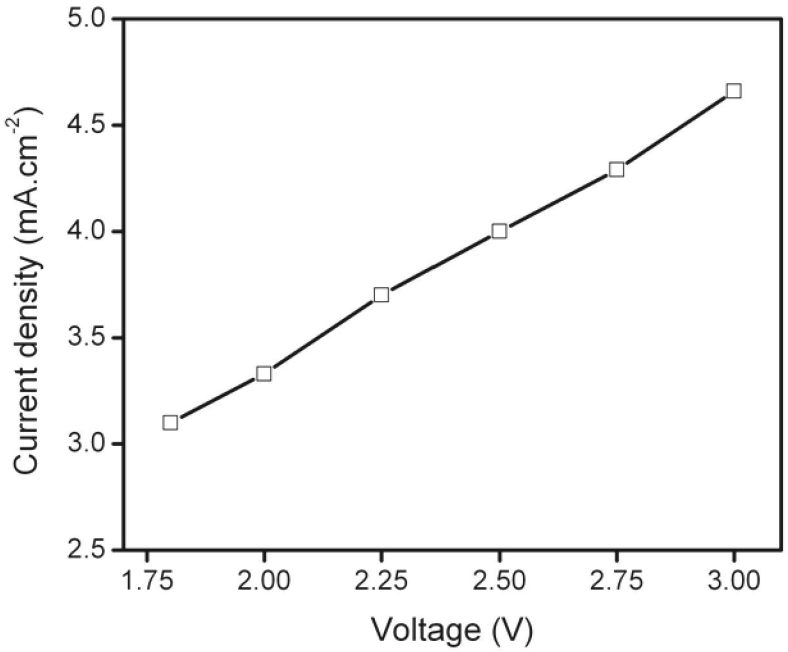

Fig. 4.24 Current density obtained as a function of applied voltage in the ERC using Amberlyst/SPEEK

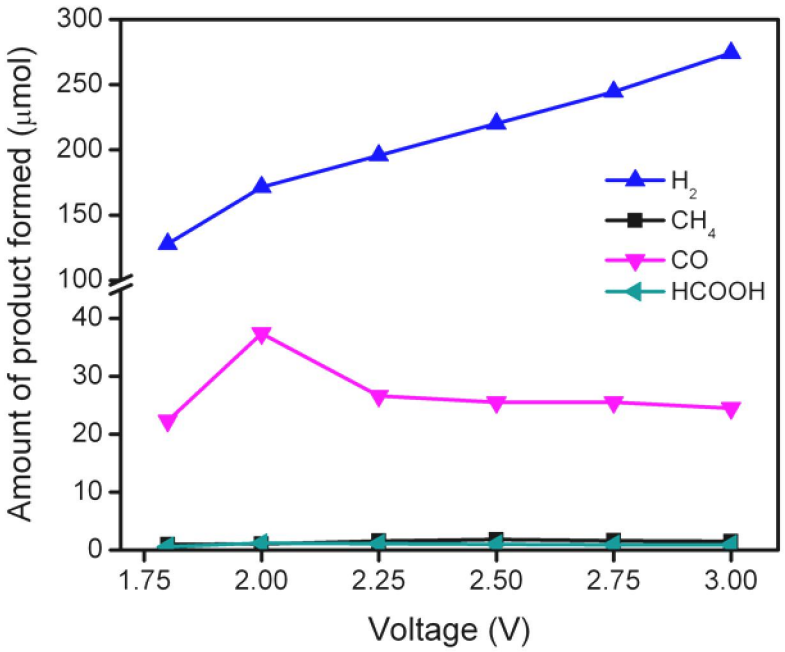

Fig. 4.25 Products obtained as a function of applied voltage in the ERC using Amberlyst/SPEEK

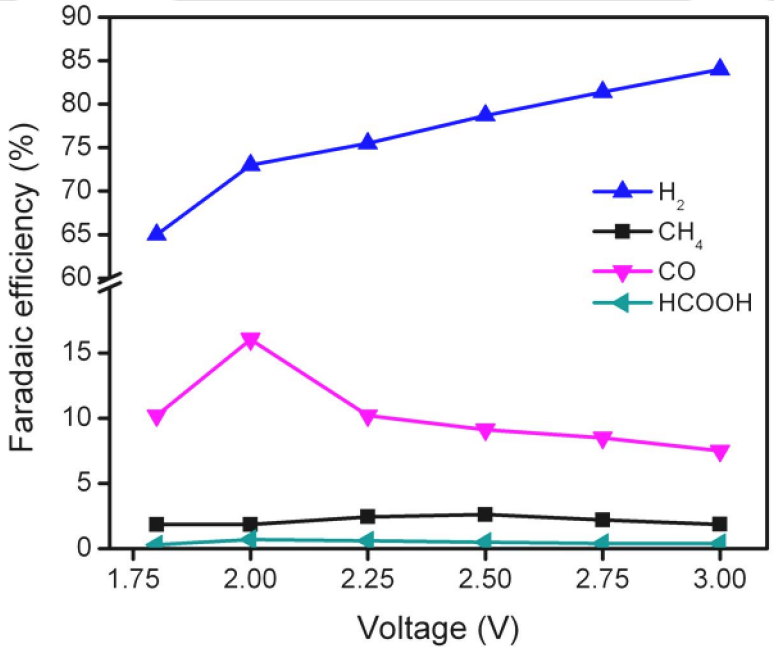

Fig. 4.26 Faradaic efficiency as a function of applied voltage in the ERC using Amberlyst/SPEEK

Figure 4.26 shows Faradaic efficiency of the products obtained in ERC using the Amberlyst/SPEEK. The CO was formed primarily and thus shows maximum Faradaic efficiency of 16% at a voltage of 2 V (fig. 4.26) and corresponding current density of 3.3 $mA \cdot cm^{-2}$ (fig. 4.24) apart from the undesired hydrogen gas as a by-product. It is observed that the anionic conductivity of the composite Amberlyst/SPEEK was significantly low as compared to alkali doped PVA and the total reaction products was lower than the alkali doped PVA membrane at particular voltage. It may be due to the low anionic conductivity of Amberlyst/SPEEK SPE (Aeshala et al., 2012).

Results were compared for the developed SPEs in the dERC and shown in table 4.2. It is observed from the table 4.2 that overpotential for the formation of major product is less in the case of anion exchange membranes even though these membranes have low ionic conductivity. The hydrogen evolution was also greatly suppressed for dERC using anion exchange membranes.

Table 4.2 Comparison of dERC performance at maximum Faradaic efficiency of the major product (2 V)

SPEs		**Product**	**Thermodynamic Voltage (V)**	**Overpotential (V)**	**SPE conductivity ($mS.cm^{-1}$)**
Cationic	Nafion	CH_4	-1.06	0.94	80
	SPEEK	CH_4	-1.06	0.94	19
Anionic	PVA/GA/KOH	CO	-1.34	0.66	1.3
	Amberlyst/SPEEK	CO	-1.34	0.66	0.06

Figure 4.27 and 4.28 shows the selectivity of the products using nafion, SPEEK, alkali doped PVA/GA, and Amberlyst/SPEEK in dERC. In cation exchange SPEs, high selectivity of CH_4 is obtained at all voltages in dERC, whereas, in case of anion exchange SPEs, high selectivity of CO was obtained at all voltages. Liquid products were also obtained in the dERC using developed SPEs. CH_3OH was obtained selectively in the range of 10-20% using cation exchange SPEs (nafion and SPEEK), whereas HCOOH was obtained selectively in the range of 2-4% using anion exchange SPEs (alkali doped PVA/GA and Amberlyst/SPEEK).

To understand the influence of the membrane effectively, it is required to know the parameters (functional groups, polymer backbone, and other vital properties) which are really playing significant role in the dERC. Based on the present observations, following changes were introduced in the dERC system for further study,

- selection of membranes, which have the same polymer backbone with different functional groups,
- pulse electrolysis instead of constant electrolysis,
- copper oxide instead of copper as cathode electrocatalyst, and
- duration of experiments for 25 min rather than 1hr.

The reasons for the above changes are based on the literature, experience, and learning on the dERC. It was reported that copper was a unique material for the formation of hydrocarbons. Therefore, in the present system, gaseous phase ERC was studied using copper as an electrocatalyst and experiments were carried out using constant mode electrolysis. However, it was observed after the dERC experiments that the electrode

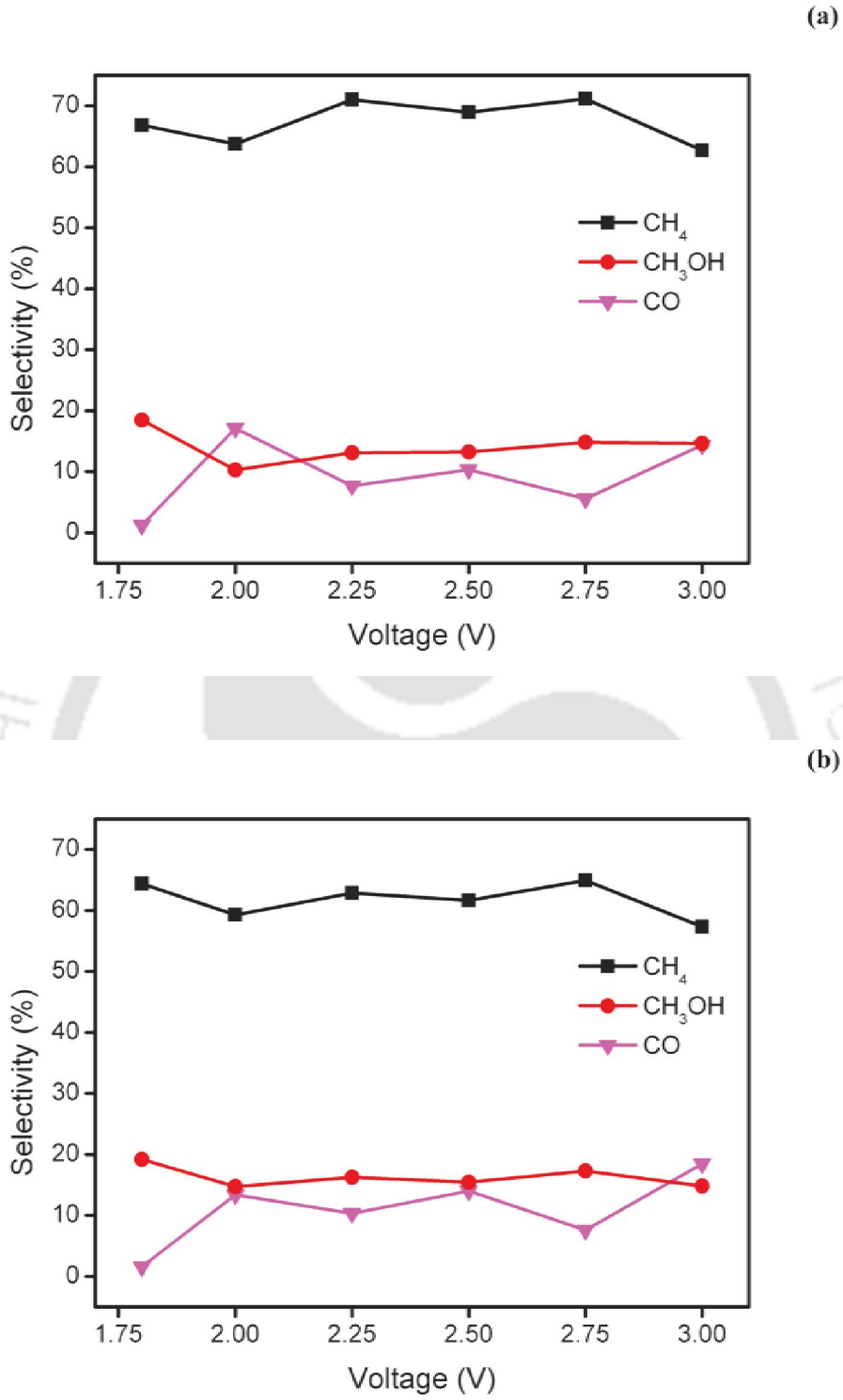

Fig. 4.27 Selectivity of the products using (a) nafion and (b) SPEEK

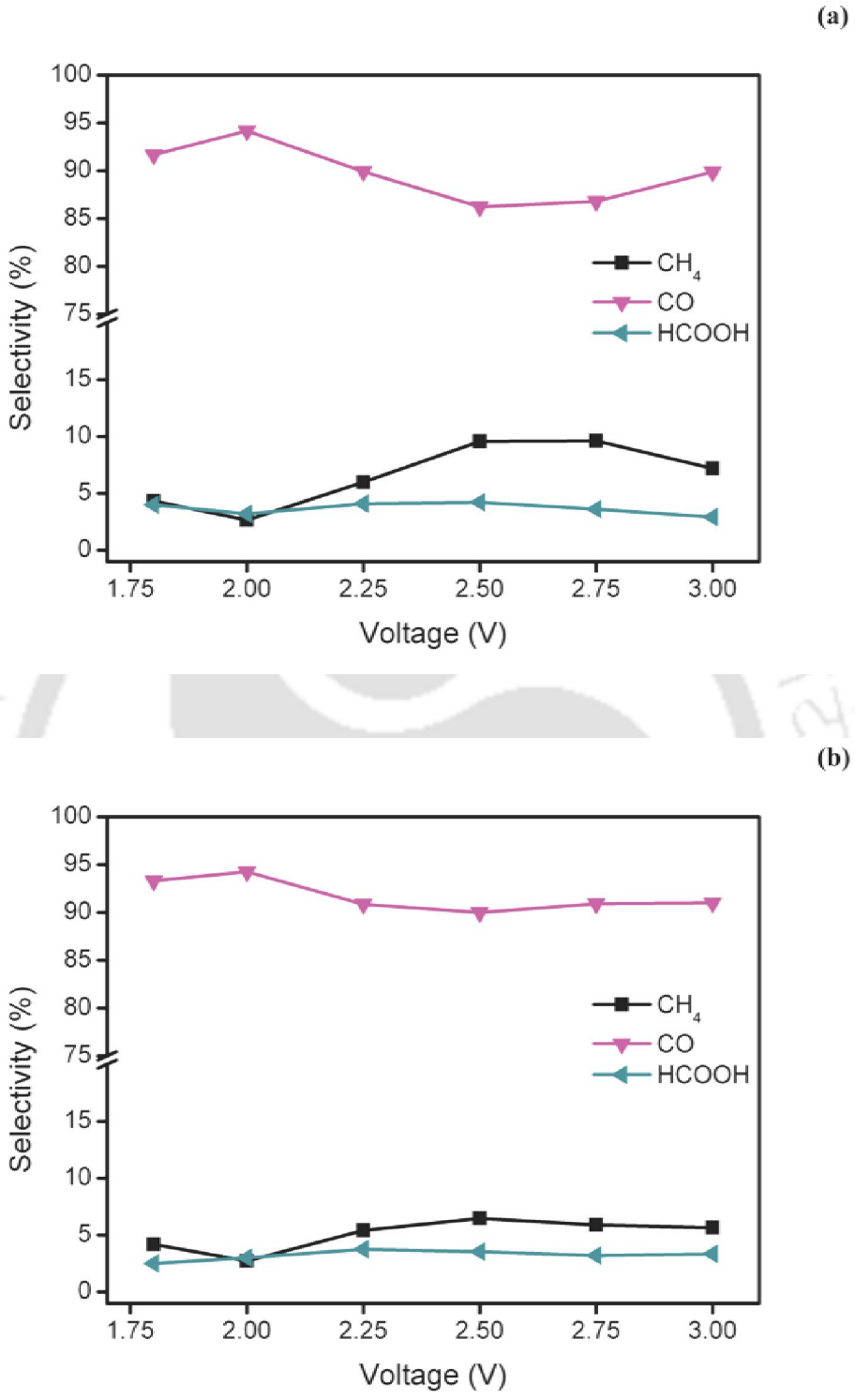

Fig. 4.28 Selectivity of the products using (a) alkali doped PVA/GA and (b) Amberlyst/SPEEK

surface has generated some malachites, which indicates some of the deactivation of copper. Therefore, in the further study Cu_2O was used for a shorter time as could not observed any deactivation (Lee and Tak, 2001). Moreover, the Faradaic efficiency was not improved significantly and also, carbon monoxide adsorbs on the electrode, which might deactivated the electrode surface thus led to the low Faradaic efficiency. Carbon monoxide was an intermediate for the formation of hydrocarbons. In the constant mode electrolysis, the CO was adsorbed on the electrode surface, which was later obtained as a major product. Thus, to elute CO and other products/by-products, pulse mode electrolysis was used in ERC as discussed in the next chapter. The pulse electrolysis may help the reaction products to come out of the reaction zone and result in clear passage for the reactants.

Chapter 5

Influence of Functional Groups in Cationic and Anionic SPEs on dERC

Chapter 5

Influence of Functional Groups in Cationic and Anionic SPEs on dERC

In this chapter, the treated cationic and anionic solid polymer electrolytes having same polymer backbone but different functional groups are used. The evaluation of these SPEs in dERC will help to understand the implications of functional groups in direct electrochemical reduction of gaseous CO_2.

5.1 Overview

It has been discussed that solid polymer electrolytes have significant role on the electrochemical reduction of CO_2. Mainly formic acid, formaldehyde, carbon monoxide, and methane were evolved with very low Faradaic efficiency. It was concluded in the chapter 4 that there is a need of systematic study for the evaluation of suitable functional groups in the solid polymer electrolyte in order to further enhance the selectivity of the products and the improvements in the Faradaic efficiency of the dERC.

In this chapter, the investigation over the influence of the functional groups in the solid polymer electrolytes on the ERC is reported. It is found that the research work on SPEs is scanty. Only a few of the literatures are available, which report the use of various SPEs along with different electrocatalysts for the product formation. However, there is hardly any literatures, which report explicitly the influence of anionic or cationic solid polymer electrolyte on the electrochemical reduction of gaseous carbon dioxide. Therefore, this chapter is focused over the evaluation of the role of cationic and anionic functional

groups in SPE on the direct electrochemical reduction of gaseous carbon dioxide. In order to study the effect of cationic and anionic SPEs, two SPEs with similar backbone structures but different functional groups were chosen for the dERC study. The dERC was conducted under pulse mode electrolysis using similar operating conditions and electrocatalyst for both the SPEs.

The electrochemical reduction of carbon dioxide in the gaseous phase was investigated using cationic and anionic solid polymer electrolytes. Influence of solid polymer electrolyte medium on electrochemical reduction of gaseous CO_2 into fuel is studied. The electrodeposited Cu_2O on porous carbon paper was used as cathode whereas Pt/C on the carbon paper was used as anode. The products formed after the ERC were analyzed by gas chromatography. Experiments were carried out at room temperature and atmospheric pressure. The subsequent sections of the chapter report about the treatment, characterization, and evaluation of the cationic and anionic SPEs on the ERC. In this study, CMI-7000 and AMI-7001 were used as cationic and anionic SPEs, respectively. It may be noted that both the SPEs were having the same polymer backbone (polystyrene crosslinked with divinyl benzene) but different functional group. The cationic SPE CMI-7000 has sulfonic acid group, whereas AMI-7001 has quaternary ammonium group.

5.2 Experimental

5.2.1 Materials

CMI-7000 and AMI-7001 were procured from Membrane International Inc, USA. The membranes have good characteristics such as high permselectivity with low permeability, wide range of chemical and temperature stability and exceptional mechanical strength. The properties of CMI-7000 and AMI-7001 are listed in table 5.1 and 5.2, respectively.

Table 5.1 General properties of CMI-7000 (as received)

Properties	Values
Appearance	Brown thin film
Ionic form	Sodium
Polymer structure	Gel polystyrene crosslinked with divinyl benzene
Thickness	450 µm
Functional group	Sulphonic acid
Functionality	Strong acid functional group

Table 5.2 General properties of AMI-7001(as received)

Properties	Values
Appearance	Light yellow thin film
Ionic form	Chloride
Polymer structure	Gel polystyrene crosslinked with divinyl benzene
Thickness	450 µm
Functional group	Quaternary ammonium
Functionality	Strong base functional group

It is known that ion exchange materials are generally used by functionalizing a suitable base polymer with the desired cationic or anionic functional groups. Generally, aromatic groups in the main chain are chosen to functionalize a suitable crosslinked base polymer. Thereafter the functional groups used to introduce according to ionic mechanisms in aromatic groups, which usually take place under mild conditions, and thus chemical attack of base polymer can be avoided (Zschocke et al., 1985; Chan and Li, 2014).

Pt/C (40 wt.%) was purchased from ElectroChem Inc., USA. Porous carbon paper (TGP-H-120) from Torayca was used as backing layer for electrode preparation. Other chemicals like H_2SO_4, and KOH were procured from Merck, India. All the chemicals were used without further purification unless specified and de-ionized water was used in all the experiments.

5.2.2 Method

5.2.2.1 Treatment of SPE

The as received CMI-7000 has sulfonic acid functional group in sodium ion form and AMI-7001 has quaternary ammonium functional group in chloride ion form. Therefore, the procured CMI-7000 and AMI-7001 SPEs were treated prior to use. The CMI-7000 membrane was treated with H_2SO_4 to exchange the sodium ions with hydrogen ions in order to get the membrane in protonic form as shown in fig. 5.1a. Similarly, AMI-7001 was prepared in hydroxyl form was prepared by treating with KOH as shown in fig. 5.1b.

(a)

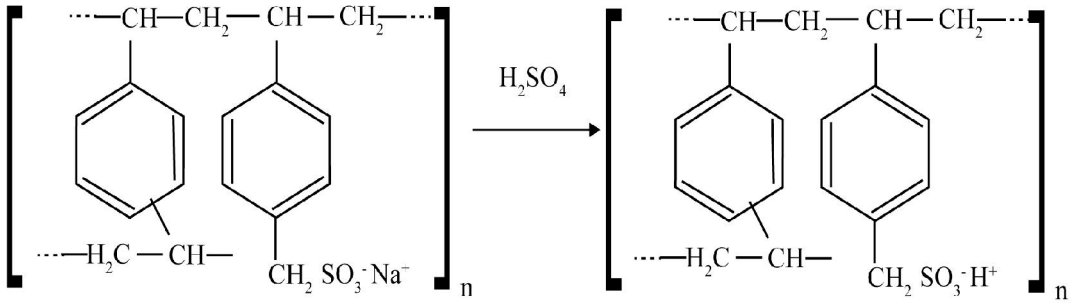

CMI-7000 (sodium ion form) CMI-7000 (proton form)

(b)

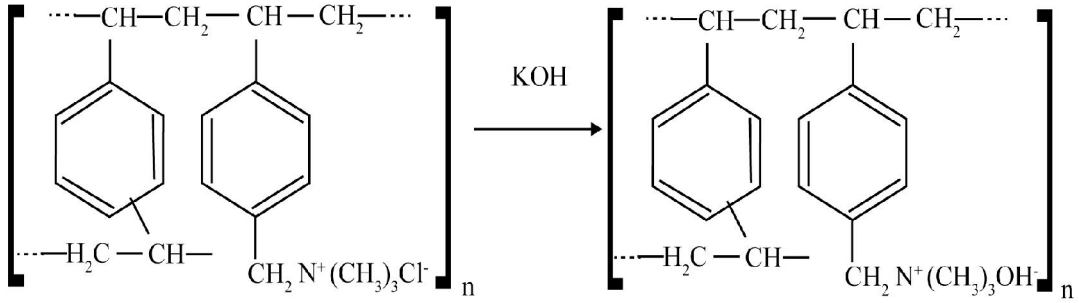

AMI-7001 (chloride ion form) AMI-7001 (hydroxyl ion form)

Fig. 5.1 Structure of (a) CMI-7000, and (b) AMI-7001

5.2.2.2 Electrode preparation

The anode was prepared as per the details given in section 4.3.2. However, as discussed earlier, the cuprous oxide will be used as cathode electrocatalyst from this chapter onwards, the electrode was developed in two steps; in the first step electroplating of copper was done in a similar manner as discussed in the section 4.3.2. In the second step, the electrodeposited copper on the carbon paper was thermally treated at a temperature of 135°C in an air oven for 17 hr to obtain cuprous oxide (Cu_2O/C) cathode (Yano and Yamasaki, 2008).

5.3 Results and Discussion

5.3.1 Membrane characterization

The treated membranes were characterized using SEM, TGA, XRD, FTIR, water uptake, swelling, ion exchange capacity, ionic conductivity, and tensile strength.

5.3.1.1 SEM images

The morphology of surface and cross-section of the cation exchange membrane (CMI-7001), and anion exchange membrane (AMI-7001) was studied using SEM. Figure 5.2a and 5.2b show the SEM images of the surface and cross-section of CMI-7000 membrane. Figure 5.2c and 5.2d shows the SEM images of the surface and cross-section of AMI-7001 membrane. These micrographs reveal certain degree of roughness on the surface of both the membranes. The surface morphology shows that these membranes are dense without any pores. The SEM micrographs of the cross-sections of CMI-7000 and AMI-7001 membranes show the presence of densely-packed micro-laminates in the membrane structure (Biljana et al., 2012).

5.3.1.2. TGA

TGA curves in fig. 5.3 show the thermal degradation of CMI-7000 and AMI-7001 membranes. These two membranes have same polymeric chain (crosslinked polystyrene with divinyl benzene) with sulfonic group for CMI-7000 and quaternary ammonium group for AMI-7001 membrane. Upto 100°C the weight loss for CMI-7000 was higher as compared to AMI-7001. It shows that CMI-7000 has higher water uptake as compared to AMI-7001, which is analyzed later while conducting water uptake study.

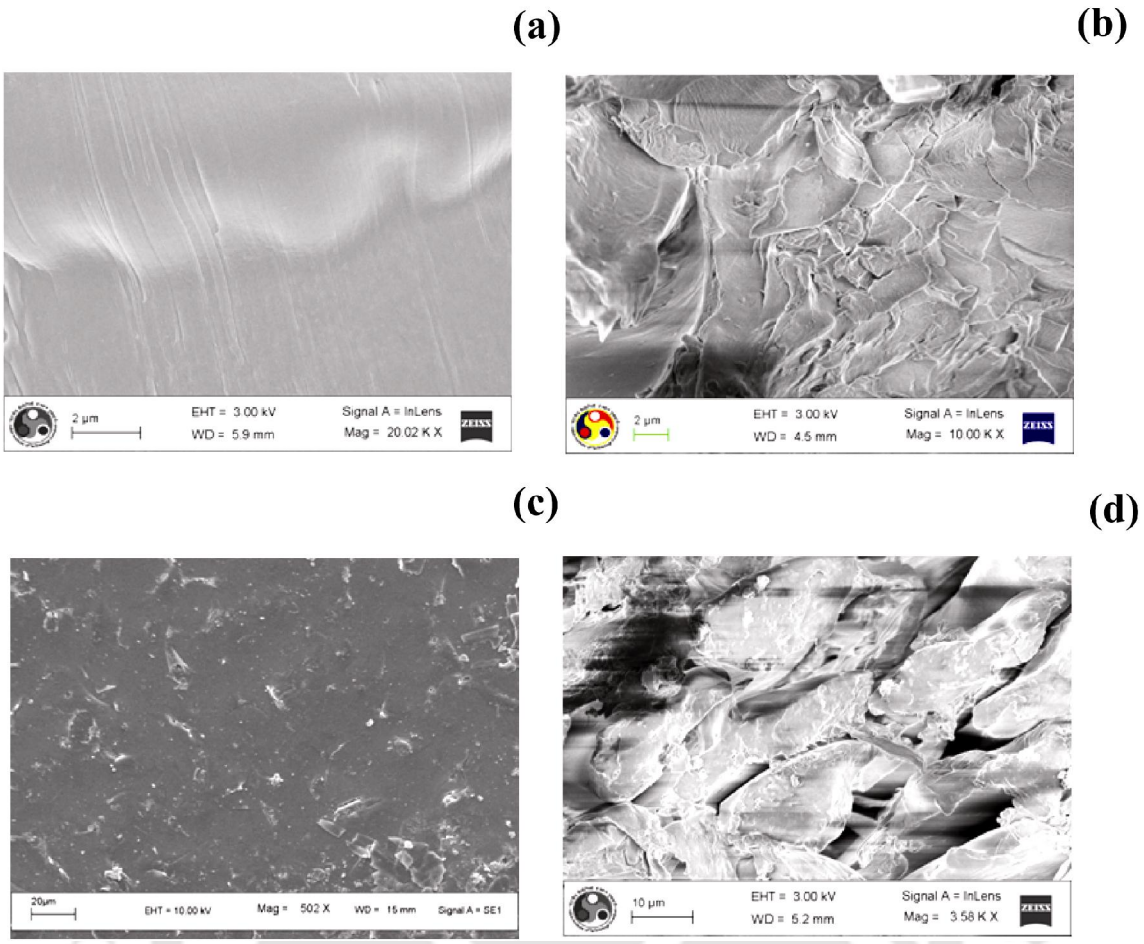

Fig. 5.2 SEM micrographs of CMI-7000: (a) surface, (b) cross-section, and AMI-7001: (c) surface, (d) cross-section

However, the CMI-7000 shows good thermal stability and main chain degradation starts at around 310°C. The thermal stability of the AMI-7001 is comparatively lower due to quaternary ammonium functional group of the membrane (Nakagawa et al., 1988). The AMI-7001 membrane exhibits a three step degradation process. The first weight loss near 100°C is attributed to the evaporation of water in the membrane. The second loss in the range of 170-280°C is due to the decomposition of quaternary ammonium groups. At the third stage (above 400°C), the weight of AMI-7001 losses rapidly due to degradation of backbone polymer structure. Although the presence of the quaternary ammonium groups

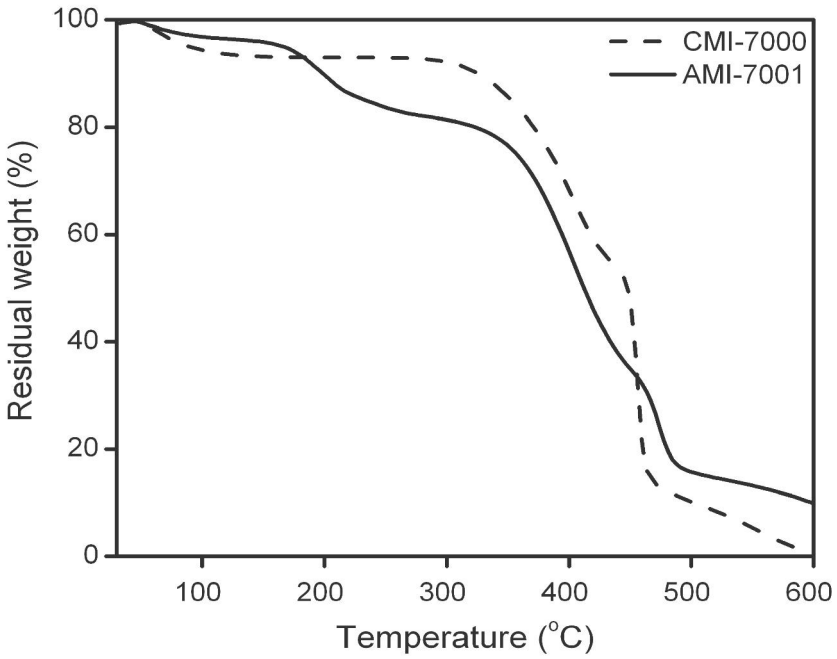

Fig. 5.3 TGA profiles of CMI-7000, and AMI-7001

decreased the thermal stability of the membranes, the AMI-7001 membrane still shows good stability atleast upto 170°C. It may be noted that although experiment was carried out at room temperature, the thermal stability test was required to ascertain the stability of the membranes for the development of the MEA at 110°C.

5.3.1.3 XRD

Figure 5.4 shows the XRD patterns of the CMI-7000 and AMI-7001 membranes. It can be observed that both CMI-7000 and AMI-7001 membranes exhibit semi-crystalline structure with characteristic peaks observed in the range of 13°–20° and a small peak in the range of 39°–40° representing the polymer base.

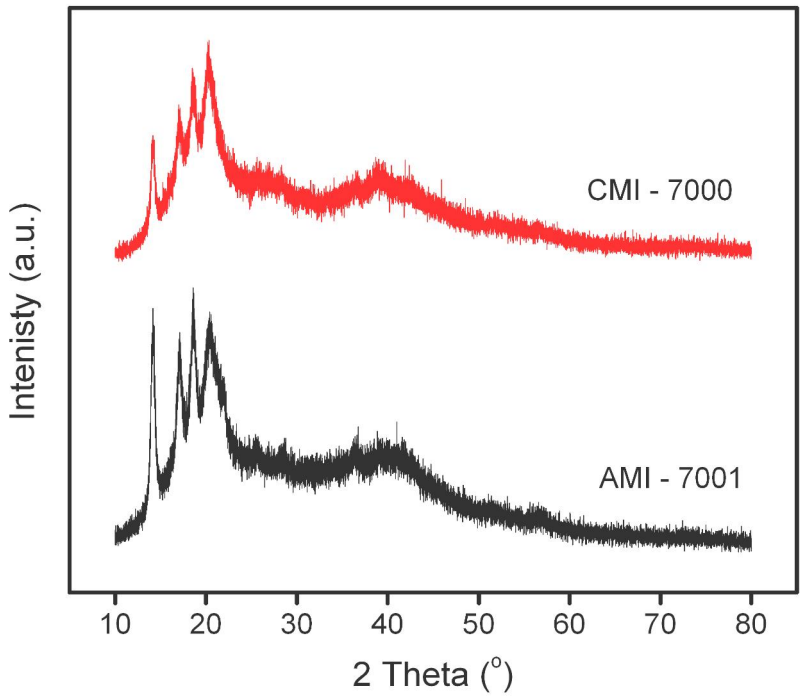

Fig. 5.4 XRD patterns of CMI-7000, and AMI-7001

5.3.1.4 FTIR

FTIR spectra of CMI-7000 and AMI-7001 are shown in fig. 5.5. In case of CMI-7000, the peaks in the range of 2850-3100 cm^{-1} represent the aliphatic stretching of C-H in polystyrene chains. The presence of benzene rings in polystyrene was confirmed by skeletal C=C stretching vibrations at 1639 cm^{-1}. The peak identified in the spectrum at 1283 cm^{-1} is due to the asymmetric stretching of S=O bond as shown in fig. 5.5a. The symmetric vibration of this bond produces the characteristic split band of absorbance at 1150-1185 cm^{-1} (Smitha et al., 2003). In case of AMI-7001, the peak at 1557 cm^{-1} represents the C-H bending of trimethyl ammonium group confirming the existence of quaternary ammonium group as shown in fig. 5.5b. The two peaks at 1118 cm^{-1} and 3439 cm^{-1} are due to stretching vibration of C-N groups and stretching vibration of O-H group, respectively.

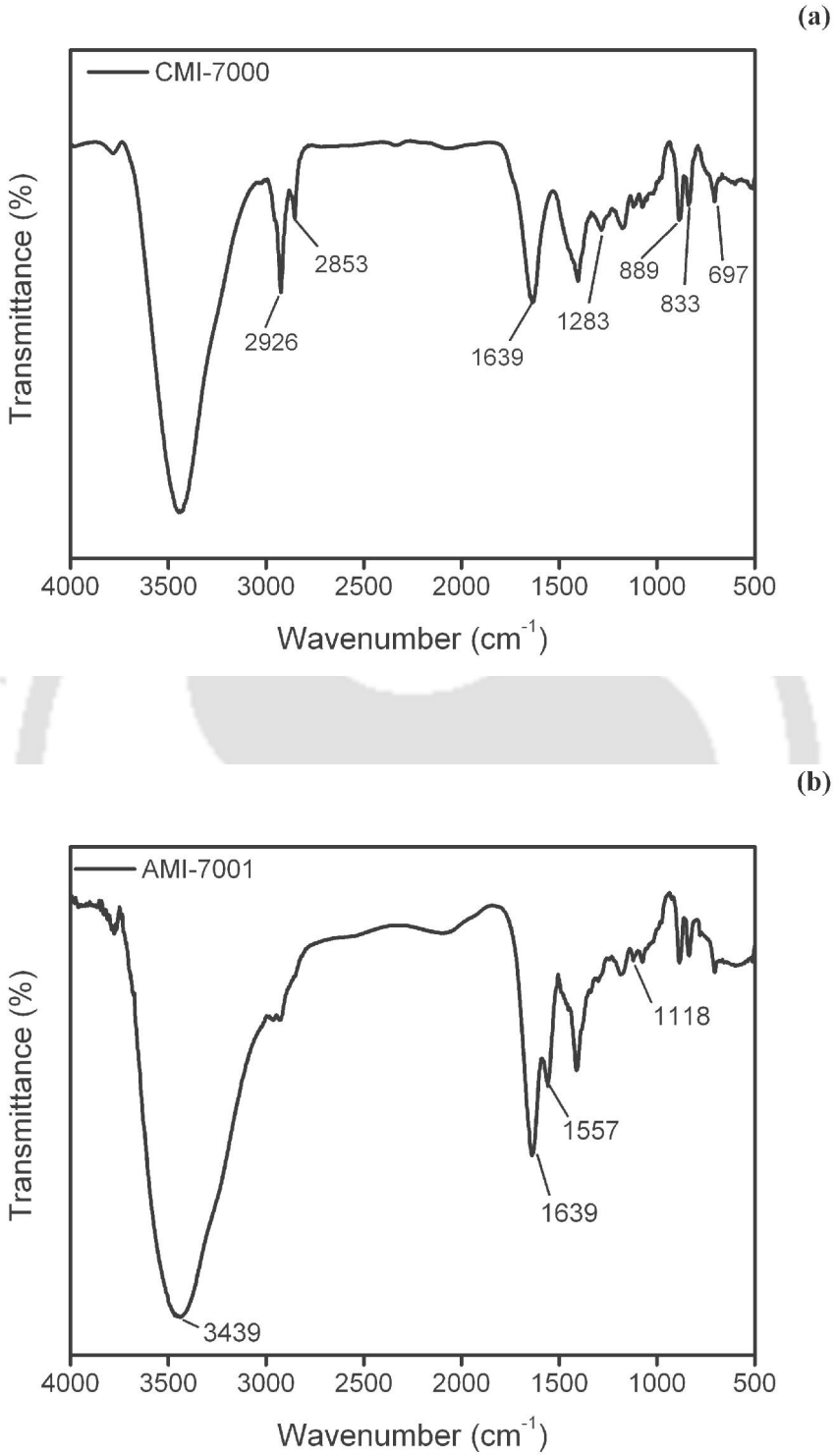

Fig. 5.5 FTIR spectra of (a) CMI-7000, and (b) AMI-7001

5.3.1.5 Water uptake

The water uptake of the CMI-7000 and AMI-7001 membrane is shown in fig. 5.6. In case of CMI-7000, the sulfonation of polymer serves to increase the water uptake, which enhances the proton transfer and thus the good conductivity of the polymer electrolyte is also expected in the presence of water. The CMI-7000 SPE shows water uptake of 32% (fig. 5.6) as compared to 25% in case of AMI-7001 SPE. It shows that hydrophobicity and hydrophilicity of the polymer and sulfonic acid groups led to the formation of nanostructures or channels in presence of water. Water uptake of AMI-7001 SPE is less than CMI-7000 due to the lower strength of hydrophilic nature of quaternary ammonium groups.

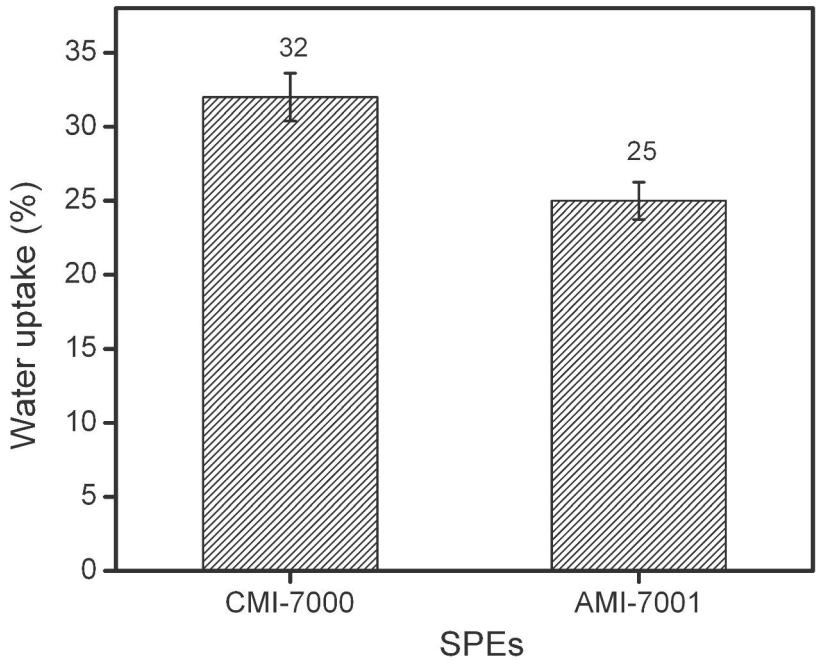

Fig 5.6 Water uptake of CMI-7000, and AMI-7001

5.3.1.6 Swelling

Swelling of the CMI-7000 and AMI-7001 is 5.7% and 4.8%, respectively, as shown in fig. 5.7. It may be noted that the water uptake is almost linearly related with the swelling for these two SPEs. The water uptake and swelling show that the SPEs may be suitable for studying the ERC. However, the IEC and ionic conductivity analysis shown in the subsequent sections will throw some more light on the application of these SPEs.

5.3.1.7 Ion exchange capacity

The ion exchange capacity (IEC) indicates the content of replaceable H^+ in the sulfonic acid groups of the CMI-7000 and quaternary ammonium group in the AMI-7001 SPE. The IEC values of the CMI-7000 and AMI-7001 are shown in fig. 5.8. The IEC of the CMI-7001 membrane is higher than the AMI-7001 membrane. It indicates that the CMI-7001 membrane have more amount of replaceable H^+ in sulfonic acid sites for its intended application in ERC as compared to AMI-7001. The ion exchange capacity follows the trend of water uptake and swelling, as expected. CMI-7000 and AMI-7001 SPEs have IEC of 1.6 $meq.g^{-1}$ and 1.2 $meq.g^{-1}$, respectively.

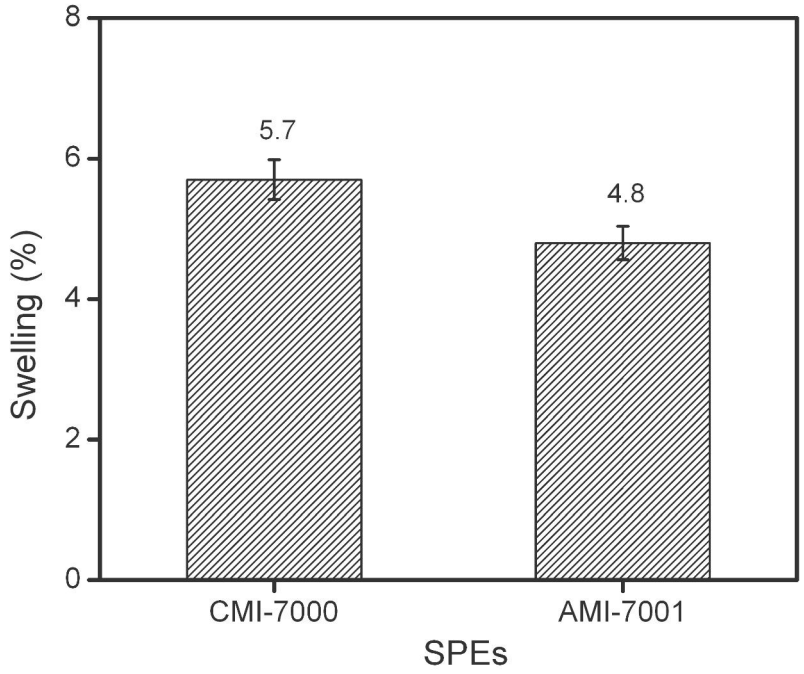

Fig. 5.7 Swelling of CMI-7000, and AMI-7001

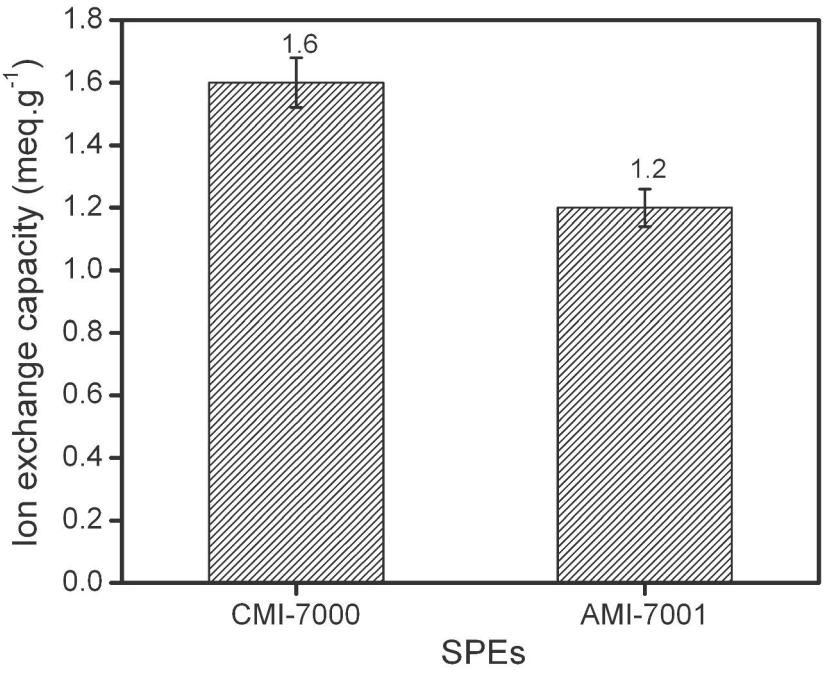

Fig. 5.8 Ion exchange capacity of CMI-7000, and AMI-7001

5.3.1.8 Ionic conductivity

The ionic conductivity indicates the ease of the proton or hydroxyl ion transport from one electrode to another through the SPE. High ionic conductivity is desirable for low ohmic overpotential during dERC. The ionic conductivity of CMI-7000 (60 $mS.cm^{-1}$) was twelve times higher than the AMI-7001 (5 $mS.cm^{-1}$) as shown in fig. 5.9. The ionic size of OH^- is more than the ionic size of H^+, moreover, the water uptake and IEC of AMI-7001 is lower than the CMI-7000, which may be the cause of low ionic conductivity in case of AMI-7001. It may be noted that the water uptake and swelling are directly related to the ionic conductivity and intactness of the SPE with the electrodes in the MEA.

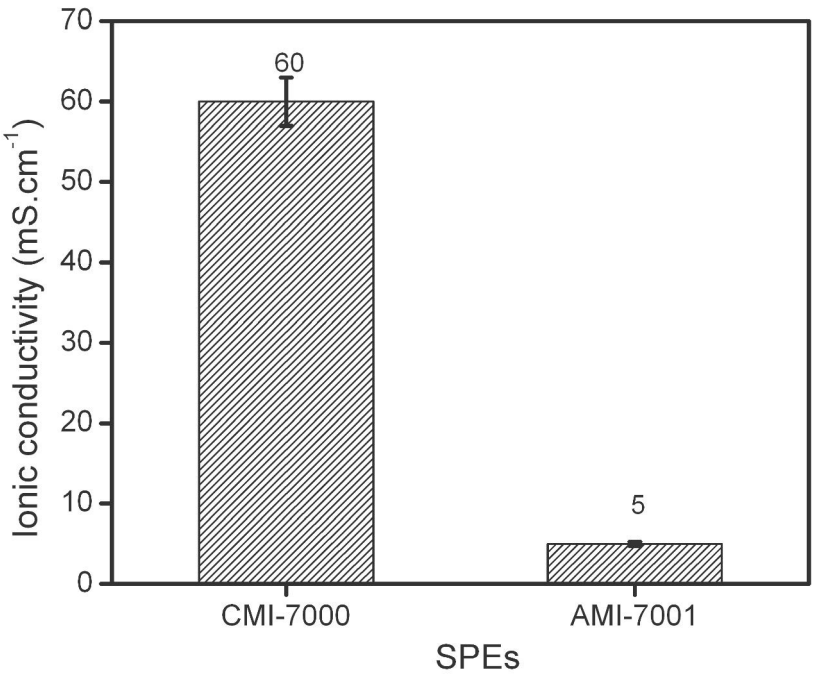

Fig. 5.9 Ionic conductivity of CMI-7000 and AMI-7001

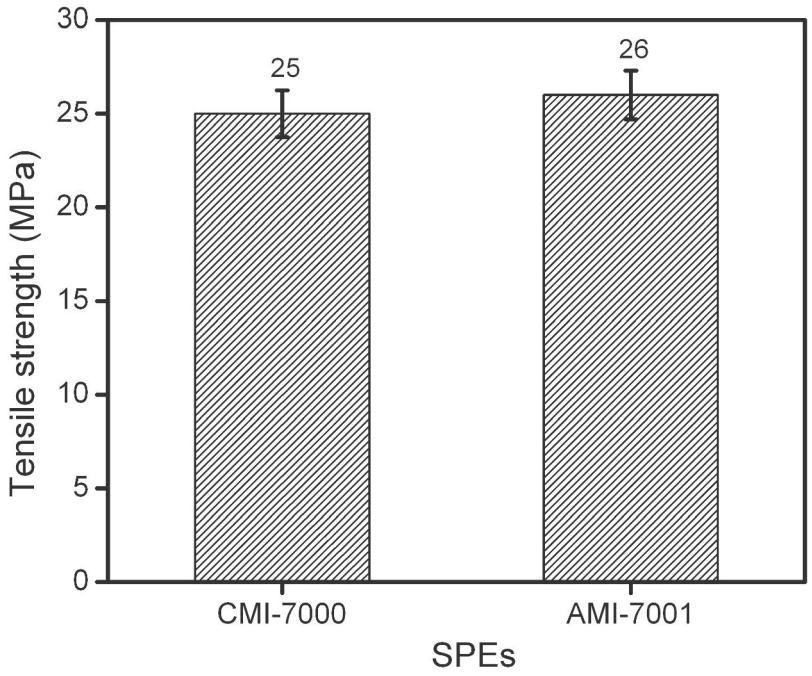

Fig. 5.10 Tensile strength of CMI-7000 and AMI-7001

5.3.1.9 Tensile strength

As discussed earlier, the mechanical strength of the SPE in such electrochemical system is usually evaluated by the tensile strength. It can be seen in the fig. 5.10 that both the SPEs have almost same tensile strength. The tensile strengths of the CMI-7000 and AMI-7001 were found to be 25 MPa and 26 MPa, respectively.

5.3.2 Electrode characterization

The cathode was prepared by electroplating technique. Thus it was important to know the surface morphology of the electrode, which was electroplated with the aim to have sufficient porosity for the transport of the CO_2 gas as well as various reaction products. Therefore, SEM analysis was conducted to know the morphology of the cathode. Figure 5.11a shows the SEM image of Cu_2O/C electrode, in which Cu_2O covers all the surface

carbon fibres of the carbon paper. It may also be seen that the cathode (Cu_2O/C) is porous in nature and thus it would facilitate the transport of the reactant and products across it. XRD analysis was conducted to confirm the conversion of Cu into Cu_2O. Figure 5.11b shows the XRD of the electroplated material and it is confirmed that the Cu_2O is successfully developed onto the carbon paper. However, different crystal nature of the Cu_2O was also observed along with some unconverted Cu.

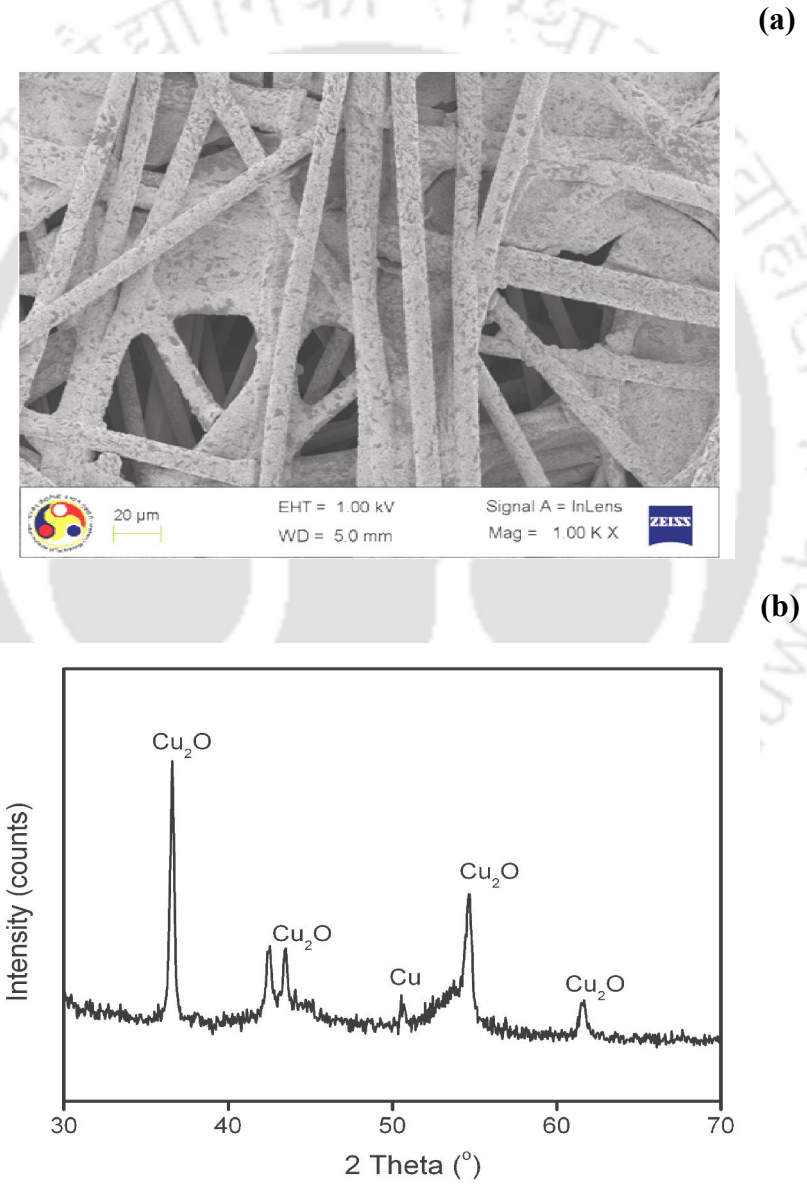

Fig. 5.11 Cu_2O on carbon paper electrode: (a) SEM image, and (b) XRD pattern

5.3.3 dERC on Cu_2O using CMI-7000 and AMI-7001 SPE

5.3.3.1 Effect of applied potential on current density

Experimental results obtained from direct electrochemical reduction of CO_2 using CMI-7000 and AMI-7001 SPEs are shown in fig. 5.12. Figure 5.12 shows current densities corresponding to various applied voltages at the terminals of the electrochemical reactor for the dERC. It can be seen that the current density increases with increase in the applied voltage for both the cationic (CMI-7000) and anionic (AMI-7001) SPEs. It indicates that rate of the reaction increases with increase in the applied voltage. The increased reaction rate corresponds to the combination of different electrochemical reactions at the electrode. Current densities increase from 2 $mA.cm^{-2}$ to 4.81 $mA.cm^{-2}$ in dERC using CMI-7000, whereas for AMI-7001, current densities increase from 3 $mA.cm^{-2}$ to 6.1 $mA.cm^{-2}$ (Aeshala et al., 2013).

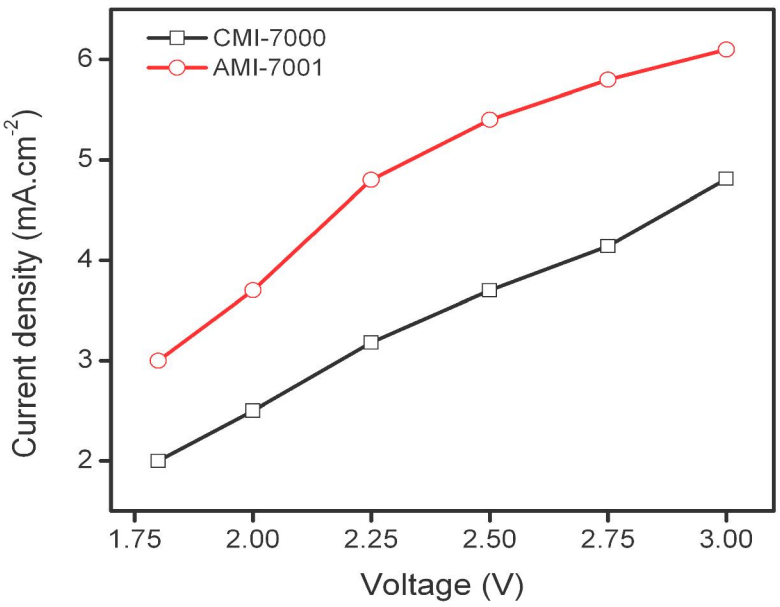

Fig. 5.12 Current density as a function of applied voltage using CMI-7000 and AMI-7001

It is interesting to note that, though the ionic conductivity of CMI-7000 is higher than AMI-7001, the current densities are higher in the case of AMI-7001 at all the voltages. Both the membranes have the same polymer backbone but different functional groups, which might play a significant role at the electrode-electrolyte interface for different rates of various electrochemical reactions. Further study was conducted to ascertain and evaluate the role of functional groups, the amount of product, Faradaic efficiency, and product selectivity and reported in the subsequent sections.

5.3.3.2 Evaluation of products, and Faradaic efficiency of dERC

Figure 5.13 shows the amount of products obtained in dERC using CMI-7000 and AMI-7001 at different applied voltages. It can be seen that the reaction product distribution (CH_4, C_2H_4, and CH_3OH) is same for CMI-7000 and AMI-7001, but the amount of products were more in AMI-7001 than CMI-7000. The amount of the products formed increases with increase in applied voltage for CMI-7000; whereas for AMI-7001, increase in the applied voltage results in more product formation up to 2 V for C_2H_4, and CH_3OH and 2.5 V for CH_4, however, decreases thereafter. Moreover, H_2 gas formation increases along with the applied voltage for both the SPEs. The interesting observation is that the H_2 formation was almost stable up to 2.5 V for anionic SPE (AMI-7001). As, the ionic conductivity of CMI-7000 was 12 times more than AMI-7001, CMI-7000 SPE could provide abundant proton availability at the interface of electrode and electrolyte, resulting in high amount of hydrogen generation. Hydrogen evolution was in the range of 117 µmol at 1.8 V to 279.6 µmol at 3 V in the case of CMI-7000. Figure 5.13a shows that maximum amount of products was obtained at 3 V. The amount of the products formed was found to be 1.85 µmol, 1.02µmol, and 4.74 µmol, for CH_4, C_2H_4, and CH_3OH respectively. Although AMI-7001 SPE is an anion exchange SPE but still the hydrogen

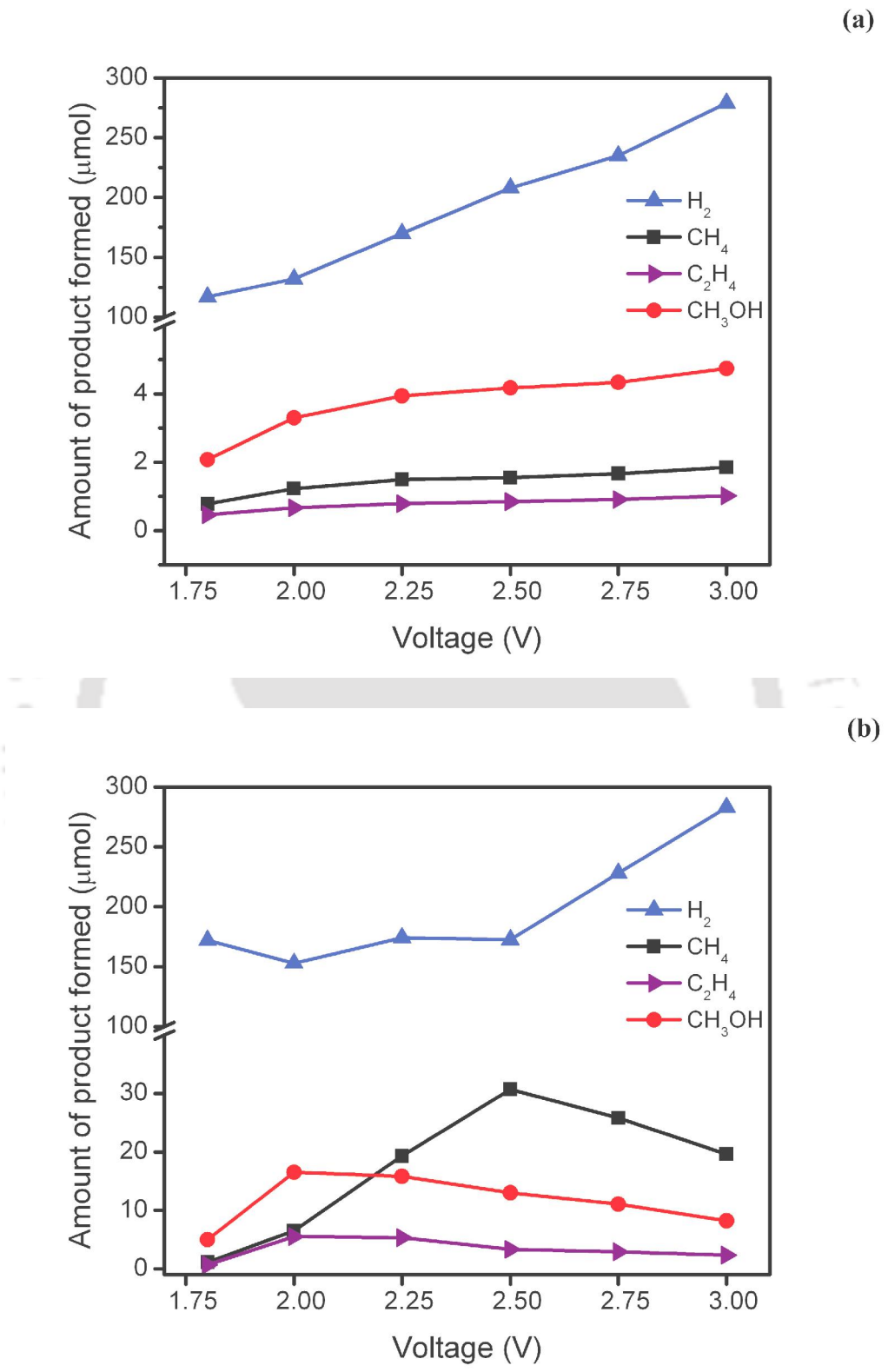

Fig. 5.13 Product distribution obtained as a function of applied voltage using (a) CMI-7000, and (b) AMI-7001

evolution was found to be significant (but lower as compared to CMI-7000) in the range of 172 µmol at 1.8 V to 283 µmol at 3 V. It may be the result of high water uptake by the AMI-7001 due to the quaternary ammonium functional group. In the anionic SPE too, the hydrogen evolution was the competitive reaction with ERC. As discussed earlier, it can be seen in the fig. 5.13b that hydrogen evolution was almost constant in the voltage range of 2 V to 2.5 V. Though the products were same for both the SPEs but the major product for CMI-7000 was CH_3OH while CH_4 for AMI-7001. Moreover, on comparing the amount of the major product formed for both the SPEs, the formation of products for AMI-7001 was found to be far more than CMI-7000. The AMI-7001 produces maximum 30.7 µmol of CH_4, whereas CMI-7000 results in maximum 4.7 µmol of CH_3OH.

Figure 5.14 shows the Faradaic efficiency obtained as a function of applied voltage in the dERC using CMI-7000, and AMI-7001 SPEs. It can be seen for AMI-7001 (fig. 5.14b) that Faradaic efficiency of CO_2 conversion initially increases sharply upto 2 V, attains maxima at 2.5 V and thereafter decreases very fast. However, in case of CMI-7000 the Faradaic efficiency slowly increases upto 2 V and then decreases gradually as shown in the fig. 5.14a, which is contrary to the trend of product formation which increases slightly. It indicates that the consumed electrical energy was utilized more for the hydrogen evolution as compared to electrochemical reduction of CO_2.

For CMI-7000 the Faradaic efficiencies were very low as compared to the AMI-7001 for all the reaction products. The maximum Faradaic efficiency for CMI-7000 was obtained at 2 V to produce CH_4, C_2H_4, and CH_3OH. Nevertheless, using AMI-7001, the maximum efficiencies were obtained at 2 V for C_2H_4 and CH_3OH production but 2.5 V for CH_4 generation. It can be seen that cationic SPE (CMI-7000) resulted in the formation of H_2

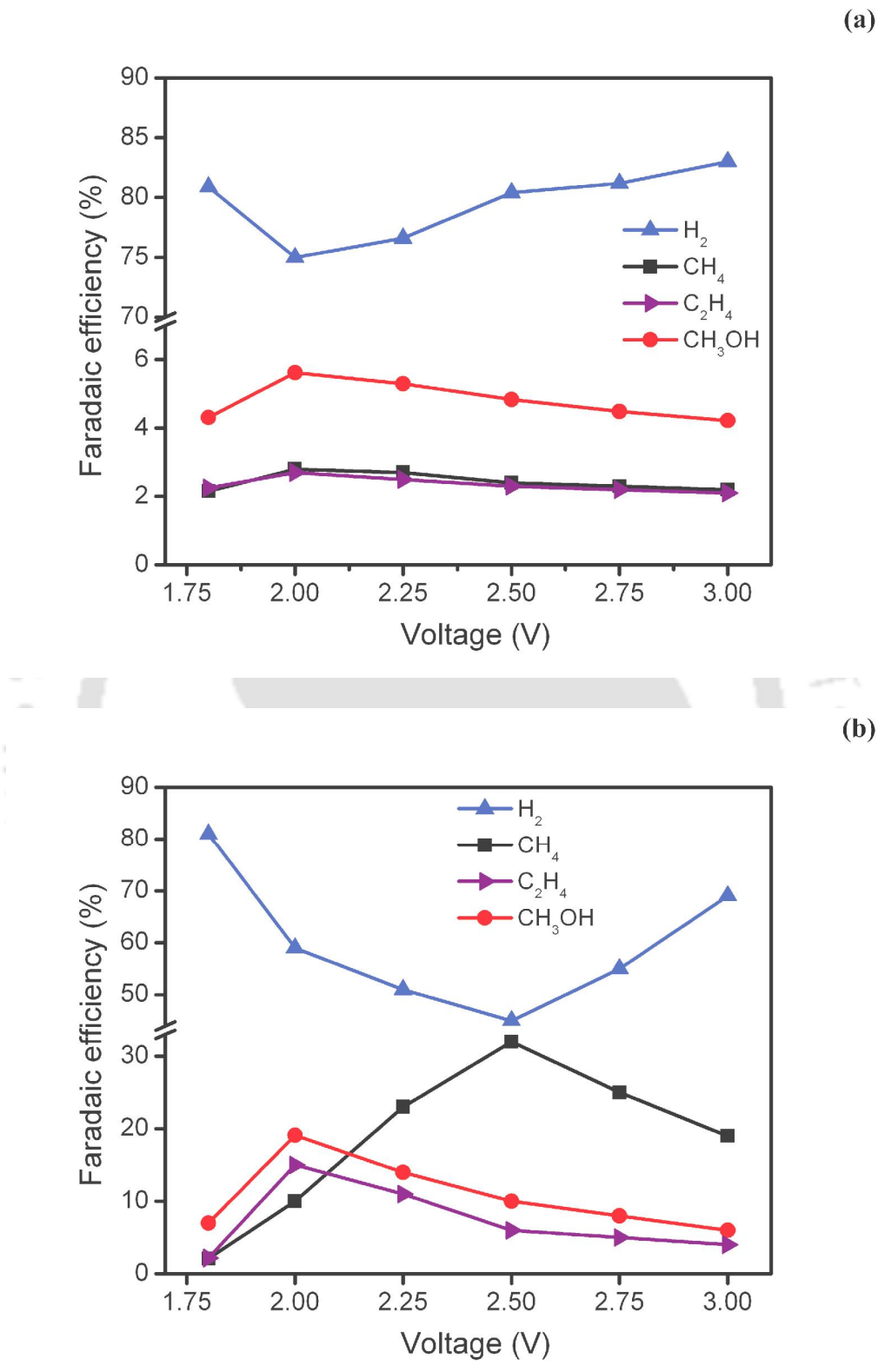

Fig. 5.14 Faradaic efficiency obtained as a function of applied voltage using (a) CMI-7000, and (b) AMI-7001

gas (by-product) more than the CO_2 reduction; whereas in anionic SPE (AMI-7001), the supplied energy was significantly utilized towards CO_2 electroreduction. The maximum Faradaic efficiency obtained for CH_4 formation is 32% at 2.5 V for AMI-7001. The Faradaic efficiencies for C_2H_4 and CH_3OH are about 15% and 19%, respectively, at 2 V (fig. 5.14b). However, it can be seen that the Faradaic efficiency for any of the products is not more than 6% using CMI-7000 (fig. 5.14a) (Aeshala et al., 2013).

The maximum Faradaic efficiency towards total CO_2 electroreduction (sum of all the products, excluding H_2) was substantially high for the anionic SPE (AMI-7001) as compared to the cationic SPE (CMI-7000). However, the applied voltage for maximum Faradaic efficiency using AMI-7001 was 2.5 V compared to 2V for CMI-7000. If the fig. 5.12 and 5.14 are compared for the maximum formation of products, it is found that the current density for AMI-7001 (5.4 $mA.cm^{-2}$ at 2.5V) was 116% higher than CMI-7000 (2.5 $mA.cm^{-2}$ at 2V). One of the reasons for the higher voltage for the above performance is the low ionic conductivity of AMI-7001 as compared to CMI-7000. Moreover, the other reasons may be the different reactions (or product formation) using different SPEs.

It clearly proves that SPE influences the system performance to a great extent. To further understand the cause of better performance by AMI-7001 than CMI-7000, an understanding has been developed and conceptual representation is shown in fig. 5.15. The quaternary ammonium ion of the AMI-7001 gets electrostatically attracted to the negative cathode, which assists the electron flow from cathode to CO_2 in the electrolysis (fig. 5.15b). However, the sulfonic acid group of CMI-7000, is hardly adsorbed onto the cathode due to the electrostatic repulsion at the negative cathode, causing hindrance to the flow of electron from the electrode to CO_2 during electrolysis (fig. 5.15a). Moreover,

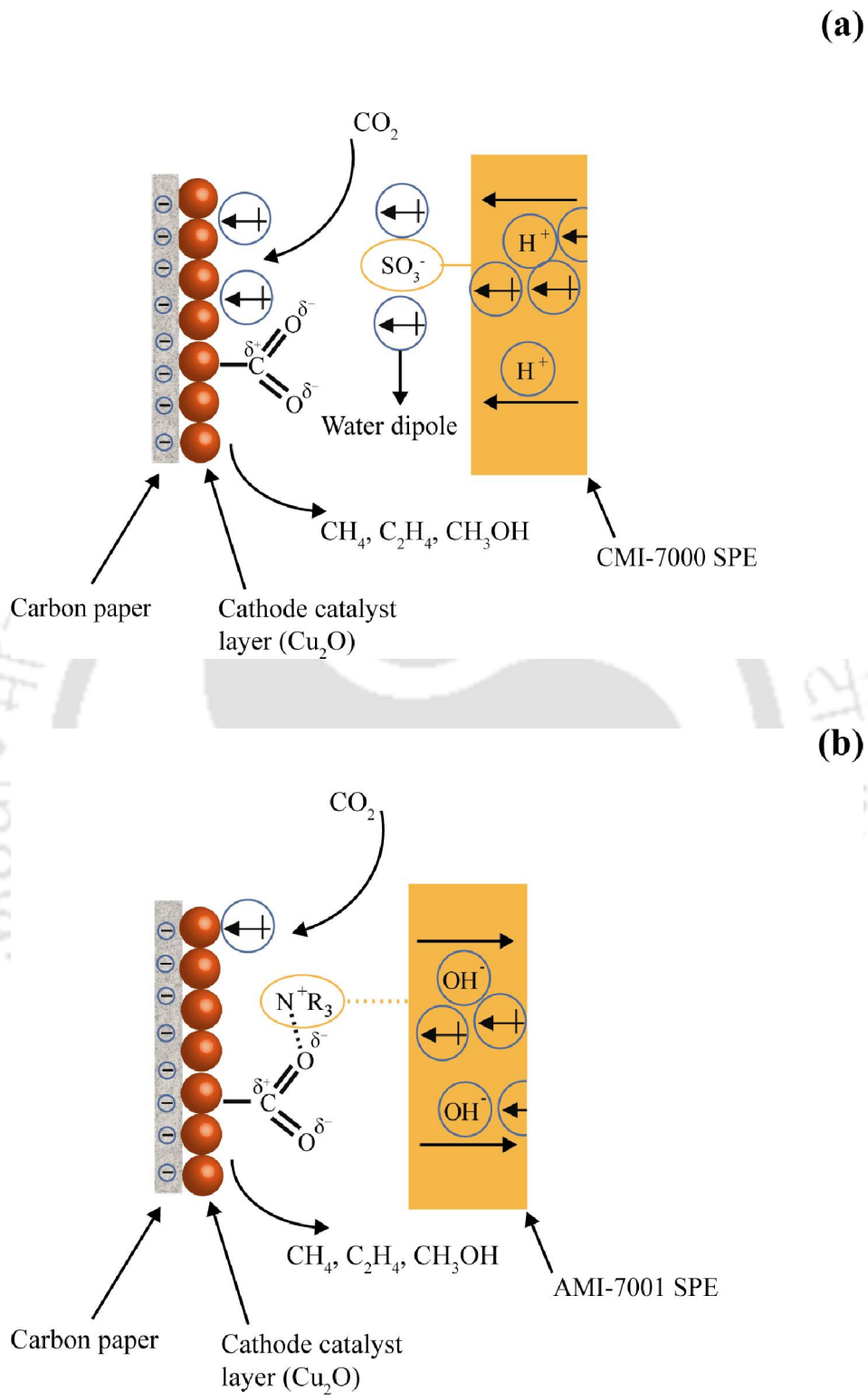

Fig. 5.15 Conceptual representation of dERC using (a) CMI-7000, and (b) AMI-7001

there may be other synergetic effects that need to be explored. It is also interesting to note that the distribution of the reaction products (CH_4, C_2H_4, and CH_3OH) in this study is quite different owing to the Cu_2O, and pulse electrolysis, as compared to the Cu and constant electrolysis as discussed in chapter 4. Infact, there is no such study, which emphasize on the role of SPE for the electrochemical reduction of CO_2. The available literatures show that using cuprous oxide as an electrocatalyst and $KHCO_3$ solution as an electrolyte, half-cell produces CH_4 and CO along with C_2H_4 as a major product (Yano et al., 2008). The other literature reports that methanol was obtained in $KHCO_3$ solutions (Le et al., 2011), whereas in case of KCl solutions, CH_4 and C_2H_4 were obtained using cuprous oxide electrode (Keerthiga et al., 2012). Good selectively of C_2H_4 was also found on Cu-halide confined copper mesh electrode (Ogura et al., 2004). It has been observed in the present study that under the experimental conditions, CH_4 was formed predominantly with significantly high Faradaic efficiency using alkaline SPE (AMI-7001). The next section reports the selectivity of the SPE for the products.

5.3.3.3 Selectivity

Selectivity was calculated to quantify the preference in the product formation using CMI-7000 and AMI-7001 SPEs. Figure 5.16 shows the selectivity of the products such as CH_4, C_2H_4, and CH_3OH in dERC using CMI-7000 and AMI-7001 at various applied voltages. It was observed that selectivity of the products was almost same in the case of CMI-7001 at all applied voltages as shown in fig. 5.16a. It is mainly due to the amount of products formed (carbon based products) using CMI-7000 constantly increase with respect to each other as shown in fig. 5.16a. Whereas, in the case of AMI-7001, amount of CH_3OH and C_2H_4 increase up to 2V and decreases thereafter. The amount of CH_4 increases up to 2.5 V thereafter slight decrease was observed as shown in fig. 5.16b. Therefore, selectivity of

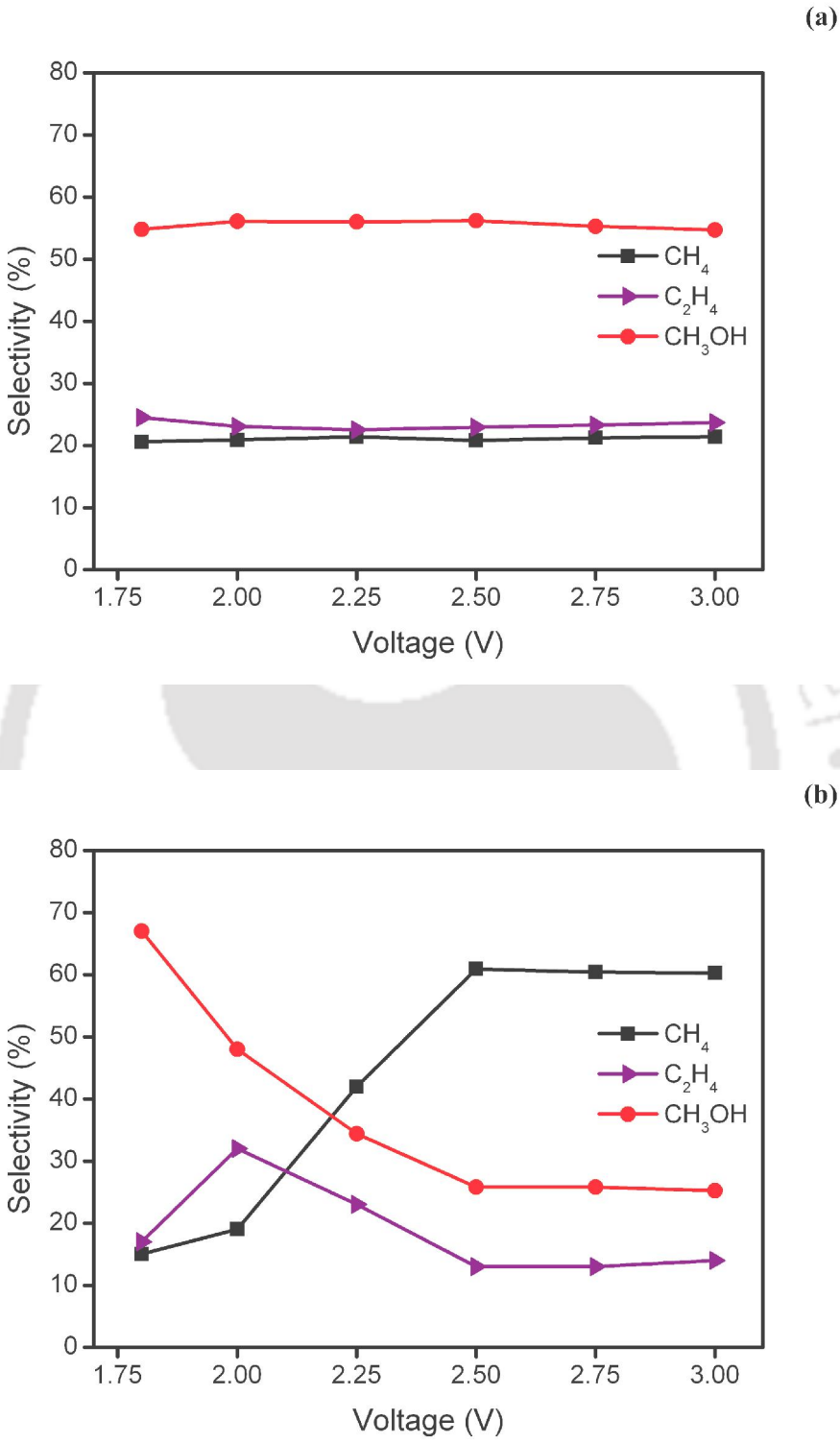

Fig. 5.16 Selectivity of products in dERC using (a) CMI-7000, and (b) AMI-7001

CH_4 was highest at 2.5 V with 60.9%, and for methanol and ethylene, selectivity increases up to 2 V and decreases thereafter. Selectivity for methane is highest in the case of AMI-7001 as compared to CMI-7000.

It may be noted that in chapter 4, the anionic and cationic SPEs were used along with Cu on carbon paper but the product distribution was not same. However, in this chapter (chapter 5), it has been seen that when all the experimental conditions, electrode as well as the backbone of the polymer electrolyte were kept same, the product distribution was same. It implies that though the functional groups are important for the rate of reaction but the polymer backbone also indirectly influences the reaction. Therefore, in order to know the effect of the functional groups, an idea has been conceptualized based on the experience gathered upto this stage. It was thought to vary the reaction products by changing the surrounding of functional group, while keeping all the other parameters fixed. Therefore, the next chapter reports about this concept and various results and discussion in tuning the reaction zone for dERC by changing the microenvironment of the reaction zone by developing an anion polymer electrolyte membrane.

Chapter 6

Tuning of Reaction Zone by Modification of Anionic SPE for dERC

Chapter 6

Tuning of Reaction Zone by Modification of Anionic SPE for dERC

In this chapter, the modified functional groups in anionic solid polymer electrolytes are evaluated for effective electrochemical reduction of CO_2.

6.1 Overview

The electrochemical reduction of CO_2 in aqueous solutions has been reported by many authors (Chen et al., 2012; Lv et al., 2014; Watkins and Bocarsly, 2014; Zhang et al., 2014). A few authors studied the role of liquid electrolyte for ERC and found that the ions (cations or anions) present in the electrolyte and supporting salts influence the ERC upto a great extent (Bockris and Wass, 1989; Saeki et al., 1995; Taniguchi et al., 1983; Thorson et al., 2013). Saeki et al., (1995) studied the effect of supporting electrolytes on the ERC in (CO_2-methanol) system. CO was found as a major product with Faradaic efficiency of 86% when tetrabutylammonium (TBA) salts were used as supporting electrolyte in ERC. Methylformate was the major CO_2 reduction product when lithium salts were used as the supporting electrolyte with a significant amount of H_2 generation. Grace et al., (2014) investigated ERC in TBA perchlorate in methanol electrolyte and HCOOH and CH_3COOH were found primarily with Faradaic efficiencies of 30.4% and 63.0%, respectively. However, liquid electrolytes offered large ohmic resistance, leakage from the reactor, liquid product dilution and/or complex separation of the products, along with significant hydrogen evolution. Therefore, researchers have investigated solid

polymer electrolytes to overcome the problems of the liquid electrolyte (Aeshala et al., 2012; Aeshala et al., 2013; Cook et al., 1988; Dewulf and Bard, 1988; Narayanan et al., 2011; Prakash et al., 2013). Moreover, solid polymer electrolyte (SPE) may be tuned as per the requirement. SPE contains polymer backbone and functional groups which may influence the ERC significantly. In our earlier studies (shown in previous chapters), it was found that cationic and anionic SPEs have some effect on the efficiency of the ERC (Aeshala et al., 2013). However, neither the mechanism of the process was clear nor the potential effect on the selectivity was known. Therefore, this chapter is aimed to find out the effect of functional groups of the SPE on the ERC and to know the possible reasons and reaction mechanism due to the functional groups. The concept behind the work is to employ the ability of amines (in SPE) for the CO_2 absorption, which may capture the CO_2 at the functional group sites. It will eventually help in the efficient conversion of CO_2 due to the increased mass transfer to the reaction site. Therefore, the use of solid polymer electrolyte having suitable functional groups is being reported, which can affect the product selectivity to accomplish efficient ERC using the direct gaseous CO_2 reduction in the developed electrochemical reactor.

To verify the proposed novel approach, branched polyethylenimine (PEI) having amine groups was chosen for synthesizing quaternized PEI (QPEI) in order to prepare anionic SPE. However, PEI does not have the film forming ability. Therefore, poly(vinyl alcohol) (PVA) was used as a polymer matrix along with glutaraldehyde as the cross-linker to form SPE membrane. Two different SPEs were developed and evaluated for ERC. One SPE was developed with direct blending of PEI with PVA (PEI/PVA) whereas another was developed with blending of quaternized PEI with PVA (QPEI/PVA) along with the doping of KOH in the SPEs. Gaseous CO_2 was used in the electrochemical study. The

product distribution, Faradaic efficiency, and selectivity of the products were evaluated to understand the rationale behind the process. It may be noted that both the SPEs (PEI/PVA/KOH and QPEI/PVA/KOH) were anionic SPEs. Moreover, the main polymer backbones were same but the functional groups were slightly different.

6.2 Experimental

6.2.1 Materials

Polyethylenimine (Mol.Wt. 7,50,000 $g.mol^{-1}$) and polyvinyl alcohol (Mol.Wt. 1,15,000 $g.mol^{-1}$) were procured from Sigma Aldrich, India. Other chemicals like bromopropane, and dimethylsulfoxide (DMSO) were procured from Merck, India and rest of the chemicals were procured from other sources as detailed in the previous chapters.

6.2.2 Method

6.2.2.1 Synthesis of PEI/PVA/KOH and QPEI/PVA/KOH

Solutions (5 wt.% each) of branched PEI and PVA were prepared in suitable solvents. The obtained solutions were mixed in 1:2 ratio of PEI and PVA. Thereafter, 10 wt.% of glutaraldehyde (GA) solution was added as crosslinking agent for PVA. The membranes were prepared by solution casting technique as described in chapter 4. The prepared membranes were doped with KOH solution for atleast 24 h and washed several times with de-ionized water to obtain PEI/PVA/KOH. In a similar way, QPEI/PVA/KOH was synthesized in which the quaternized PEI was used instead of PEI. The quarternization was done by adding bromopropane solution into PEI solution under stirring at 60^{o}C until clear homogeneous solution of quaternized PEI was obtained. Figure 6.1 and 6.2 shows

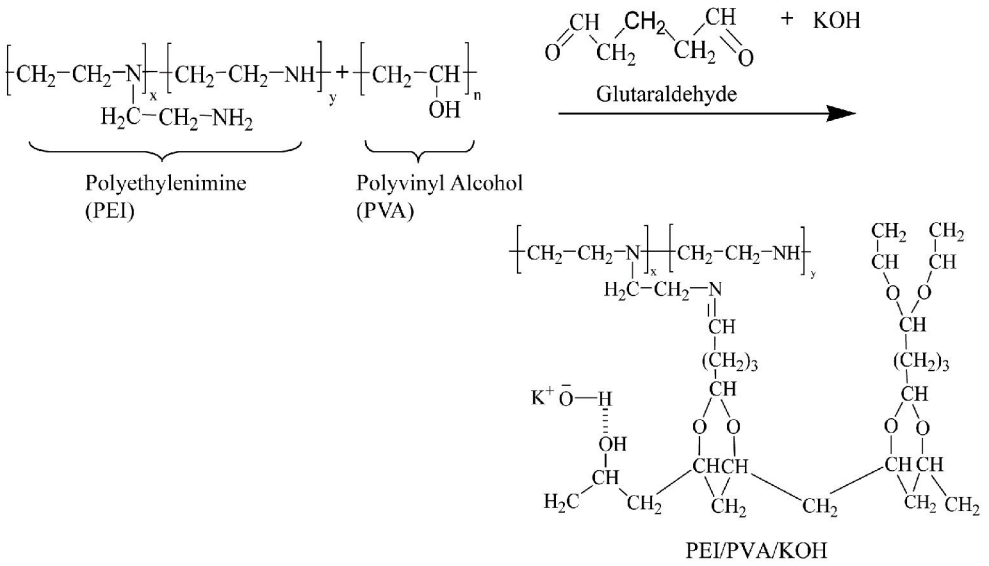

Fig. 6.1 Structural representation of PEI/PVA/KOH SPE

the representative reaction schemes along with the structural representations of PEI/PVA/KOH and QPEI/PVA/KOH SPEs, respectively (Aeshala et al., 2014).

6.3 Results and Discussion

6.3.1 SPE Characterizations

6.3.1.1 SEM images

Figure 6.3 shows the SEM images of PEI/PVA/KOH and QPEI/PVA/KOH SPEs. It can be seen in the SEM images that the SPEs are dense membranes. Moreover, the surface morphology of the membranes appears uniform without any formation of pores or cracks. The thickness of both the membrane was 80±10 µm.

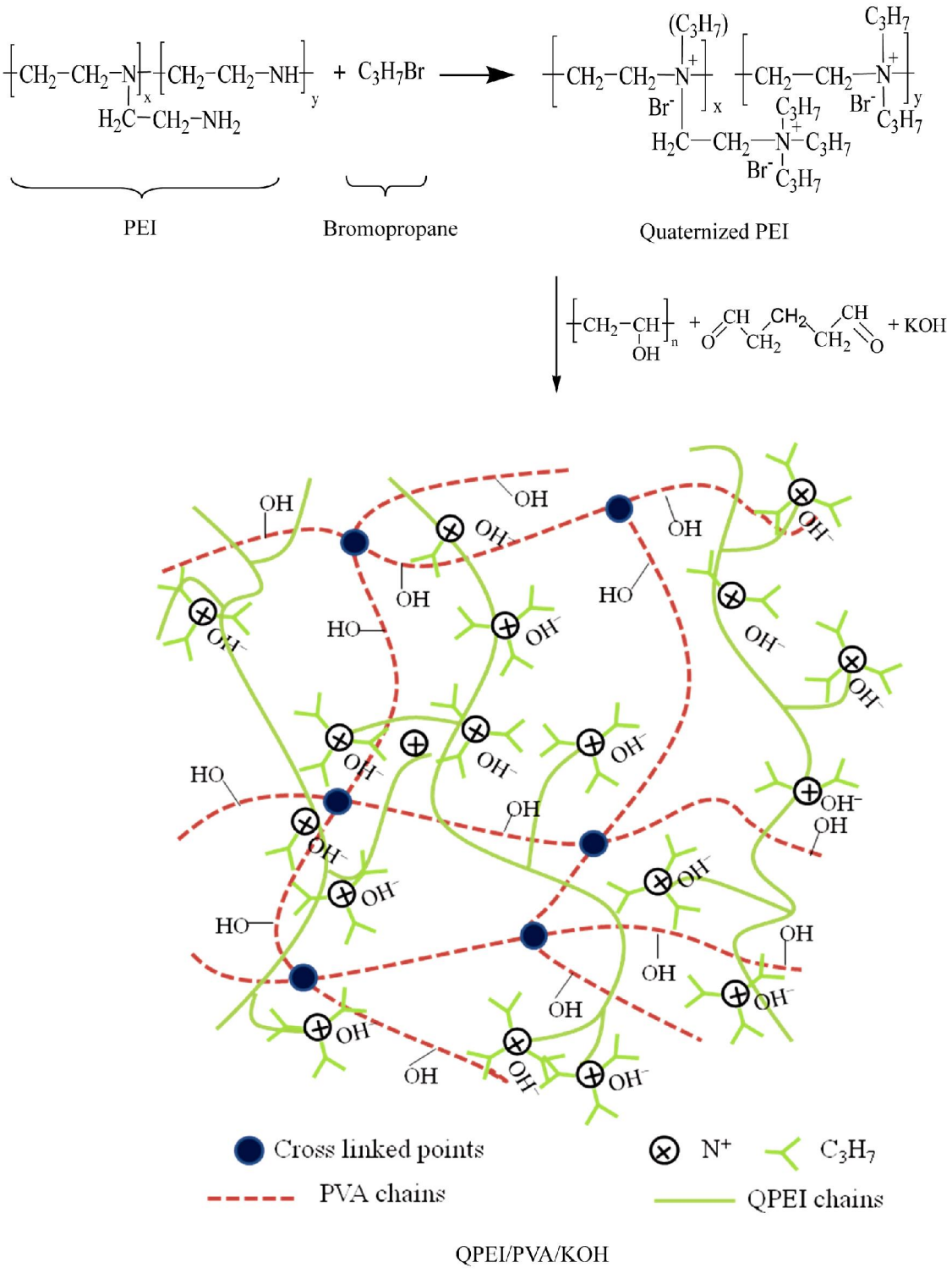

Fig. 6.2 Structural representation of QPEI/PVA/KOH SPE

(a)

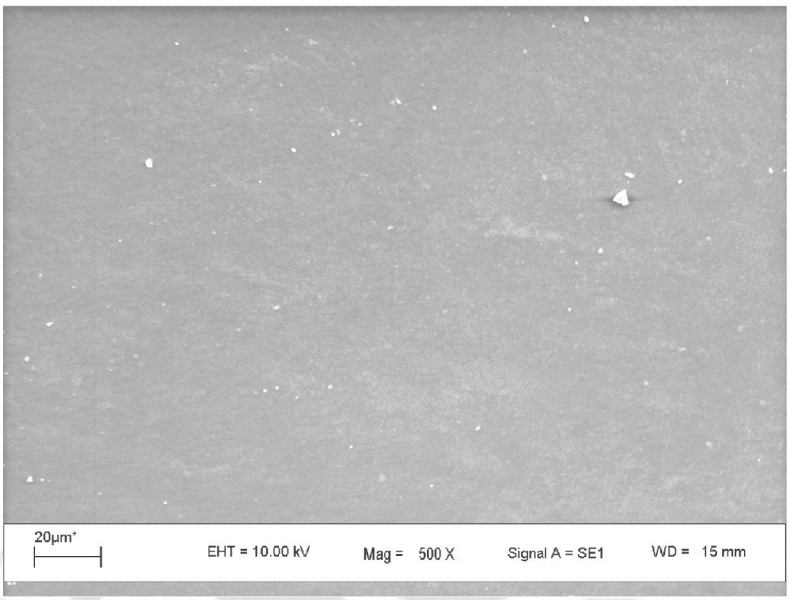

(b)

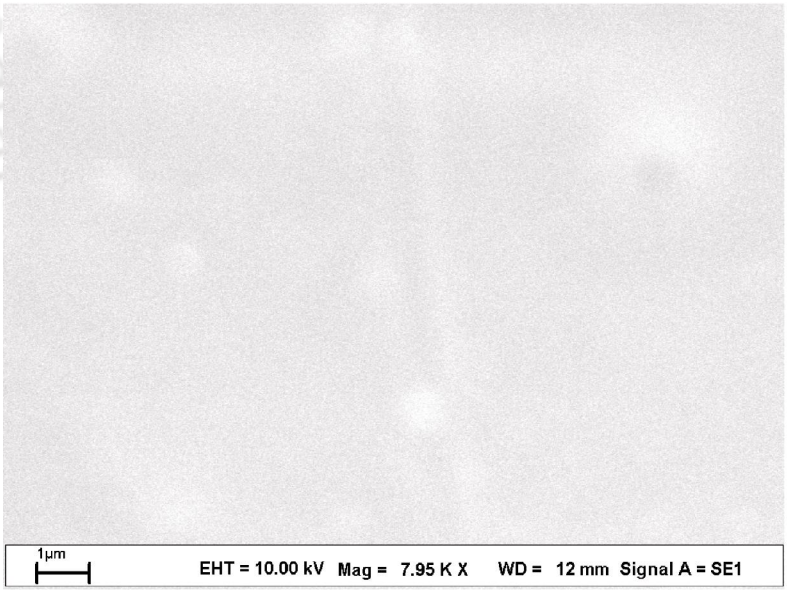

Fig. 6.3 SEM images of (a) PEI/PVA/KOH, and (b) QPEI/PVA/KOH

6.3.1.2 TGA

Figure 6.4 shows the thermal degradation behavior of PEI/PVA/KOH and QPEI/PVA/KOH SPEs. In the initial stage, up to a temperature of around 210°C the weight reduction of the membranes is due to evaporation of bound water in the membrane. It can be seen that PEI/PVA/KOH has higher water loss compared to the QPEI/PVA/KOH due to high water uptake of the former membrane, which is confirmed and reported in later section of the chapter. It can be noted that PEI/PVA/KOH membrane exhibits two sharp weight losses ranging from approximately 210°C to 260°C and 370°C to 450°C as shown in the fig. 6.4. The first weight loss may be due to the splitting of the ionic groups and the second weight loss may be due to the main chain splitting prior to the final decomposition of the polymer (Aeshala et al., 2014).

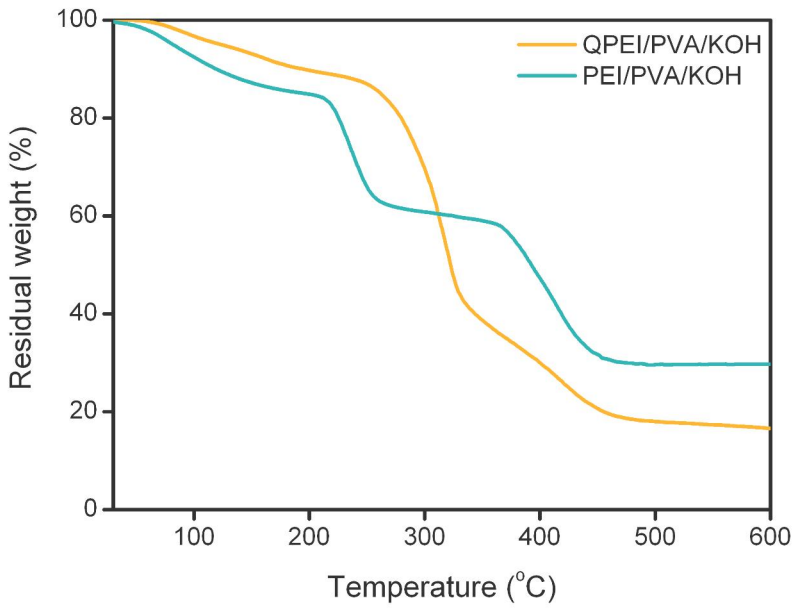

Fig. 6.4 TGA profile of PEI/PVA/KOH, and QPEI/PVA/KOH

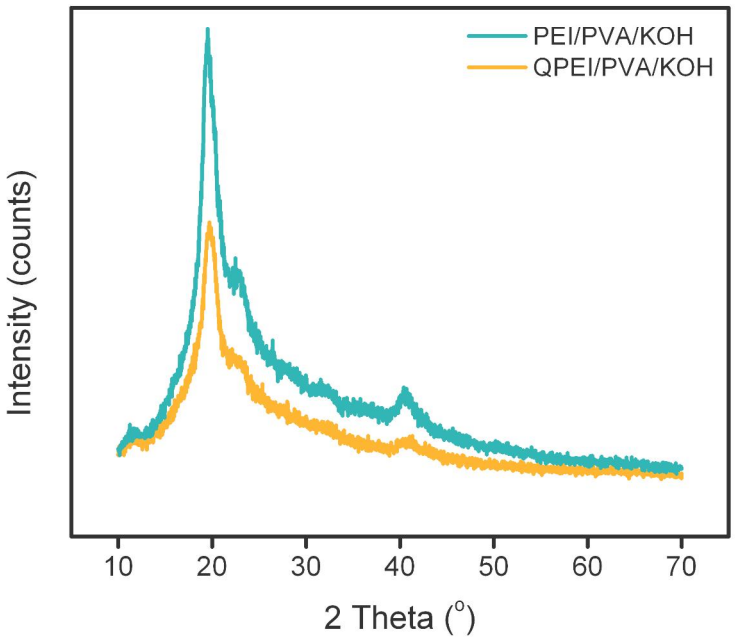

Fig. 6.5 XRD patterns of PEI/PVA/KOH, and QPEI/PVA/KOH

In case of QPEI/PVA/KOH too, two sharp weight losses ranging from approximately 250°C to 220°C and 390°C to 460°C are shown in the fig. 6.4. The first weight loss was attributed to decomposition of isopropyl groups in the quaternized membrane and the second weight loss, was due to the main chain splitting prior to the final decomposition of the polymer, as in the case of PEI/PVA/KOH.

6.3.1.3 XRD

Figure 6.5 shows the XRD patterns of PEI/PVA/KOH and QPEI/PVA/KOH. Both the membranes exhibit semi-crystalline structure with a broad peak at 2θ angle of 18°–22° and a small peak at 39°–40°. However, it can be seen that the intensity of the peaks in QPEI/PVA/KOH was less than PEI/PVA/KOH. As the ion transport is facilitated when the crystallinity is decreased, higher ionic conductivity is expected for QPEI/PVA/KOH.

6.3.1.4 FTIR

FTIR spectra of PEI/PVA and QPEI/PVA are shown in fig. 6.6. In both the cases the peaks at 2836 cm^{-1} and 1716 cm^{-1}, correspond to C–H stretching related to aldehydes and carbonyl group (C=O) respectively. These peaks are the result of crosslinking of glutaraldehyde. In the case of PEI/PVA SPE, the peak at 1635 cm^{-1} represents the formation of imine (C=N) linkage, which confirms the crosslinking between -NH_2 sites of PEI polymer and crosslinked polyvinyl alcohol (Rao et al., 2006). The quaternization of the PEI was confirmed by the disappearance of imine linkage at 1635 cm^{-1} and increased intensity of the C–H stretching bond. The appearance of deformation vibration bands at 1656 and 1461 cm^{-1} and the quaternary ammonium absorption band at 916 cm^{-1} further confirms the quaternization of the PEI (Yudovin-Farber et al., 2010).

6.3.1.5 Other important properties of the SPEs

Figure 6.7 shows the various properties of PEI/PVA/KOH and QPEI/PVA/KOH. The ionic conductivity and ion exchange capacity of the SPEs are very important properties. The ionic conductivity indicates the ease in the transportation of the hydroxyl ion from cathode to anode through the SPE, whereas ion exchange capacity signifies the amount of replaceable ions (meq.gm^{-1} of polymer) in the SPE. The branched QPEI was interpenetrated in the crosslinked PVA chains to form the semi-interpenetrating polymer network structure as shown in the fig. 6.2. Therefore, the quaternization has a dominant influence on the ionic conductivity and tensile strength of the membranes (fig. 6.7b). The ionic conductivity of QPEI/PVA/KOH was 10 times more than the PEI/PVA/KOH. The probable reason may be that quaternary ammonium cation are having higher amount of

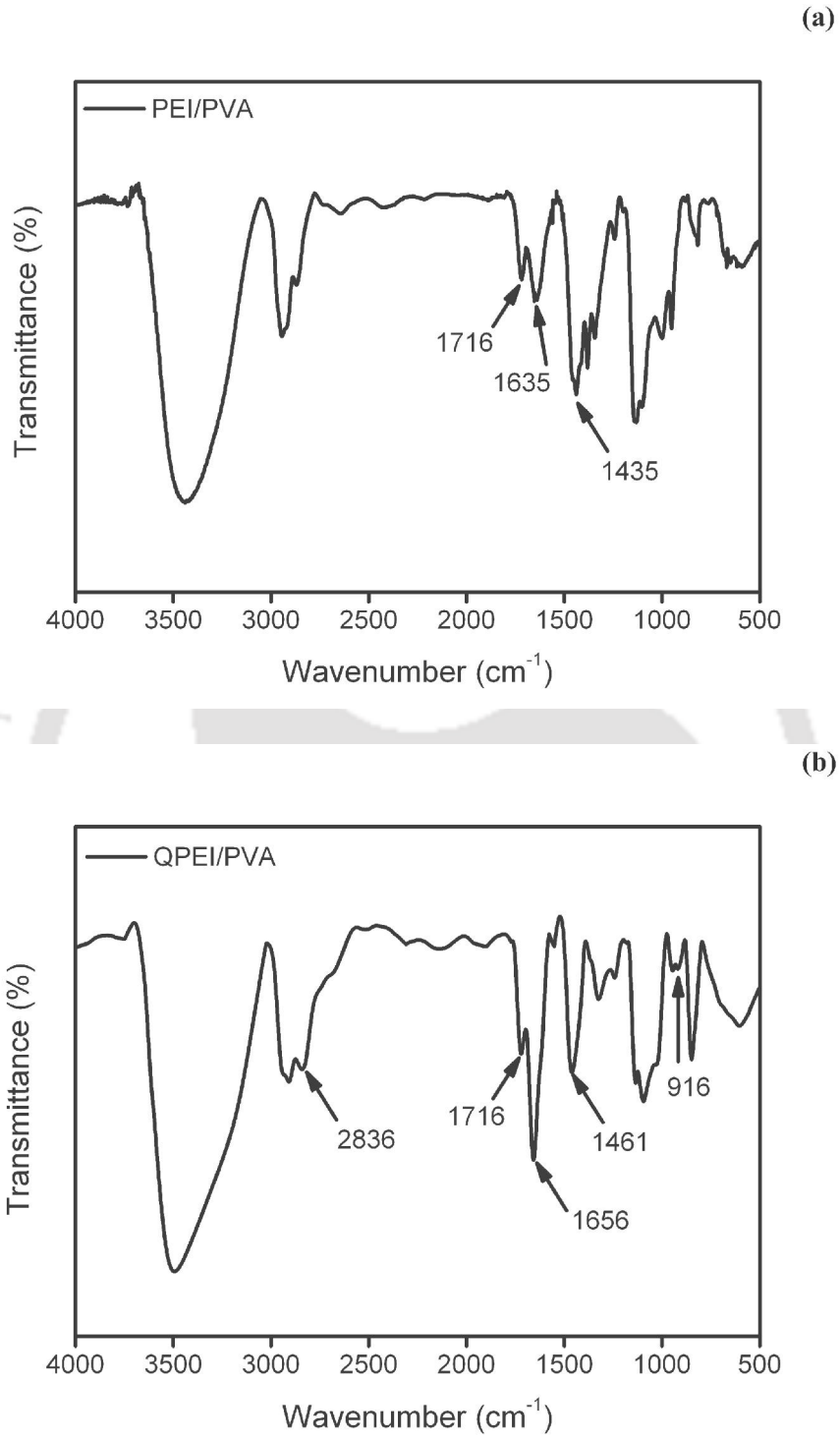

Fig. 6.6 FTIR spectra of (a) PEI/PVA, and (b) QPEI/PVA

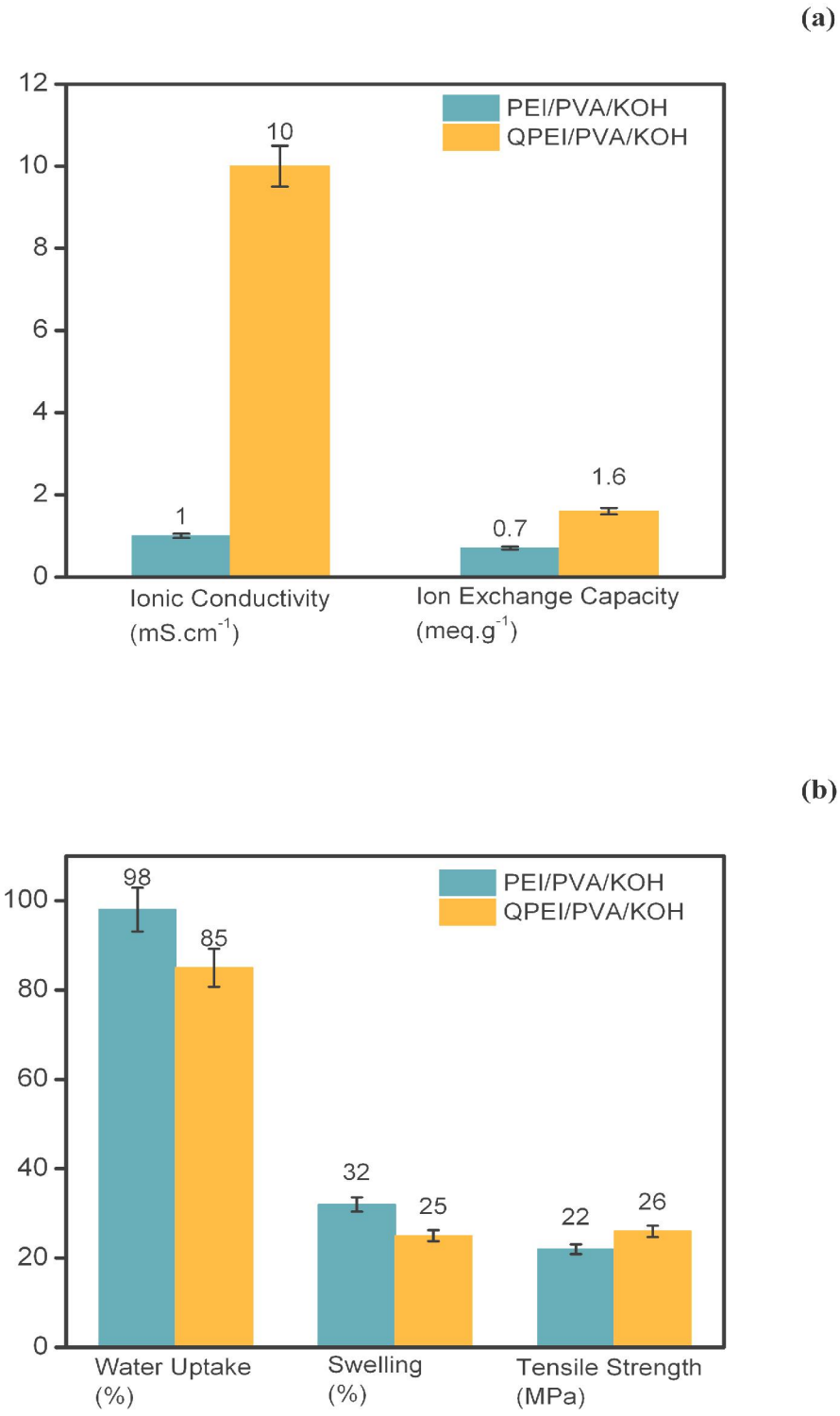

Fig. 6.7 (a) Ionic conductivity and ion exchange capacity, and (b) water uptake, swelling and tensile strength of PEI/PVA/KOH and QPEI/PVA/KOH SPEs

loosely held hydroxide ions (Starks et al., 1994), which resulted in the higher ionic conductivity through Grotthuss mechanism in the electric field.

It can be seen in the fig. 6.7a that the IEC of the SPE is affected by the quaternization and it was found to increase significantly after quaternization. It may be due to the bulky quaternary ammonium ion, which has higher anion activation stability due to the longer distance between cation and anion and thus hydroxyl ions are loosely held with the quaternary ammonium ion enhancing the ion exchange capacity (Starks et al., 1994). The electrostatic attraction between cation and anion will be weaker, resulting in more nucleophilic nature of the anion. In the case of PEI/PVA/KOH, solvation effects of primary and secondary amines increase the electron density on the amine nitrogen to a great extent (Pan et al., 2013), which leads to higher water uptake and swelling. The hydrophilicity of the QPEI/PVA/KOH was reduced by introducing alkyl groups via quaternization, resulting in slight decrease in water content as shown in fig. 6.7b. Therefore, the above results show that the membranes chosen for the ERC are suitable to be used as SPEs and thus evaluated in the electrochemical reactor which is discussed in the subsequent sections.

6.3.2 Influence of functional groups in SPE on dERC

The gaseous CO_2 was fed into the electrochemical reactor and various products were obtained at different applied voltages in the range of 1.8 V to 3 V. Figure 6.8 shows that the current density increases with the increase in the applied voltage for both the SPEs, which indicate that the rate of the reactions increase with increase in the applied voltage. The increased reaction rate corresponds to the increased electrical charge consumption by the various electrochemical reactions at the electrodes. In case of PEI/PVA/KOH SPE,

current density increases from 2.42 mA.cm^{-2} at 1.8 V to 5.83 mA.cm^{-2} at 3 V, whereas the current densities of 1.42 mA.cm^{-2} at 1.8 V to 4.81 mA.cm^{-2} at 3V are obtained using QPEI/PVA/KOH. Higher current density was observed for PEI/PVA/KOH as compared to QPEI/PVA/KOH at all the voltages. However, it is interesting to note in fig. 6.9 that, though the experimental conditions were same but the product formation was greatly influenced because of the variation in the functional groups of SPEs.

It is interesting to note (fig. 6.8) that on increasing the applied voltage up to a certain extent, the product formation was increased. However, further increase in the applied voltage results in the enhanced H_2 evolution and reduced product formation. The probable reason for this can be the significantly higher reaction kinetics at higher applied voltages,

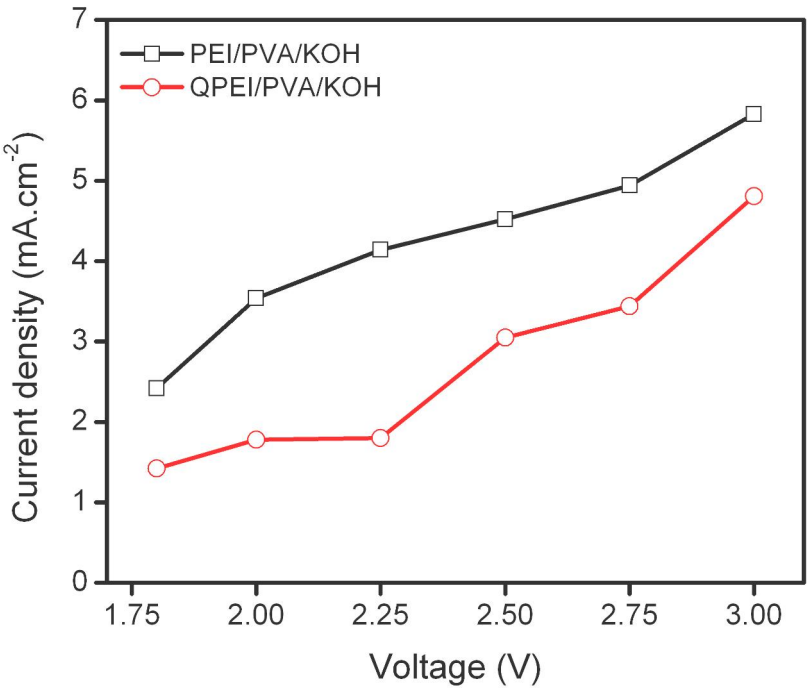

Fig. 6.8 Current density obtained as a function of applied potential in the ERC using PEI/PVA/KOH, and QPEI/PVA/KOH SPEs

which resulted in the formation of more amount of water at anode due to electroosmotic drag as well as anodic reaction. This may imbalance the water concentrations in the anode and cathode, resulting in the diffusion of the water from anode to the cathode. Therefore, cathode catalyst layer gets flooded with the water and the applied potential is primarily used up for the hydrogen generation. It hampers the ERC due to low solubility of gaseous CO_2 in the liquid water formed on the electrocatalyst. Additionally, the escape of H_2 from the reaction site offers diffusional resistance to the incoming CO_2.

Figure 6.9 shows that the amount of product formed also increases along with the applied voltage. However, the amount of CH_4 increases up to a certain voltage depending upon the SPE used and on further increase in voltage, CH_4 formation decreases. The formation of H_2 increases along with the applied voltage. In case of PEI/PVA/KOH (fig. 6.9a), CH_4 was the main product, whereas C_2H_6 and CH_4 were the major products for the QPEI/PVA/KOH (fig. 6.9b), along with comparatively minor quantities of CO, and CH_3OH in both the cases. Hydrogen gas was formed as a by-product due to water electrolysis (a competitive reaction at the cathode) in both the cases. However, the formation of H_2 gas was reduced as high as upto 50% when quaternized SPE was used for the dERC.

Based on the results, the process was conceptualized along with the reaction mechanism and is depicted in fig. 6.10. Figure 6.10 shows a representative cartoon of membrane electrode assembly having anode-SPE-cathode structure. The FESEM micrograph of the electroplated cathode on the carbon paper (Cu_2O/C) is also shown in the fig. 6.10. In order to have good contact among these components, the assembly was fabricated using hot press method. The membrane electrode assembly shows the various components such

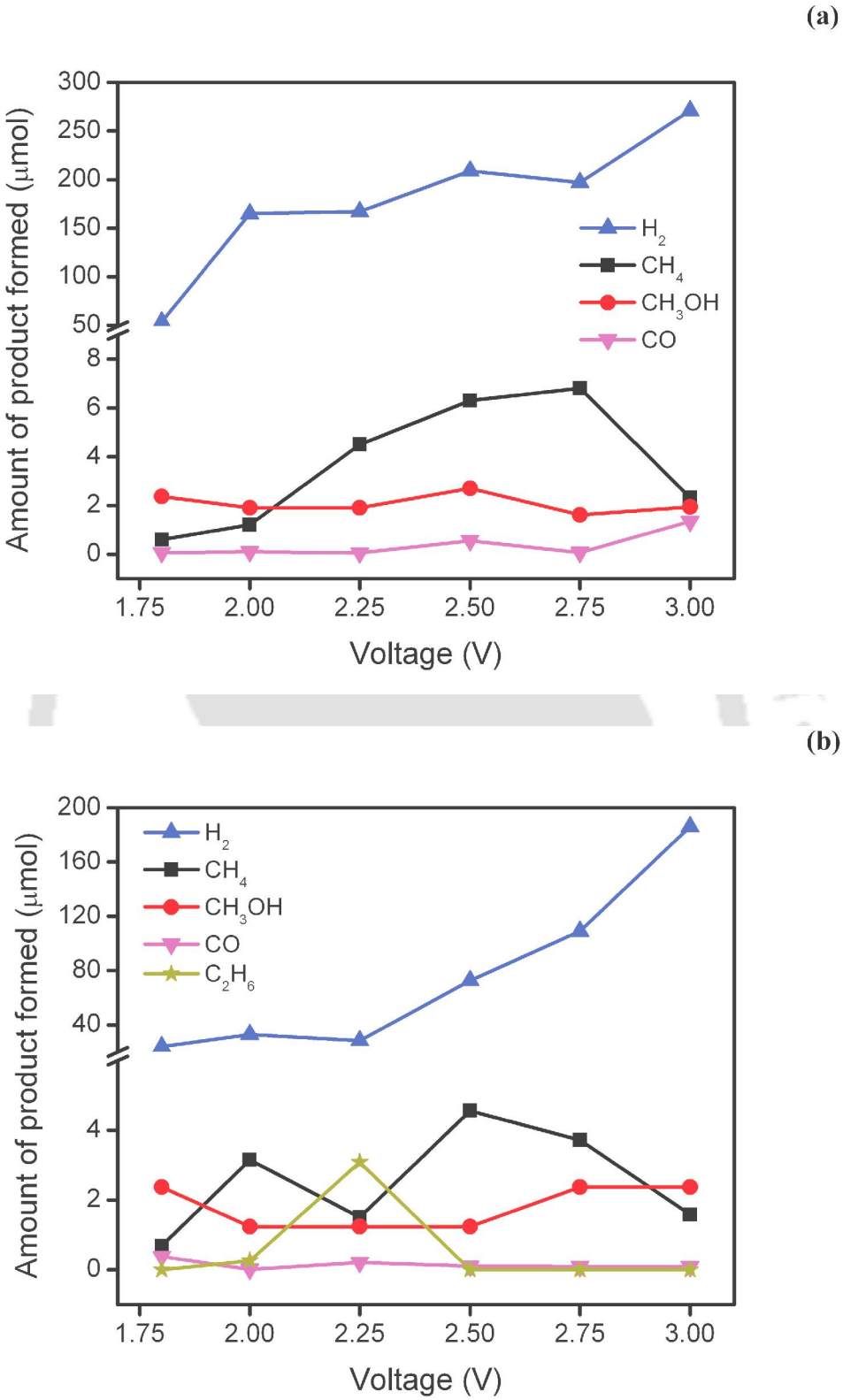

Fig. 6.9 Product distribution obtained as a function of applied potential using (a) PEI/PVA/KOH, and (b) QPEI/PVA/KOH SPEs

as anode gas diffusion layer, which is having porous structure for the transport of various reactants and products. The gas diffusion layer has a thin film of anode catalyst layer in contact to the SPE. Similarly, the cathode structure along with catalyst layer can be seen in the fig. 6.10. It can be anticipated that hot press process might result in the bulging of SPE in between the catalyst particles.

Figure 6.11 shows the representation where the bulging of the SPE into the catalyst particle can be visualized in a better way. The bulging of the polymer around the electrocatalyst is infact an added advantage as it provides large and effective triple phase boundary for electrochemical reactions.

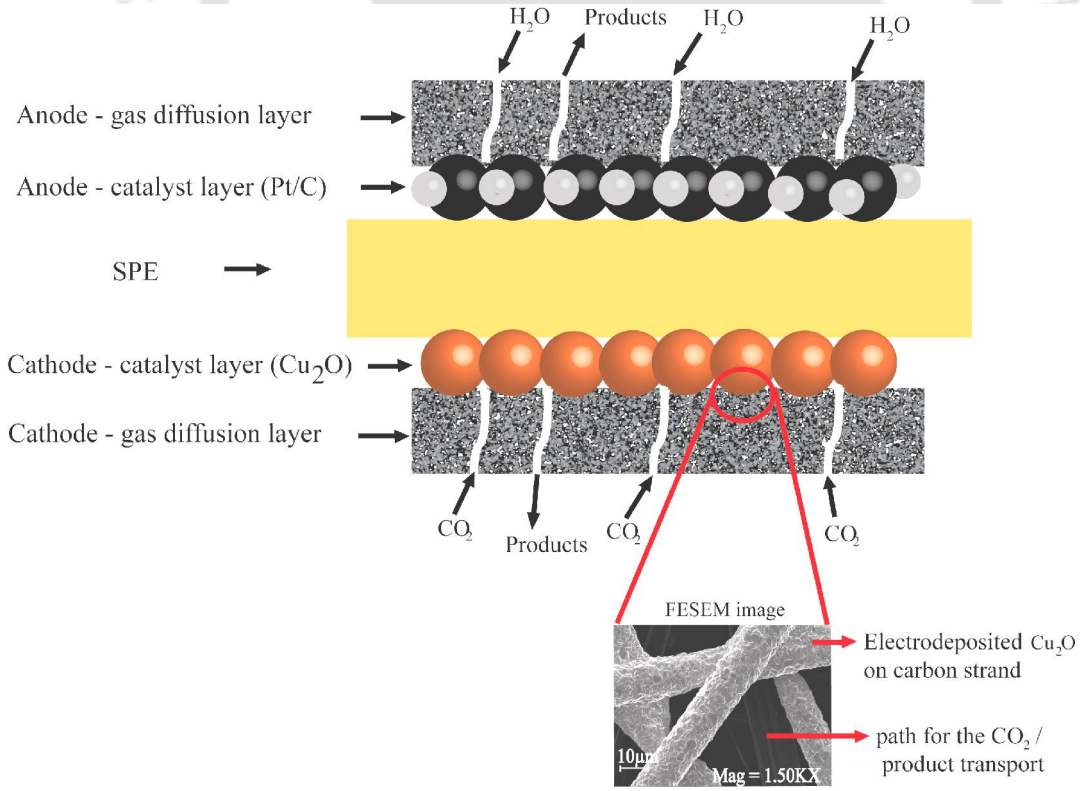

Fig. 6.10 Representation of membrane electrode assembly

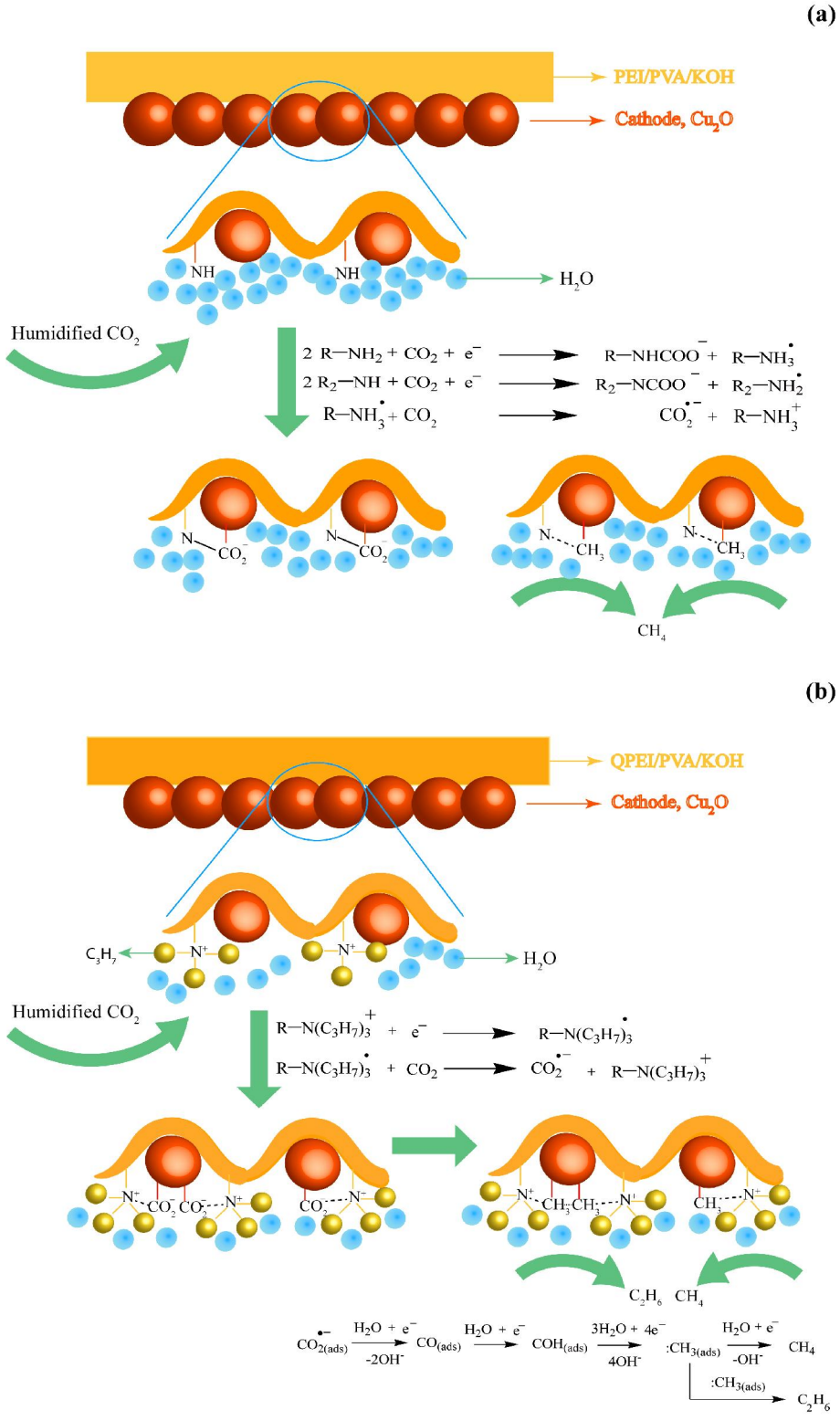

Fig. 6.11 Conceptualized representation of ERC using (a) PEI/PVA/KOH, and (b) QPEI/PVA/KOH (Aeshala et al., 2014)

Figure 6.11a shows the PEI/PVA/KOH as SPE (having primary, secondary, and tertiary amines as shown in the fig. 6.1). CO_2 reaching to the interface gets absorbed by the amine group and its linear stable structure bends by forming the carbamate via intermediates possibly composed of the loosely-bound encounter complex and zwitterions (Czaun et al., 2013; Pan et al., 2013).

Moreover, the electrocatalyst present at the interface along with the solvated water molecules form the reaction product and hydroxyl ion. These hydroxyl ions move from cathode to the anode and transform to water and O_2 gas in the presence of the anode electrocatalyst. The quaternized SPE (QPEI/PVA/KOH) (fig. 6.11b) having bulky alkyl groups hinders the water molecules to get associated with the quaternary group and thus decrease the solvation effect due to weaker electrostatic interactions (Sarode et al., 2014). In case of QPEI/PVA/KOH SPE, which is having bulky alkyl groups (fig. 6.10b), the incoming CO_2 does not form carbamate but ammonium group increases the CO_2 absorption capacity by forming an ion pair and/or bicarbonate (Saeki et al., 1995). The reason of (fig. 6.9b) getting low H_2 production (by-product of ERC) for the quaternized SPE as well as formation of C_2H_6 by C-C coupling can be the low water availability at the interface. It is interesting to observe that the maximum amount of formation of CH_4 (peak value) shifted to the lower potential (2.5 V for QPEI/PVA/KOH as compared to 2.75 V for PEI/PVA/KOH) due to higher ionic conductivity and co-catalyzation effect of quaternized SPE. The other reason may be the difference in covalent bond formation (in carbamate) and ions-pair formation energy differences.

Based on the above discussion it may be agreed that quaternary ammonium ion in the QPEI/PVA/KOH helps as a mediator or co-catalyst in the reduction of CO_2. It may also be suggested that electrostatically attracted quaternary ammonium ion to the negative

cathode also assist the electron flow from cathode to CO_2 molecule for ERC. Once $CO_{2ads}^{\bullet-}$ is formed, the remaining reaction pathways to produce the products in the electroreduction of CO_2 are proposed by several authors (Kuhl et al., 2012; Nie et al., 2013; Schouten et al., 2011). However, the pathway for the formation of C_2H_6 is not clear in the literature available for ERC. Therefore, the reaction pathway is being extended and proposed in the fig. 6.11b, in which the formation of C-C coupling through 2 molecules of $:CH_{3ads}$ to generate C_2H_6.

The cathode reactions for the different products formed during dERC are shown in the eq. (6.1-6.4) along with the standard half-cell potentials. The half-cell potential for the C_2H_6 formation was not available in the literature and thus standard calculation procedure (bond strength, enthalpy change, Gibb's free energy change) was opted to find the standard half-cell potential (Dean and Lange, 1999). It may be noted that the CH_4 and C_2H_6 have almost similar standard electrode potentials (E^o) and that may be another probable reason of the formation of one species at the expense of other even in a slightly changed interface environment.

$$CO_{2(g)} + 2H_2O_{(l)} + 2e^- \rightarrow CO_{(g)} + 2OH^- \quad E^o = -0.934\ V \qquad (6.1)$$

$$CO_{2(g)} + 5H_2O_{(l)} + 6e^- \rightarrow CH_3OH_{(l)} + 6OH^- \quad E^o = -0.812\ V \qquad (6.2)$$

$$CO_{2(g)} + 6H_2O_{(l)} + 8e^- \rightarrow CH_{4(g)} + 8OH^- \quad E^o = -0.659\ V \qquad (6.3)$$

$$CO_{2(g)} + 10H_2O_{(l)} + 14e^- \rightarrow C_2H_{6(g)} + 14OH^- \quad E^o = -0.685V \qquad (6.4)$$

To quantify the preference of the product formation on others, selectivity was calculated for the CH_4 using PEI/PVA/KOH as SPE; CH_4 and C_2H_6 using QPEI/PVA/KOH as SPE at various applied voltages. Selectivity is defined as the amount of desired product to amount of total CO_2 reduction products obtained (based on the carbon content) during the

Table 6.1 Selectivity of products obtained as a function of applied potential using PEI/PVA/KOH and QPEI/PVA/KOH

Voltage (V)	Selectivity (%)		
	PEI/PVA/KOH	QPEI/PVA/KOH	
	CH_4	CH_4	C_2H_6
1.8	19.6	19.9	0
2	37.4	64	10.6
2.25	68.4	16.4	67.6
2.5	65.8	77.3	0
2.75	80	60.18	0
3	41.2	39.19	0

reaction time of 25 min (Ogura et al., 2004). Maximum selectivity of 80% for CH_4 is obtained at 2.75 V using PEI/PVA/KOH whereas, 77.3% for CH_4 at 2.5 V in the case of QPEI/PVA/KOH. The selectivity of C_2H_6 at 2.25 V was 67.6% using QPEI/PVA/KOH, whereas the selectivity of CH_4 was reduced to around 16.4% as shown in table 6.1. It was observed that the quaternization has strong role on the formation of CH_4, C_2H_6, and H_2. However, the other minor reaction products were hardly influenced. Faradaic efficiency was calculated for different ERC products obtained using PEI/PVA/KOH and QPEI/PVA/KOH after 25 min of electrolysis at different voltages. Figure 6.12 shows that the the maximum Faradaic efficiency of CH_4 is 7.97% obtained at 2.5 V at corresponding current density of 4.52 $mA.cm^{-2}$ (fig. 6.8) in the case of PEI/PVA/KOH. It may be seen that to form any reaction product, either a potential window or a particular voltage is

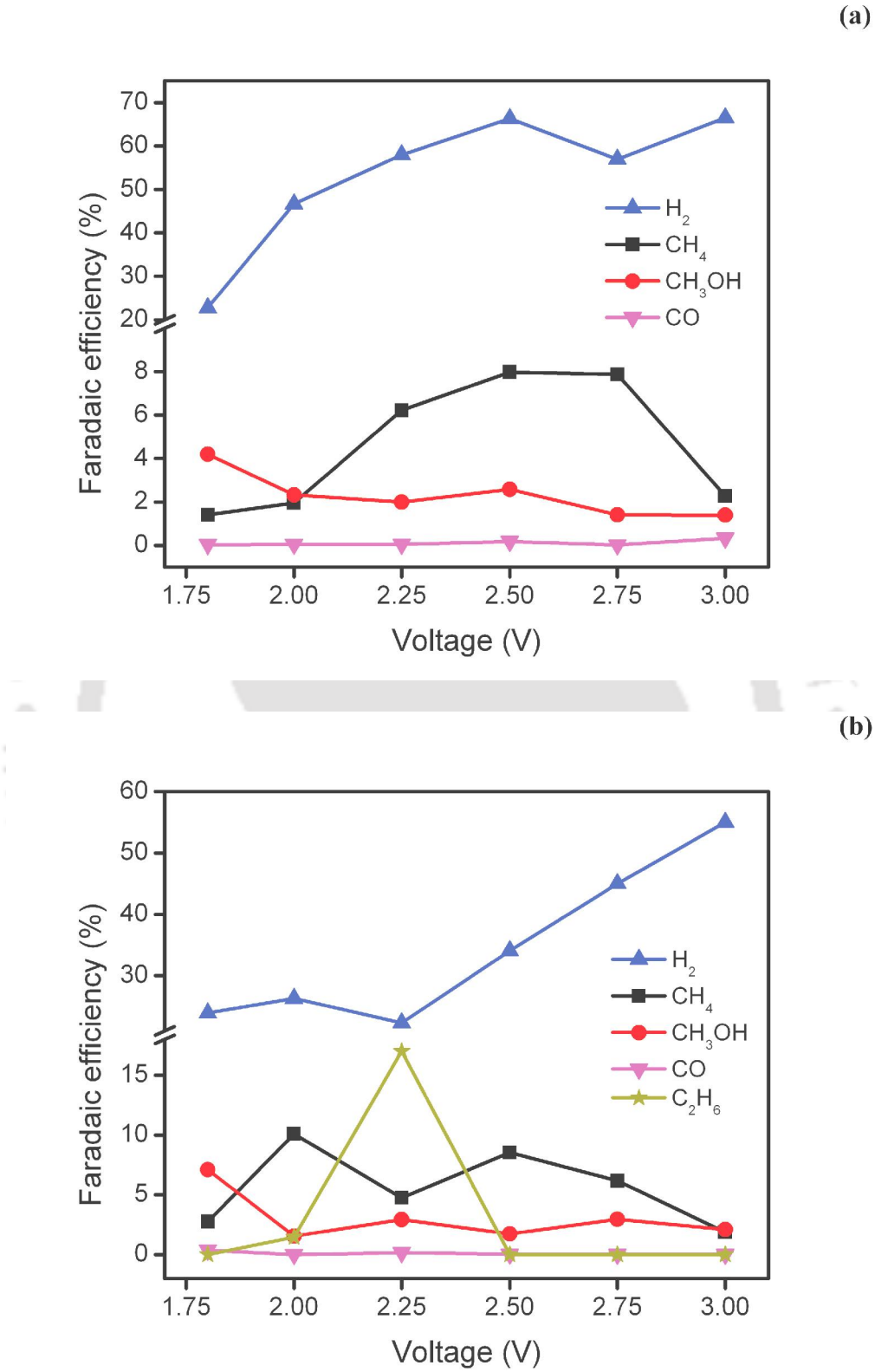

Fig. 6.12 Faradaic efficiency obtained as a function of applied potential using (a) PEI/PVA/KOH and (b) QPEI/PVA/KOH SPEs

more favorable. However, with lowering or raising the applied voltage, the adverse effect is found for the reaction products. At higher voltages the hydrogen evolution is favoured and at lower potentials the Faradaic efficiencies for the products generally reduces with significant hydrogen evolution. On further reduction of the applied potentials, there is no significant formation of either the reaction products or hydrogen by-product. The maximum Faradaic efficiency for CH_4 is around 6% for the potential window of 2.25 V to 2.75 V using PEI/PVA/KOH, whereas the use of QPEI/PVA/KOH suppressed the Faradaic efficiency of the CH_4 and selectively formed C_2H_6 with the maximum efficiency of 17.06% at 2.25V. Therefore, in order to further understand, the Faradaic efficiency was evaluated only for CH_4, C_2H_6, and H_2 (for different time intervals instead at the end of 25 min. duration) using PEI/PVA/KOH and QPEI/PVA/KOH.

Figure 6.13 shows that the Faradaic efficiency for CH_4 decreases with the time, whereas Faradaic efficiency for H_2 increases at the same voltage (2.75 V) using PEI/PVA/KOH. However, on comparing these results with the QPEI/PVA/KOH, it can be noted that after quaternization of the membrane, the Faradaic efficiency of CH_4 and C_2H_6 increases with the time or almost maintains the higher Faradaic efficiency as compared to its initial value at 5 min. The trend of the hydrogen Faradaic efficiency is also influenced by the QPEI/PVA/KOH and reduced to 50% compared to PEI/PVA/KOH at all time intervals. The maximum Faradaic efficiency of C_2H_6 is 17% using QPEI/PVA/KOH SPE at 2.25V at the end of 25 min.

It can be concluded that the reaction zone can be tuned with the modification of the functional group, which in turn affects the reaction mechanism for the electrochemical reduction of carbon dioxide.

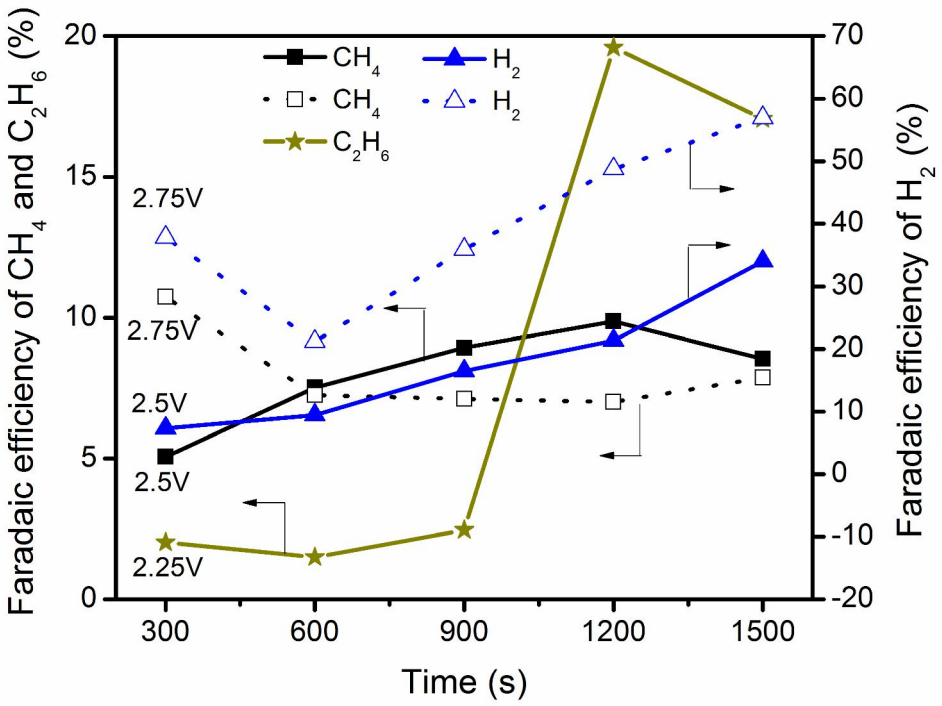

Fig. 6.13 Faradaic efficiency of CH_4, and H_2 obtained as a function of time in the ERC using both SPEs and C_2H_6 for QPEI/PVA/KOH at the maximum selectivity. (solid lines and closed symbols for QPEI/PVA/KOH and dotted lines and open symbols for PEI/PVA/KOH)

Chapter 7

Conclusions and Future Scope

Chapter 7

Conclusions and Future Scope

7.1 Conclusions

In this study, various solid polymer electrolytes were synthesized and characterized for the direct electrochemical reduction of CO_2 and particularly the role of SPE in dERC was investigated. Moreover, cationic and anionic exchange SPEs, functional groups and the reaction zone tuning by the modification of functional groups in SPE were studied and evaluated for dERC. The main findings emanating from this study are summarized ahead.

The work was focused on the development of an electrochemical reactor for continuous electrochemical reduction of carbon dioxide in gas phase using solid polymer electrolytes. Cationic (nafion and SPEEK) and anionic (alkali doped PVA/GA and Amberlyst/SPEEK) solid polymer electrolyte membranes were synthesized by casting method. The synthesized membranes were extensively characterized by SEM, TGA, XRD, FTIR, water uptake, swelling, ion exchange capacity, ionic conductivity, and tensile strength. The anode and cathode were prepared using Pt/C and copper electrocatalysts, respectively to form a membrane electrode assembly. The reactor was developed successfully and the preliminary study shows encouraging results for continuous gas phase CO_2 electroreduction in different solid electrolyte environment.

SEM images of the cationic and anionic SPEs appears uniform without formation of pores or cracks. Thermal stability of the membranes was evaluated as the membranes experience temperature of 110°C during the fabrication of membrane electrode assembly.

It has been observed that all the cationic and anionic membranes used in the study were stable not only upto the desired temperature (110^{o}C) but also upto a significantly higher temperature range.

In case of cation exchange SPEs, the water uptake of the SPEEK membrane was found to be more than nafion. Similar to water uptake, IEC was also higher for SPEEK as compared to nafion. However, in case of ionic conductivity, the trend was reversed and nafion exhibited higher conductivity as compared to SPEEK. It may be due to lower mean separation distance between the sulphonic acid groups in SPEEK than the nafion. The mean separation distance between the sulfonic acid groups decreases upon increasing the IEC. The equivalent weight of SPEEK (degree of sulfonation-50%) was 657 g.eq^{-1} and for nafion, it was 1100 g.eq^{-1}. Immersion of SPEEK membrane in water allows the molecular rearrangements in the nanostructure of the membrane and provides a well-defined interface between hydrophilic and hydrophobic phases. However, the intrinsic nano-phase separation of hydrophilic and hydrophobic zones in nafion explains the higher ionic conductivity of nafion than SPEEK.

In the case of anion exchange SPEs, Amberlyst/SPEEK composite membrane has shown higher water uptake than alkali doped PVA/GA but the ionic conductivity of Amberlyst/SPEEK was significantly low as compared to alkali doped PVA/GA. It may be due to the incorporation of quaternary ammonium based resin in the SPEEK. There might be some disruption in the continuum of hydrophilic channels or the sulfonic group clusters. Thus the ion movement either took a longer path or the hindered movement resulted in the drop of the hydroxyl ion conductivity. It was noticed that higher water uptake do not inevitably result into higher hydroxyl ion conductivity. Inclusion of additives in SPEEK changes the morphology of the membrane by changing the shape of

the ionic cluster and water content, which subsequently result in variation of the ionic conductivity of the composite membranes.

When pure cast nafion membrane was used, the products obtained were CH_3OH, HCHO, CO, and CH_4 with Faradaic efficiencies of 0.54%, 0.42%, 0.3%, and 4.5% respectively at current density of 11.1 mA cm^{-2}. SPEEK membrane also produced the same reaction products with Faradaic efficiencies of 0.44%, 0.35%, 0.4%, and 3.3%, respectively, at current density of 8.9 mA cm^{-2}. When alkali doped PVA/GA was used, the main products were formic acid (HCOOH), and carbon monoxide (CO) with the Faradaic efficiencies of 1%, and 12%, respectively, at current density of 5.6 mA cm^{-2}. The Amberlyst/SPEEK composite membrane worked as an anionic SPE and produced HCOOH and CO with a Faradaic efficiency of 0.7% and 16%, respectively, at current density of 3.3 mA cm^{-2}. The results were very encouraging especially for the composite membrane (Amberlyst/SPEEK) because it worked probably in the low alkaline region as desired. At higher potentials, the applied voltage was primarily utilized for hydrogen evolution, which was in competition with CO_2 reduction reaction due to higher reaction kinetics. Moreover, lower overpotential was found towards the formation of major product in dERC using anionic SPEs as compared to cationic SPEs.

The role of cationic and anionic SPE on the direct electrochemical reduction of gaseous CO_2 has been emphasized. The CMI-7000 and AMI-7001 were procured and successfully treated with H_2SO_4 and KOH, respectively, to get protonic and hydroxyl ion conductivity. Both the SPEs were characterized using ex-situ methods. It was observed that ionic conductivity of CMI-7000 was twelve times higher than AMI-7001 SPE and followed the same trend for ion exchange capacity and water uptake.

Current densities increase from 2 $mA.cm^{-2}$ to 4.81 $mA.cm^{-2}$ using CMI-7000, whereas for AMI-7001, current densities increase from 3 $mA.cm^{-2}$ to 6.1 $mA.cm^{-2}$. Both the membranes have the same polymer backbone but different functional groups, which might play a significant role at the electrode-electrolyte interface for the various electrochemical reactions.

In case of CMI-7000, the maximum amount of CH_4, C_2H_4, and CH_3OH was obtained at 3V with the concentration of 1.85 µmol, 1.02 µmol, and 4.74 µmol, respectively. Hydrogen evolution was more and it was found in the range of 117 µmol at 1.8 V to 279.6 µmol at 3 V. In case of AMI-7001, maximum amount of CH_4 obtained was 30.7 µmol at 2.5 V and the hydrogen evolution was also significant in the range from 172 µmol at 1.8 V to 283 µmol at 3 V. It may be due to the high water uptake of the membrane due to the quaternary ammonium functional group in the AMI-7001. The maximum Faradaic efficiency obtained for CH_4 formation was 32% at 2.5 V. The Faradaic efficiencies for C_2H_4 and CH_3OH were about 15% and 19%, respectively, at 2 V. In case of CMI-7000, Faradaic efficiency for any of the products was not more than 6%. Selectivity of methane was highest at 2.5 V with 60.9%, and for methanol and ethylene, selectivity was increased up to 2V and decreased thereafter. Selectivity for methane was more in the case of AMI-7001 than CMI-7000. The probable reason may be the electrostatically attracted quaternary ammonium ion of the AMI-7001 to the negative cathode and thus assisting the electron flow from cathode to the CO_2 in the electrolysis. However, anionic sulfonic group of CMI-7000, which might hardly be adsorbed onto the cathode due to the electrostatic repulsion at the negative cathode and thus caused hindrance to the flow of electron to CO_2 during electrolysis. It may be concluded that quaternary ammonium

group in anionic SPE played major role in the activation of CO_2 and thus enhanced the efficiency of the dERC.

It has been observed that though the functional groups are important for the rate of reaction but the polymer backbone, which infact does not take part in the reaction influences the reaction indirectly. Therefore, with this information, we have conceptualized the idea of active reaction zone and thought that it would be possible to change the reaction products by changing the surroundings of the functional group, while keeping all the other parameters fixed.

The anionic SPE (PEI/PVA/KOH and QPEI/PVA/KOH) membranes were successfully prepared and characterized. FTIR analysis confirmed the formation of quaternary amine functional group. The ionic conductivity of QPEI/PVA/KOH was 10 times higher than the PEI/PVA/KOH. It might be because quaternary ammonium cation can have higher amount of loosely held hydroxide ions, which led to the higher ionic conductivity through Grotthuss mechanism in the electric field. The IEC of the SPE was affected by the quaternization and it increased significantly after quaternization. It may be due to the bulky quaternary ammonium ion having higher anion activation stability due to the longer distance between cation and anion and thus hydroxyl ions were loosely held with the quaternary ammonium ion and enhanced the ion exchange capacity. In the case of PEI/PVA/KOH, solvation effects of primary and secondary amines increased the electron density on the amine nitrogen to a greater extent, which led to the higher water uptake and swelling.

In case of PEI/PVA/KOH SPE, current density was increased from 2.42 $mA.cm^{-2}$ at 1.8 V to 5.83 $mA.cm^{-2}$ at 3V, whereas 1.42 $mA.cm^{-2}$ at 1.8 V to 4.81 $mA.cm^{-2}$ at 3V were obtained using QPEI/PVA/KOH. Ethane was selectively formed in case of

QPEI/PVA/KOH. However, the generation of H_2 gas was reduced as high as upto 50% when quaternized SPE was used for the dERC.

The conceptual reaction mechanism was successfully proposed. The bulging of the polymer around the electrocatalyst showed an added advantage to provide effective three-phase boundary for electrochemical reactions. In case of PEI/PVA/KOH, CO_2 reached to the interface gets absorbed by the amine group and its linear stable structure bends by forming the carbamate via intermediates possibly composed of the loosely-bound encounter complex and zwitterions. In case of QPEI/PVA/KOH SPE which is having bulky alkyl groups, the incoming CO_2 does not form carbamate but ammonium group increases the CO_2 absorption capacity by forming an ion pair and/or bicarbonate. The observations to get low H_2 production (by-product of ERC) for the quaternized SPE as well as formation of C_2H_6 by C-C coupling was might be due to low water availability at the interface. The reaction pathway was extended and proposed that C-C coupling might be formed through 2 molecules of $:CH_{3ads}$ to generate C_2H_6.

The maximum Faradaic efficiency for CH_4 was around 6% for the potential window of 2.25 V to 2.75 V using PEI/PVA/KOH, whereas the use of QPEI/PVA/KOH suppressed the Faradaic efficiency of the CH_4 and selectively formed C_2H_6 with the maximum efficiency of 17.06% at 2.25 V. Maximum selectivity of 80% for CH_4 was obtained at 2.75V using PEI/PVA/KOH whereas, 77.3% for CH_4 at 2.5V in the case of QPEI/PVA/KOH. The selectivity of C_2H_6 at 2.25V was 67.6% using QPEI/PVA/KOH, whereas the selectivity of CH_4 was reduced to around 16.4%.

It was found that the anionic solid polymer electrolyte with suitable functional groups played an important role to enhance direct electrochemical reduction of CO_2. It was seen that the reaction zone can be tuned by the modification of functional groups for selective

formation of products for dERC. Moreover, the developed solid polymer electrolyte showed higher electrochemical reduction of CO_2 and greater suppression of H_2 evolution. Thus the study fulfills the aim of the research work along with the objective. It may be noted that though the selectivity of the products increased but still need improvements in the Faradaic efficiency and energy efficiency of the system. However, in order to further make the effective solid polymer electrolyte and electrocatalyst, some future scope along with future direction for the research is shown in the next section.

7.2 Future scope

- A study on the kinetics of reactions occuring in dERC may be conducted to study the mass transfer limitations of CO_2 at the interface of the electrode and electrolyte.
- Study on the stability of SPEs to improve the performance of dERC is required.
- Electrocatalysis for the dERC should be studied.

References

References

Aeshala, L.M., Rahman, S.U., Verma, A., 2011. Proceedings of ASME 5th International Conference on Energy Sustainability, Washington, DC, USA.

Aeshala, L.M., Rahman, S.U., Verma, A., 2012. Effect of solid polymer electrolyte on electrochemical reduction of CO_2. Sep. Purif. Technol. 94, 131-137.

Aeshala, L.M., Uppaluri, R.G., Verma, A., 2013. Effect of cationic and anionic solid polymer electrolyte on direct electrochemical reduction of gaseous CO_2 to fuel. J. CO_2 Util. 3–4, 49-55.

Aeshala, L.M., Uppaluri, R.G., Verma, A., 2014. Electrochemical conversion of CO_2 to fuels: Tuning of reaction zone using suitable functional group in solid polymer electrolyte. Phys. Chem. Chem. Phys., DOI: 10.1039/C4CP02389G.

Agel, E., Bouet, J., Fauvarque, J.F., 2001. Characterization and use of anionic membranes for alkaline fuel cells. J. Power Sources 101, 267-274.

Ahmad, M.I., Zaidi, S.M.J., Rahman, S.U., 2006. Proton conductivity and characterization of novel composite membranes for medium-temperature fuel cells. Desalination 193, 387-397.

Akahori, Y., Iwanaga, N., Kato, Y., Hamamoto, O., Ishii, M., 2004. New electrochemical process for CO_2 reduction to from formic acid from combustion flue gases. Electrochemistry 72, 266-270.

Alvarez-Guerra, M., Quintanilla, S., Irabien, A., 2012. Conversion of carbon dioxide into formate using a continuous electrochemical reduction process in a lead cathode. Chem. Eng. J. 207–208, 278-284.

Armand, M.B., Chabagno, J.M., Duclot, M.J., 1979. Fast ion transport in solids, North Holland Publishers, Amsterdam, 131-136.

Armaroli, N., Balzani, V., 2011. Towards an electricity-powered world. Energy Environ. Sci. 4, 3193-3222.

Aydin, R., Koleli, F., 2004. Electrocatalytic conversion of CO_2 on a polypyrrole electrode under high pressure in methanol. Synth. Met. 144, 75-80.

Azuma, M., Hashimoto, K., Hiramoto, M., Watanabe, M., Sakata, T., 1990. Electrochemical reduction of carbon dioxide on variuos metal electrodes in low-temperature aqueous $KHCO_3$ media. J. Electrochem. Soc. 137, 1772-1778.

Baglio, V., Aric`o, A.S., Di Blasi, A., Antonucci, V., Antonucci, P.L., Licoccia, S., Traversa, E., Fiory, S.F., 2005. Nafion–TiO_2 composite DMFC membranes: physico-chemical properties of the filler versus electrochemical performance. Electrochim. Acta 50, 1241–1246.

Bahar, B., Hobson, A.R., Kolde, J.A., Zuckerbrod, D., 1996. Ultrathin integral composite membrane. US Patent, 5,547,551.

Barbora, L., Acharya, S., Singh, R., Scott, K., Verma, A., 2009a. A novel composite Nafion membrane for direct alcohol fuel cells. J. Membr. Sci. 326, 721-726.

Barbora, L., Acharya, S., Verma, A., 2009b. Synthesis and ex-situ characterization of nafion/TiO_2 composite membranes for direct ethanol fuel cell. Macromol. Symp. 277, 177-189.

Barbora, L., Singh, R., Shroti, N., Verma, A., 2010. Synthesis and characterization of neodymium oxide modified nafion membrane for direct alcohol fuel cells. Mater. Chem. Phys. 122, 211–216.

Barbora, L., Verma, A., 2012. Enhanced performance of direct methanol fuel cell using talc modified nafion membrane. Int. J. Innov. Res. Dev. 7, 128-133.

Biljana, S., Ana, L.M., Diogo, M.F.S., Cesar, A.C.S., 2012. Anion- or cation-exchange membranes for NaBH4/H_2O_2 Fuel Cells?. Membranes (Basel).Sep 2, 478-492.

Bockris, J.O.M., Wass, J.C., 1989. The Photoelectrocatalytic reduction of carbon dioxide. J. Electrochem. Soc. 136, 2521-2528.

BP, 2013. Statistical review of world energy June 2013. Retrieved from: http://www.bp.com/content/dam/bp/pdf/statistical-review/statistical_review_of_world_energy_2013.pdf.

Centi, G., Perathoner, S., Wine, G., Gangeri, M., 2007. Electrocatalytic conversion of CO_2 to long carbon-chain hydrocarbons. Green Chem. 9, 671-678.

Chan, K.Y., Li, C.Y.V., 2014. Electrochemically Enabled Sustainability: Devices, Materials and Mechanisms for Energy Conversion. CRC Press, Taylor and Francis group, Florida, US.

Chang, T., Liang, R., Wu, P., Chen, J., Hsieh, Y., 2009. Electrochemical reduction of CO_2 by Cu_2O-catalyzed carbon clothes. Mater. Lett. 63, 1001-1003.

Chen, Y., Kanan, M.W., 2012. Tin oxide dependence of the CO_2 reduction efficiency on tin electrodes and enhanced activity for Tin/Tin oxide thin-film catalysts. J. Am. Chem. Soc. 134, 1986-1989.

Choi, P., Jalani, N.H., Datta, R., 2005a. Thermodynamics and proton transport in nafion II. proton diffusion mechanisms and conductivity. J. Electrochem. Soc. 152, E123-E130.

Choi, Y.J., Park, J.M., Yeon, K.H., Moon, S.H., 2005b. Electrochemical characterization of poly(vinyl alcohol)/formyl methyl pyridinium (PVA-FP) anion-exchange membranes. J. Membr. Sci. 250, 295-304.

Christophe, J., Doneux, Th., Buess-Herman, C., 2012. Electroreduction of carbon dioxide on copper-based electrodes: Activity of copper single crystals and copper-gold alloys. Electrocatal 3, 139-146.

Cook, R.L., MacDuff, R.C., Sammells, A.F., 1988. Ambient temperature gas phase CO_2 reduction to hydrocarbons at solid polymer electrolyte cells. J. Electrochem. Soc. 135, 1470-1471.

Czaun, M., Goeppert, A., May, R.B., Peltier, D., Zhang, H., Prakash, G.K.S., Olah, G.A., 2013. Organoamines-grafted on nano-sized silica for carbon dioxide capture. J. CO_2 Util. 1, 1-7.

Dean, J.A., Lange, N.A., 1999. Lange's Handbook of Chemistry. McGraw-Hill Inc. USA.

Delacourt, C., Ridgway, P.L., Kerr, J.B., Newman, J., 2008. Design of an electrochemical cell making syngas ($CO+H_2$) from CO_2 and H_2O reduction at room temperature. J. Electrochem. Soc. 155, B42-B49.

Dewulf, D., Bard, A., 1988. The electrochemical reduction of CO_2 to CH_4 and C_2H_4 at Cu/nafion electrodes (solid polymer electrolyte structures). Catal. Lett. 1, 73-79.

Dimitrova P., Friedrich K.A., Stimming U., Vogt B., 2002. Modified nafion based membranes for use in direct methanol fuel cells. Solid State Ionics 150, 115-122.

Druger, S.D., Ratner, M.A., Nitzan, A., 1985. Generalized hopping model for frequency-dependent transport in a dynamically disordered medium, with applications to polymer solid electrolytes. Phys. Rev. B 31, 3939-3947.

Eberle, U., von Helmolt, R., 2010. Sustainable transportation based on electric vehicle concepts: a brief overview. Energy Environ. Sci. 3, 689-699.

Fenton, D.E., Parker, J.M., Wright, P.V., 1973. Complexes of alkali metal ions with poly(ethylene oxide). Polymer 14, 589.

Galeazzi, L., 1976. Process for the chloromethylation of styrene-divinyl benzene copolymers. US 3997706, USA.

Gangeri, M., Perathoner, S., Caudo, S., Centi, G., Amadou, J., Begin, D., Pham-Huu, C., Ledoux, M.J., Tessonnier, J.P., Su, D.S., Schlogi, R., 2009. Fe and Pt carbon nanotubes for the electrocatalytic conversion of carbon dioxide to oxygenates. Catal. Today 143, 57-63.

Gattrell, M., Gupta, N., Co, A., 2007. Electrochemical reduction of CO_2 to hydrocarbons to store renewable electrical energy and upgrade biogas. Energy Convers. Manage. 48, 1255-1265.

Gonçalves, M.R., Gomes, A., Condeço, J., Fernandes, R., Pardal, T., Sequeira, C.A.C., Branco, J.B., 2010. Selective electrochemical conversion of CO_2 to C_2 hydrocarbons. Energy Convers. Manage. 51, 30-32.

Grace, A.N., Choi, S.Y., Vinoba, M., Bhagiyalakshmi, M., Chu, D.H., Yoon, Y., Nam, S.C., Jeong, S.K., 2014. Electrochemical reduction of carbon dioxide at low overpotential on a polyaniline/Cu_2O nanocomposite based electrode. Appl. Energy 120, 85-94.

Hara, K., Kudo, A., Sakata, T., 1995. Electrochemical reduction of carbon dioxide under high pressure on various electrodes in an aqueous electrolyte. J. Electroanal. Chem. 391, 141-147.

Hara, K., Sakata, T., 1997. Electrocatalytic formation of CH_4 from CO_2 on Pt gas diffusion electrode. J. Electrochem. Soc. 144, 539-545.

Hori, Y., Kikuchi, K., Murata, A., Suzuki, S., 1986. Production of methane and ethylene in electrochemical reduction of carbon dioxide at copper electrode in aqueous hydrogen carbonate solution. Chem. Lett. 15, 897-898.

Hori, Y., Murata, A., Takahashi, R., 1989. Formation of hydrocarbons in the electrochemical reduction of carbon dioxide at a copper electrode in aqueous solution. J. Chem. Soc., Faraday Trans. 1 85, 2309-2326.

Hori, Y., Konishi, H., Futamura, T., Murata, A., Koga, O., Sakurai, H., Oguma, K., 2005. "Deactivation of copper electrode" in electrochemical reduction of CO_2. Electrochim. Acta 50, 5354-5369.

Huda, M.S., Kiyono, R., Tasaka, M., Yamaguchi, T., Sata, T., 1998. Thermal membrane potential across anion-exchange membranes with different benzyltrialkylammonium groups. Sep. Purif. Technol. 14, 95-106.

Ikeda, S., Ito, T., Azuma, K., Ito, K., Noda, H., 1995. Electrochemical mass reduction of carbon dioxide using Cu-loaded gas diffusion electrodes I. Preparation of electrode and reduction products. Denki Kagaku 63, 303-309.

Ikeda, S., Taragi, T., Ito, K., 1987. Selective formation of formic acid, oxalic acid, carbon monoxide by electrochemical reduction of carbon dioxide. Bull. Chem. Soc. Jpn. 60, 2517-2522.

Innocent, B., Liaigre, D., Pasquier, D., Ropital, F., Léger, J.M., Kokoh, K.B., 2009. Electro-reduction of carbon dioxide to formate on lead electrode in aqueous medium. J. Appl. Electrochem. 39, 227-232.

Intaraprasit, N., Kongkachuichay, P., 2011. Preparation and properties of sulfonated poly(ether ether ketone)/Analcime composite membrane for a proton exchange membrane fuel cell (PEMFC). J. Tai. Inst. Chem. Eng. 42, 190–195.

Jhong, H.M., Ma, S., Kenis, P.J., 2013. Electrochemical conversion of CO_2 to useful chemicals: current status, remaining challenges, and future opportunities. Curr. Opin. Chem. Eng. 2, 191-199.

Kaneco, S., Hiei, N., Xing, Y., Katsumata, H., Ohnishi, H., Suzuki, T., Ohta, K., 2003. High-efficiency electrochemical CO_2 to methane reduction method using aqueous $KHCO_3$ media at less than 273 K. J. Solid State Electrochem. 7, 152-156.

Kaneco, S., Iiba, K., Ohta, K., Mizuno, T., 1999. Electrochemical reduction of carbon dioxide on copper in methanol with various potassium supporting electrolytes at low temperature. J. Solid State Electrochem. 3, 424-428.

Keerthiga, G., Viswanathan, B., Pulikottil, C.A., Chetty, R., 2012. Electrochemical reduction of carbon dioxide at surface oxidized copper electrodes. Bonfring Inter. J. Eng. Manag. Sci. 2, 41-43.

Kim, J.J., Summers, D.P., Frese, K.W., 1988. Reduction of CO_2 and CO to methane on Cu foil electrodes. J. Electroanal. Chem. 245, 223-244.

Kobayashi, K., Tanaka, K., 2014. Approach to multi-electron reduction beyond two-electron reduction of CO_2. Phys. Chem. Chem. Phys. 16, 2240-2250.

Koleli, F., Ropke, T., Hamann, C.H., 2004. The reduction of CO_2 on polyaniline electrode in a membrane cell. Synth. Met. 140, 65-68.

Komatsu, S., Tanaka, M., Okumura, A., Kungi, A., 1995. Preparation of Cu-solid polymer electrolyte composite electrodes and application to gas-phase electrochemical reduction of CO_2. Electrochim. Acta 40, 745-753.

Kreuer, K.D., 2001. On the development of proton conducting polymer membranes for hydrogen and methanol fuel cells. J. Membr. Sci. 185, 29-39.

Kuhl, K.P., Cave, E.R., Abram, D.N., Jaramillo, T.F., 2012. New insights into the electrochemical reduction of carbon dioxide on metallic copper surfaces. Energy Environ. Sci. 5, 7050-7059.

Kumar, M., Singh, S., Shahi, V.K., 2010. Cross-linked poly(vinyl alcohol)-poly(acrylonitrile-CO_2-dimethylamino ethylmethacrylate) based anion-exchange membranes in aqueous media. J. Phys. Chem. B 114, 198-206.

Kumutha, K., Alias, Y., 2006. FTIR spectra of plasticized grafted natural rubber–$LiCF_3SO_3$ electrolytes. Spectrochim. Acta 64, 442-447.

Kyriacou, G.Z., Anagnostopoulos, A.K., 1993. Influence of CO_2 partial pressure and the supporting electrolyte cation on the product distribution in CO_2 electroreduction. J. Appl. Electrochem. 23, 483-486.

Le, M., Ren, M., Zhang, Z., Sprunger, P.T., Kurtz, R.L., Flake, J.C., 2011. Electrochemical reduction of CO_2 to CH_3OH at copper oxide surfaces. J. Electrochem. Soc. 158, E45-E49.

Lebrun, L., Silva, E.D., Metayer, M., 2002. Elaboration of ion-exchange membranes with semi-interpenetrating polymer networks containing poly(vinyl alcohol) as polymer matrix. J. Appl. Polym. Sci. 84, 1572–1580.

Lebrun, L., Follain, N., Metayer, M., 2004. Elaboration of a new anion-exchange membrane with semi-interpenetrating polymer networks and characterisation. Electrochim. Acta 50, 985-993.

Lee, K.R., Lim, J.H., Lee, J.K., Chun, S.H., 1999. Reduction of carbon dioxide in 3-dimensional gas diffusion electrodes. Korean. J. Chem. Eng. 16, 829-836.

Lee, J., Tak, Y., 2001. Electrocatalytic activity of Cu electrode in electroreduction of CO_2. Electrochim. Acta 46, 3015-3022.

Lewandowski, A., Skorupska, K., Malinska, J., 2000. Novel poly(vinyl alcohol)-KOH-H_2O alkaline polymer electrolyte. Solid State Ionics 133, 265-271.

Li, H., Oloman, C., 2005. The Electroreduction of carbon dioxide in a continuous reactor. J. Appl. Electrochem. 35, 955-965.

Li, H., Oloman, C., 2006. Development of a continuous reactor for the electro-reduction of carbon dioxide to formate – Part 1: Process variables. J. Appl. Electrochem. 36, 1105-1115.

Li, H., Oloman, C., 2007. Development of a continuous reactor for the electro-reduction of carbon dioxide to formate – Part 2: Scale-up. J. Appl. Electrochem. 37, 1107-1117.

Li, L., Zhang, J., Wang, Y., 2003. Sulfonated poly(ether ether ketone) membranes for direct methanol fuel cell. J. Membr. Sci. 226, 159-167.

Liu, F., Yi, B., Xing, D., Yu, J., Zhang, H., 2003. Nafion/PTFE composite membranes for fuel cell applications. J. Membr. Sci. 212, 213–223.

Ludvigsson, M., Lindgren J., Tegenfeldt, J., 2000. FTIR study of water in cast nafion films. Electrochim. Acta 45, 2267-2271.

Lv, W., Zhang, R., Gao, P., Lei, L., 2014. Studies on the faradaic efficiency for electrochemical reduction of carbon dioxide to formate on tin electrode. J. Power Sources 253, 276-281.

MacHunda, R.L., Lee, J., Lee, J., 2010. Microstructural surface changes of electrodeposited Pb on gas diffusion electrode during electroreduction of gas-phase CO_2. Surf. Interface Anal. 42, 564-567.

Mansur, H.S., Sadahira, C.M., Souza, A.N., Mansur, A.A.P., 2008. FTIR spectroscopy characterization of poly (vinyl alcohol) hydrogel with different hydrolysis degree and chemically crosslinked with glutaraldehyde. Mater. Sci. Eng. 28, 539–548.

Mahreni, A.B., Mohamad, A.B., Kadhum, A.A.H., Daud, W.R.W., Iyuke S.E., 2009. Nafion/silicon oxide/phosphotungstic acid nanocomposite membrane with enhanced proton conductivity. J. Memb. Sci. 327, 32-40.

Menidil-Jakani, H., Lopez, I., Legrand, P.M., Mareau, V.H., Gonon, L., 2014. A new interpretation of SAXS peaks in sulfonated poly(ether ether ketone) (sPEEK) membranes for fuel cells. Phys. Chem. Chem. Phys. 16, 11243-11250.

Minier, M., Berthier, C., Gorecki, W., 1984. Thermal analysis and NMR study of poly(ethylene oxide) complex electrolyte: PEO($LiCF_3SO_3$). Journal de physique Paris 45, 739-744.

Mohamad, A.A., Mohamed, N.S., Alias, Y., Arof, A.K., 2002. Studies of alkaline solid polymer electrolyte and mechanically alloyed polycrystalline Mg_2Ni for use in nickel metal hydride batteries. J. Alloys Compd. 337, 208-213.

Mohamad, A.A., Mohamed, N.S., Yahya, M.Z.A., Othman, R., Ramesh, S., Alias, Y., Arof, A.K., 2003. Ionic conductivity studies of poly(vinyl alcohol) alkaline solid polymer electrolyte and its use in nickel-zinc cells. Solid State Ionics 156, 171-177.

Motupally, S., Becker, A.J., Weidner, J.W., 2000. Diffusion of water in nafion 115 membranes. J. Electrochem. Soc. 147, 3171-3177.

Murata, A., Hori, Y., 1991. product selectivity affected by cationic species in electrochemical reduction of CO_2 and CO at a Cu electrode. Bull. Chem. Soc. Jpn. 64, 123-127.

Nakagawa, H., Tsuge, S., Mohanraj, S., Ford, W.T., 1988. Characterization of chloromethyl-substituted polystyrene networks by high-resolution pyrolysis-gas chromatography. Macromolecules. 21, 930-933.

Narayanan, S.R., Haines, B., Soler, J., Valdez, T.I., 2011. Electrochemical conversion of carbon dioxide to formate in alkaline polymer electrolyte membrane cells. J. Electrochem. Soc. 158, A167-A173.

Nie, X., Esopi, M.R., Janik, M.J., Asthagiri, A., 2013. Selectivity of CO_2 reduction on copper electrodes: The role of the kinetics of elementary steps. Angew. Chem. Int. Ed. 52, 2459-2462.

Nishimura, M., Higa, M., Akamine, K., Masudaya, S., 2008. Preparation and characterization of anion-exchange membranes with a semi-interpenetrating network structure of poly(vinyl alcohol) and poly(allyl amine). Desalination 233, 157-165.

Nishimura, Y., Yoshida, D., Mizuhata, M., Asaka, K., Oguro, K., Takenaka, H., 1995. Solid polymer electrolyte CO_2 reduction. Energy Convers. Manage. 36, 629-632.

Ogura, K., Yano, H., Shirai, F., 2003. Catalytic reduction of CO_2 to ethylene by electrolysis at a three-phase interface. J. Electrochem. Soc. 150, D163-D168.

Ogura, K., Yano, H., Tanaka, T., 2004. Selective formation of ethylene from CO_2 by catalytic electrolysis at a three-phase interface. Catal. Today 98, 515-521.

Ohya, S., Kaneco, S., Katsumata, H., Suzuki, T., Ohta, K., 2009. Electrochemical reduction of CO_2 in methanol with aid of CuO and Cu_2O. Catal. Today 148, 329-334.

Olah, G.A., Goeppert, A., Prakash, G.K.S., 2009. Chemical Recycling off Carbon Dioxide to Methanol and Dimethyl Ether: From Greenhouse Gas to Renewable, Environmentally Carbon Neutral Fuels and Synthetic Hydrocarbons. J. Org. Chem. 74, 487-498.

Oloman, C., Li, H., 2008. Electrochemical Processing of Carbon Dioxide. ChemSusChem 1, 385-391.

Palacios, I., Castillo, R., Vargas, R.A., 2003. Thermal and transport properties of the polymer electrolyte based on poly(vinyl alcohol)-KOH-H_2O. Electrochim. Acta 48, 2195-2199.

Pan, X., Wang, G., Lay, C.L., Tan, B.H., He, C., Liu, Y., 2013. Photoluminescence from amino-containing polymer in the presence of CO_2: Carbamato anion formed as a fluorophore. Sci. Rep. 3, 2763, doi:10.1038/srep02763.

Park, Y.S., Yamazaki, Y., 2005. Low water uptake content and low water/methanol transport in CP/nafion hybrid membrane with high non-hydrogen bonding. J. Membr. Sci. 261, 58-66.

Park, J., Wang, L., Advani, S.G., Prasadz, A.K., 2012. Durability analysis of nafion/hydrophilic pretreated PTFE membranes for PEMFCs. J. Electrochem. Soc. 159, F864-F870.

Parry, M.L., Canziani, O.F., Palutikof, J.P., Van der Linden, P.J., Hanson, C.E., Eds., 2007. ClimateChange 2007: Impacts, adaptation and vulnerability. Contribution of working group II to the fourth assessment report of the Intergovernmental Panel on Climate Change, Cambridge University Press, Cambridge, UK, pp. 982.

Prakash, G.K.S., Viva, F.A., Olah, G.A., 2013. Electrochemical reduction of CO_2 over Sn-Nafion® coated electrode for a fuel-cell-like device. J. Power Sources 223, 68-73.

Ramani, V., Kunz, H.R., Fenton, J.M., 2005. Effect of particle size reduction on the conductivity of nafion/phosphotungstic acid composite membranes. J. Membr. Sci. 266, 110-114.

Rackley, S., 2009. Carbon Capture and Storage. Elsevier Science, Gulf Professional Publishing, USA.

Rao, P.S., Smitha, B., Sridhar, S., Krishnaiah, A., 2006. Preparation and performance of poly(vinyl alcohol)/polyethyleneimine blend membranes for the dehydration of 1,4-dioxane by pervaporation: Comparison with glutaraldehyde cross-linked membranes. Sep. Purif. Technol. 48, 244-254.

Saeki, T., Hashimoto, K., Kimura, N., Omata, K., Fujishima, A., 1995. Electrochemical reduction of CO_2 with high current density in a CO_2 + methanol medium II. CO formation promoted by tetrabutylammonium cation. J. Electroanal. Chem. 390, 77-82.

Sandhu, S.S., Crowther, R.O., Fellner, J.P., 2005. Prediction of methanol and water fluxes through a direct methanol fuel cell polymer electrolyte membrane. Electrochim. Acta 50, 3985-3991.

Sang, S., Wu, Q., Gan, Z., 2008. Influences of doping approach on conductivity of composite alkaline solid polymer electrolyte PVA-HA-KOH-H_2O. Electrochim. Acta 53, 5065-5070.

Sarode, H.N., Lindberg, G.E., Yang, Y., Felberg, L.E., Voth, G.A., Herring, A.M., 2014. Insights into the transport of aqueous quaternary ammonium cations: A combined experimental and computational study. J. Phys. Chem. B 118, 1363-1372.

Sata, T., 1978. Modification of properties of ion-exchange membranes - 4. change of transport properties of cation-exchange membranes by various polyelectrolytes. J. Polym. Sci. Polym. Chem. Ed 16, 1063-1080.

Sata, T., Teshima, K., Yamaguchi, T., 1996. Permselectivity between two anions in anion exchange membranes crosslinked with various diamines in electrodialysis. J. Polym. Sci., Part A: Polym. Chem. 34, 1475-1482.

Sata, T., Yamane, Y., Matsusaki, K., 1998. Preparation and properties of anion exchange membranes having pyridinium or pyridinium derivatives as anion exchange groups. J. Polym. Sci. Part A: Polym. Chem. 36, 49-58.

Senthil K.R., Senthil K.S., Anbu K.M., 2012. Highly selective electrochemical reduction of carbon dioxide using Cu based metal organic framework as an electrocatalyst. Electrochem. Commun. 25, 70-73.

Schouten, K.J.P., Kwon, Y., van der Ham, C.J.M., Qin, Z., Koper, M.T.M., 2011. A new mechanism for the selectivity to C_1 and C_2 species in the electrochemical reduction of carbon dioxide on copper electrodes. Chem. Sci. 2, 1902-1909.

Silva, V.S., Ruffmann, B., Vetter, S., Mendes, A., Madeira, L.M., Nunes S.P., 2005. Characterization and application of composite membranes in DMFC. Catal. Today 104, 205-212.

Singh, S., Aeshala, L.M., Verma, A., 2012. Sustainable Production of Fuel from Electrochemical Reduction of Carbon Dioxide. Int. J. Innov. Res. Dev. 1, 155-160.

Smitha, B., Sridhar, S., Khan, A.A., 2003. Synthesis and characterization of proton conducting polymer membranes for fuel cells. J. Memb. Sci. 225 (2003) 63-76.

Sperling, L.H., 1981. Interpenetrating Polymer Networks and Related Materials. Plenum, Newyork.

Starks, C., Liotta, C., Halpern, M., 1994. Basic Concepts in Phase-Transfer Catalysis, Phase-Transfer Catalysis. Springer Netherlands, pp. 1-22.

Strathmann, H., 1995. Chapter 6 Electrodialysis and related processes, pp. 213-281.

Subramanian, K., Asokan, K., Jeevarathinam, D., Chandrasekaran, M., 2007. Electrochemical membrane reactor for the reduction of carbondioxide to formate. J. Appl. Electrochem. 37, 255-260.

Taniguchi, I., Aurian-Blajeni, B., Bockris, J.O.M., 1983. Photo-aided reduction of carbon dioxide to carbon monoxide. J. Electroanal. Chem. Interfacial Electrochem. 157, 179-182.

Tazi, B., Savadago, O., 2001. New cation exchange membranes based on nafion, Silicotungstic acid and thiophene. J. New Mater. Electrochem. Syst. 185, 3–27.

Terunuma, Y., Saitoh, A., Momose, Y., 1997. Relationship between hydrocarbon production in the electrochemical reduction of CO_2 and the characteristics of the Cu electrode. J. Electroanl. Chem. 434, 69-75.

Thorson, M.R., Siil, K.I., Kenis, P.J.A., 2013. Effect of cations on the electrochemical conversion of CO_2 to CO. J. Electrochem. Soc. 160, F69-F74.

Vargas, R.A., Zapata, V.H., Delgado, M.I., Palacios, I., 2004. Effect of water vapor on the ion transport in polymer films of PVOH/LiH_2PO_4/H_2O. Solid State Ionics 175, 729-732.

Vinodh, R., Ilakkiya, A., Elamathi, S., Sangeetha, D., 2010. A novel anion exchange membrane from polystyrene (ethylene butylene) polystyrene: Synthesis and characterization. Mat. Sci. Eng., B: Solid. 167, 43-50.

Wang, J., Zhao, Z., Gong, F., Li, S., Zhang, S., 2009a. Synthesis of soluble poly(arylene ether sulfone) ionomers with pendant quaternary ammonium groups for anion exchange membranes. Macromolecules 42, 8711-8717.

Wang, G., Weng, Y., Chu, D., Chen, R., Xie, D., 2009b. Developing a polysulfone-based alkaline anion exchange membrane for improved ionic conductivity. J. Membr. Sci. 332, 63-68.

Wasmus, S., Valeriu, A., Mateescu, G.D., Tryk, D.A., Savinell, R.F., 2000. Characterization of H_3PO_4-equlibriated nafion 117 membranes using ^{1}H and ^{31}P NMR spectroscopy. J. Membr. Sci. 185, 78-85.

Watkins, J.D., Bocarsly, A.B., 2014. Direct reduction of carbon dioxide to formate in high-gas-capacity ionic liquids at post-transition-metal electrodes. ChemSusChem 7, 284-290.

Wilcox, J., 2012. Introduction to Carbon Capture, Carbon Capture. Springer New York, pp. 1-34.

Yang, C.C., Hsu, S.T., Chien, W.C., 2005. All solid-state electric double-layer capacitors based on alkaline polyvinyl alcohol polymer electrolytes. J. Power Sources 152, 303-310.

Yang, C.C., Lin, S.J., 2002. Preparation of composite alkaline polymer electrolyte. Mater. Lett. 57, 873-881.

Yang, C.C., Lin, S.J., Hsu, S.T., 2003. Synthesis and characterization of alkaline polyvinyl alcohol and poly(epichlorohydrin) blend polymer electrolytes and performance in electrochemical cells. J. Power Sources 122, 210-218.

Yudovin-Farber, I., Beyth, N., Weiss, E., Domb, A., 2010. Antibacterial effect of composite resins containing quaternary ammonium polyethyleneimine nanoparticles. J. Nanopart. Res. 12, 591-603.

Yano, H., Tanaka, T., Nakayama, M., Ogura, K., 2004. Selective electrochemical reduction of CO_2 to ethylene at a three-phase interface on copper(I) halide-confined Cu-mesh electrodes in acidic solutions of potassium halides. J. Electroanal. Chem. 565, 287-293.

Yano, J., Yamasaki, S., 2008. Pulse-mode electrochemical reduction of carbon dioxide using copper and copper oxide electrodes for selective ethylene formation. J. Appl. Electrochem. 38, 1721-1726.

Zaidi, S.M.J., Mikhailenko, S.D., Robertson, G.P., Guiver, M.D., Kaliaguine, S., 2000. Proton conducting composite membranes from polyether ether ketone and heteropolyacids for fuel cell applications. J. Membr. Sci. 173, 17-34.

Zeng, Q.H., Liu, Q.L., Broadwell, I., Zhu, A.M., Xiong, Y., Tu, X.P., 2010. Anion exchange membranes based on quaternized polystyrene-block-poly(ethylene-ran-butylene)-block-polystyrene for direct methanol alkaline fuel cells. J. Membr. Sci. 349, 237-243.

Zhang, Q.G., Liu, Q.L., Zhu, A.M., Xiong, Y., Ren, L., 2009. Pervaporation performance of quaternized poly(vinyl alcohol) and its crosslinked membranes for the dehydration of ethanol. J. Membr. Sci. 335, 68-75.

Zhang, S., Kang, P., Meyer, T.J., 2014. Nanostructured tin catalysts for selective electrochemical reduction of carbon dioxide to formate. J. Am. Chem. Soc. 136, 1734-1737.

Zschocke, P., Quellmalz, D., 1985. Novel ion exchange membranes based on an aromatic polyethersulfone. J. Membr. Sci. 22, 325-332.

Research Output

Research Output

Papers published in peer reviewed international journals

1. **Aeshala, L.M.**, Uppaluri, R.G., Verma, A., "Electrochemical Conversion of CO_2 to Fuels: Tuning of Reaction Zone using suitable Functional Group in Solid Polymer Electrolyte", Physical Chemistry Chemical Physics, 2014, doi: 10.1039/C4CP02389G (RSC Publication).
2. **Aeshala, L.M.**, Uppaluri, R.G., Verma, A., "Effect of Cationic and Anionic Solid Polymer Electrolyte on Direct Electrochemical Reduction of Gaseous CO_2 to Fuel", Journal of CO_2 Utilization, 2013, 3-4, 49-55 (Elsevier Publication).
3. **Aeshala, L.M.**, Rahman, S.U., Verma, A., "Electrochemical Reduction of CO_2 to Value Added Products Using Solid Polymer Electrolyte Reactor", Separation and Purification and Technology, 2012, 94, 131-137 (Elsevier Publication).
4. Singh, S., **Aeshala, L.M.**, Verma, A., "Sustainable Production of Fuel from Electrochemical Reduction of Carbon Dioxide" International Journal of Innovative Research and Development, 2012, 1(7), 155-160 (IJIRD Publication).
5. **Aeshala, L.M.,** Rahman, S.U., Verma, A., **"**Development of a Reactor for Continuous Electrochemical Reduction of CO_2 using Solid Electrolyte, ASME Proceedings, ES 2011, 1193-1199 (ASME Publication).

Papers in international conferences

1. **Aeshala, L.M.**, Verma, A.*, International Conference on Environmental Technology and Sustainable Developments: Challenge and Remedies, 21-23 February, 2014, Lucknow, India.

2. **Aeshala, L.M.***, Rapally, R., Verma, A., International Conference on Harnessing Natural Resources for Sustainable Development, 29-31 January, 2014, Cotton College, Guwahati, Assam, India.

3. Singh, S., **Aeshala, L.M.***, Verma, A., International Seminar and Workshop on Energy, Sustainability and Development, 12-14 October, 2012, Sibsagar, Assam, India.

4. **Aeshala, L.M.***, Rahman, S.U., Verma, A., International Conference on Recent Advance in Chemical Engineering and Technology (RACET), IIChE, 10-12 March, 2011, Kochi, India.

5. **Aeshala, L.M.**, Rahman, S.U., Verma, A.*, Proceedings of the 5th International Conference on Energy Sustainability, 7-10 August, 2011, Washington DC, USA.

Papers in national conferences

1. **Aeshala, L.M.***, Rapally, R., Verma, A., Reflux- Annual Chemical Engineering Symposium, 29-30 March, 2014, IIT Guwahati, Guwahati, India.
2. **Aeshala, L.M.**, Yadav, V.S.K., Uppaluri, R.G., Verma, A.*, Seminar on Carbon Management for Sustainable Development, Institute of Engineers, 14-16 November, 2013, Duliajan, Assam.

3. **Aeshala, L.M.***, Uppaluri, R.G., Verma, A., Next Generation Clean Fuels, Growdiesel, 17-18 September, 2013, New Delhi, India.

4. **Aeshala, L.M.***, Verma, A., REFLUX-2013, A Technical Annual Meeting, Department of Chemical Engineering, 3-4 April, 2013, IIT Guwahati, Assam.

5. Ghosh, A., **Aeshala, L.M.***, Verma, A., CHEMCON-2012, 65th Annual Meeting of Indian Institute of Chemical Engineers, 27-30 December, 2012, NIT Jalandhar, Punjab.

6. **Aeshala, L.M.***, Rahman, S.U., Verma, A., CHEMCON-2012, 65th Annual Meeting of Indian Institute of Chemical Engineers, 27-30 December, 2012, NIT Jalandhar, Punjab.

7. **Aeshala, L.M.***, Rahman, S.U., Verma, A., CHEMCON-2011, 64th Annual Meeting of Indian Institute of Chemical Engineers, 27-29 December, 2011, Bangalore.

Awards

1. **Best poster award** (**3rd prize**) has been conferred to the paper entitled as "Electrochemical Reduction of Atmospheric CO_2 to Generate Fuel and Simultaneous Storage of Solar Energy", held at Reflux-Chemical Engineering Annual Symposium, 29-30 March, 2014, IIT Guwahati, Guwahati, India.

2. Secured **2nd prize** in exhibition competition to the concept entitled as "Electrochemical Reduction of CO_2 using Solar Energy and Developed Electrochemical Reactor", held at Reflux-Chemical Engineering Annual Symposium, 29-30 March, 2014, IIT Guwahati, Guwahati, India.

3. Secured **2nd prize** in Green-Tech competition to the topic entitled as "Solar Energy Driven Electrochemical Reduction of CO_2 for Generation of Renewable Fuel", held at Reflux-Chemical Engineering Annual Symposium, 29-30 March, 2014, IIT Guwahati, Guwahati, India.

4. **Best poster award** has been conferred to the paper entitled as "Effect of Solid Electrolyte on Electrochemical Reduction of CO_2 to Generate Fuel", held at International Conference on Environmental Technology and Sustainable Developments: Challenge and Remedies, 21-23 February, 2014, Lucknow, India.

5. **Best paper award** has been conferred to the paper entitled as "Electrochemical Reduction of CO_2 using Solid Polymer Electrolyte Reactor", in Reaction Engineering and Transport Phenomena Session held at International Conference on Recent advance in Chemical Engineering and Technology (RACET), IIChE, 10-12 March, 2011, Kochi, India.

About the Author

The author joined Sustainable Environergy Electrochemical Research Group (*SEERG*) in the Department of Chemical Engineering, Indian Institute of Technology Guwahati, Assam, India, as a full time Ph.D. scholar in December 2009. Before joining IIT Guwahati, the author has completed M.Tech. in Chemical Engineering from Andhra University, Andhra Pradesh, India in 2009.

The author has published 5 research papers in several peer reviewed high impact factor international journals. He has also presented several scientific and technical research papers in national and international seminars and symposiums. He has secured best poster and paper awards in various national and international conferences. The author has recently joined as an Assistant Professor in Department of Chemical Engineering, National Institute of Technology, Agartala, India.